



ADVANCED MASTERS IN STRUCTURAL ANALYSIS
OF MONUMENTS AND HISTORICAL CONSTRUCTIONS



Master's Thesis

Giulia Grecchi

Monitoring and Structural Assessment of Monuments in the Historical Centre of L'Aquila struck by the 2009 Earthquake: the Case Study of St. Silvestro Church

This Masters Course has been funded with support from the European Commission. This publication reflects the views only of the author, and the Commission cannot be held responsible for any use which may be made of the information contained therein.

DECLARATION

Name: Giulia Grecchi

Email: giuliagrecchi@yahoo.it

Title of the Msc Dissertation: Monitoring and Structural Assessment of Monuments in the Historical Centre of L'Aquila struck by the 2009 Earthquake: The Case Study of St. Silvestro Church

Supervisors: Claudio Modena, Filippo Casarin, Bruno Silva

Year: 2012

I hereby declare that all information in this document has been obtained and presented in accordance with academic rules and ethical conduct. I also declare that, as required by these rules and conduct, I have fully cited and referenced all material and results that are not original to this work.

I hereby declare that the MSc Consortium responsible for the Advanced Masters in Structural Analysis of Monuments and Historical Constructions is allowed to store and make available electronically the present MSc Dissertation.

University: Università degli Studi di Padova

Date: 25th July, 2012

Signature: _____

ACKNOWLEDGEMENTS

First of all I would like to acknowledge the Consortium for the scholarship provided: without it, it would have been impossible to live this wonderful experience!

I am grateful to Prof. Claudio Modena for the interesting topic given. Thank you also to Filippo Casarin for his advises and to Bruno Silva for his continuous and really constructive guidance even from Portugal.

My gratitude to Filippo Lorenzoni for the priceless time he dedicated to discuss with me part of this work. Thank you also to Giulia Bettiol and Giovanni Guidi for the helpful hints given.

Grazie to everybody in Padova working in the Master Room: it was nice to share these months with you!

Going back to the experience lived in Portugal, I would like to thank all the Professors I met in Guimarães during the coursework part of this Master: it was really a privilege to learn from you.

A giant *obrigada* goes to my classmates: it was great to live with you all for 7 months! And thank you also to Elizabeth for being my family in Guimarães!

Finally, I cannot forget my family and my friends in Pavia: now I know the feeling of missing you! Mum, Dad, Cecilia, and Amit: thank you for being always my reference point!

Last but not least, thank you Fede! This year has been strange, difficult but at the same time wonderful: besides the distance, we built a lot together! Little by little, step by step we can do everything: what does not destroy us, makes us stronger!

ABSTRACT

The research work carried out throughout this thesis concerns the study carried out on the Church of St. Silvestro in L'Aquila. This Church was damaged during the earthquake in April 2009 and has been included in the Niker Project as a case study, together with other Historical Buildings. The objective of this project is to mitigate the seismic risk in Cultural Heritage of all over the World through the use of integrated methodologies.

The work starts by describing the research that was already done on the Church and was made available. Then, a numerical model of the Church was built to able to simulate its behaviour during the seismic event and assess the strengthening interventions both temporary and permanent.

The Church's bell tower is under continuous static and dynamic monitoring. Data coming from these systems was considered as a reference for the calibration process of the model.

The first model built aimed at the calibration of the elastic material properties of the bell tower and the front façade. Modal analyses were run and modal shapes were checked in order to assess the model behaviour. Values and assumptions made for this model were then included in a global model of the entire church. Modal analyses and a linear dynamic analysis were performed to see the global behaviour of the Church.

Results coming from different analyses have been compared between them. Also, for the linear dynamic analysis, numerical accelerations were validated with the data coming from the monitoring system.

The model built showed a behaviour similar to the real Church, but a deeper investigation is recommend, especially for what concern the material parameters of the different type of masonry that have been recognized through visual inspection.

SOMMARIO

Monitoraggio e valutazione strutturale dei monumenti nel centro storico della città di L'Aquila colpita dal terremoto 2009: il caso studio della Chiesa di San Silvestro

Il lavoro di ricerca descritto in questa tesi riguarda lo studio portato avanti sulla chiesa di San Silvestro a L'Aquila. La chiesa è stata danneggiata durante il terremoto avvenuto nell'Aprile del 2009 ed è stata inclusa, insieme con altri Edifici Storici, nel progetto Niker. Questo progetto ha come obiettivo principale quello di migliorare dal punto di vista sismico le prestazioni degli edifici del Patrimonio Culturale mondiale attraverso lo sviluppo e l'applicazione di tecnologie integrate.

Questo lavoro comprende anche ciò che è già stato fatto e ciò che è a disposizione sulla Chiesa e ha come obiettivo quello di costruire un modello numerico capace di simulare il comportamento della Chiesa in caso di eventi sismici e utile per verificare possibili interenti permanenti sulla struttura.

Il campanile è sotto continuo monitoraggio sia statico sia dinamico; i dati provenienti da entrambi i sistemi sono stati presi come punto di riferimento durante il processo di calibrazione del modello.

Con primo modello costruito si aveva come intento quello di calibrare i parametri elastici del campanile e dalla facciata. Per tutte le analisi modali effettuate per verificare il comportamento del modello, sono state controllate le forme modali. I valori ottenuti e le ipotesi fatte per questo primo modello, sono stati poi inseriti nel modello globale della Chiesa. Di questo, sono state eseguite non solo analisi modali, ma anche un'analisi dinamica lineare con lo scopo di veder il comportamento della Chiesa nella sua globalità.

I risultati provenienti dalle diverse analisi sono stati messi a confronto. Inoltre per l'analisi dinamica lineare, le accelerazioni numeriche sono state controllate con le accelerazioni sperimentali provenienti dal sistema di monitoraggio.

Il modello costruito ha dimostrato un comportamento simile a quello reale della Chiesa, ma si raccomanda un'investigazione più completa, specialmente per quanto riguarda i parametri dei materiali di diversi tipi di muratura che sono stati riconosciuti durante l'ispezione visiva.

LIST OF CONTENT

1	INTRODUCTION	1
1.1	MOTIVATION.....	1
1.2	OBJECTIVES.....	1
1.3	OUTLINE.....	2
2	INVESTIGATION: STATE OF THE ART	3
2.1	STEP 1: HISTORICAL EVOLUTION.....	6
2.2	STEP 2: GEOMETRICAL SURVEY.....	7
2.3	STEP 3: DAMAGE SURVEY.....	7
2.4	STEP 4: ON SITE INVESTIGATION.....	7
2.4.1	<i>Non Destructive Tests - NDT</i>	7
2.4.2	<i>Minor Destructive Tests - MDT</i>	11
2.5	STEP 5: LABORATORY TESTS.....	14
2.6	STEP 6: STRUCTURAL CONTROL WITH MONITORING.....	14
3	MODELING: STATE OF THE ART	17
3.1	RIGID BLOCK ANALYSIS.....	17
3.2	STRUCTURAL ELEMENT MODELS (SEM).....	18
3.2.1	<i>Equivalent Strut</i>	18
3.2.2	<i>POR method</i>	18
3.2.3	<i>Macro-elements and Frame Models</i>	19
3.3	FINITE ELEMENT METHODS (FEM).....	20
3.4	DISCRETE ELEMENT METHODS (DEM).....	22
3.5	MODELLING OF HISTORICAL CONSTRUCTIONS.....	22
4	THE CHURCH OF ST. SILVESTRO	23
4.1	INTRODUCTION.....	23
4.2	HISTORY.....	24
4.3	ARCHITECTURAL AND STRUCTURAL DESCRIPTION.....	25
4.4	MATERIALS.....	27
4.5	DAMAGE AFTER THE 6.4.2009 EARTHQUAKE.....	28
5	STRUCTURAL CONTROL: MONITORING	35

5.1	INTRODUCTION.....	35
5.2	THE MONITORING SYSTEM IN ST. SILVESTRO.....	36
5.2.1	<i>Static</i>	36
5.2.2	<i>Dynamic</i>	37
5.3	THE STATIC CONTROL.....	38
5.4	THE DYNAMIC IDENTIFICATION.....	40
6	STRUCTURAL ANALYSIS: MODELING	55
6.1	INTRODUCTION.....	55
6.2	GEOMETRY	55
6.3	MATERIALS, PROPERTIES, AND BOUNDARY CONDITIONS	55
6.4	MESH: QUADRILATERAL AND TRIANGULAR CURVED SHELL ELEMENTS (DIANA USER'S MANUAL, 2012)	59
6.5	LOADS	61
6.5.1	<i>Roof weight</i>	61
6.5.2	<i>Other loads</i>	62
6.5.3	<i>Load Combination</i>	62
7	ANALYSES AND CALIBRATION OF THE MODEL	63
7.1	INTRODUCTION.....	63
7.2	THE CALIBRATION PROCESS: FIRST LEVEL	66
7.2.1	<i>Bell Tower & façade</i>	66
7.2.2	<i>Global model</i>	71
7.3	THE CALIBRATION PROCESS: SECOND LEVEL.....	75
8	CONCLUSIONS AND FUTURE WORKS	83
	BIBLIOGRAPHY	85
9	ANNEXES.....	A
9.1	STRAINS.....	A
9.2	STRESSES.....	C

LIST OF FIGURES

Figure 1-1: The Church of St. Silvestro (actual state - May 2012).....	1
Figure 2-1: The most important crack pattern after earthquakes in churches (Linee Guida per la valutazione e riduzione del rischio sismico del patrimonio culturale (in Italian), 2010).....	4
Figure 2-2: Out of plane mechanisms for general buildings (D'Ayala & Speranza, 2002).....	4
Figure 2-3: Experimental survey (Binda, Mirabella, & Abbaneo, 1994).....	5
Figure 2-4: Information required and corresponding investigation.....	6
Figure 2-5: Thermovision: detection of a vertical rod behind the plaster,.....	8
Figure 2-6: Sonic Test (left) and Possible layouts hammer-receiver (right).....	9
Figure 2-7: Sonic tomography of the hor. section of two pillars, (Binda, Saisi, & Zanzi, 2003).....	9
Figure 2-8: Radargrams of the walls sections of Fontanella Church Bergamo, Italy.....	10
Figure 2-9: Schmidt Hammer.....	11
Figure 2-10: Single Flat jack test.....	12
Figure 2-11: Calculation method of the tangent E modulus in the loading part (left) and of the secant E in the unloading (right). (Binda, Cantini, Saisi, & Tiraboschi, 2007).....	13
Figure 3-1: Modelling of a masonry panel (left) and a masonry building (right).....	18
Figure 3-2: Macro elements approach.....	19
Figure 3-3: SAM method (Magenes, Bolognini, & Braggio, 2000).....	20
Figure 3-4: FEM modelling of Masonry (adapted from (Lourenço, 1996)).....	21
Figure 4-1: The Italian Peninsula and L'Aquila.....	23
Figure 4-2: St. Silvestro.....	24
Figure 4-3: Building phases according to O. Antonini.....	25
Figure 4-4: South-West (left) and South-East (right) views.....	25
Figure 4-5: North-West (left) and North-East (right) views.....	26
Figure 4-6: St. Silvestro Façade.....	26
Figure 4-7: The "apparecchio aquilano" layout of the east wall (left) and west wall (right).....	27
Figure 4-8: Masonry in the interior part of the bell tower.....	28
Figure 4-9: The RC curb (Borri, et al., 2010).....	28

Figure 4-10: The seismic activity in L'Aquila (updated to 15 th June 2009)	28
Figure 4-11: Bell tower: cracks on the North side (left) and East side (right)	29
Figure 4-12: Cracks pattern on the front façade (left) and in the apse (right)	30
Figure 4-13: Overturning mechanisms of the bell tower (Borri, et al., 2010).....	30
Figure 4-14: Overturning of the façade (Borri, et al., 2010).....	31
Figure 4-15: Cracks in Cappella Branconio.....	31
Figure 4-16: Overturning of the apses and shear cracks (Borri, et al., 2010)	32
Figure 4-17: Graphic reproduction of the overturning in the apses (Borri, et al., 2010)	32
Figure 4-18: Roof collapse (Borri, et al., 2010)	33
Figure 4-19: Hammering process and effects inside the Church (Borri, et al., 2010)	33
Figure 5-1: Tiltmeter (a), displacement transducer (b), and sensor for the temperature	36
Figure 5-2: Static monitoring at (starting from left): 2.5 m, 6.8 m, 8.6 m, and 26 m (Caccin, 2012)	36
Figure 5-3: Static monitoring system (green: displacement, Ciano: temperature, orange: tiltmeter) (Caccin, 2012)	37
Figure 5-4: The accelerometer in St. Silvestro (Fattoretto, 2012)	37
Figure 5-5: Dynamic monitoring system in the bell tower of St. Silvestro: ground level (left), +14.5m (centre), +26m (right).....	38
Figure 5-6: 3D view of St. Silvestro and the accelerometers (Fattoretto, 2012)	38
Figure 5-7: Cracks opening and time (dash lines are the temperature) (Caccin, 2012)	39
Figure 5-8: Tiltmeter data (red and green lines) (Caccin, 2012)	39
Figure 5-9: Tiltmeter data (red and green lines) (Caccin, 2012)	40
Figure 5-10: Sensors used for the dynamic identification of the structure (Fattoretto, 2012)	40
Figure 5-11: Singularities of the spectral density matrix (FDD).....	42
Figure 5-12: Singularities of the spectral density matrix (EFDD)	43
Figure 5-13: Modal estimation parameters.....	43
Figure 5-14: Stabilization diagram.....	45
Figure 5-15: First five modal frequencies of St. Silvestro (Fattoretto, 2012).....	47
Figure 5-16: Modal frequencies and MAC value of the first mode (Fattoretto, 2012)	48
Figure 5-17: Modal frequencies and MAC value of the second mode (Fattoretto, 2012)	48

Figure 5-18: Modal frequencies and MAC value of the third mode (Fattoretto, 2012).....	49
Figure 5-19: Modal frequencies and MAC value of the fourth mode (Fattoretto, 2012)	49
Figure 5-20: Modal frequencies and MAC value of the fifth mode (Fattoretto, 2012).....	50
Figure 5-21: Damping with time for the first mode (Fattoretto, 2012)	50
Figure 5-22: Damping with time for the second mode (Fattoretto, 2012)	51
Figure 5-23: Damping with time for the third mode (Fattoretto, 2012).....	51
Figure 5-24: Damping with time for the fourth mode (Fattoretto, 2012).....	52
Figure 5-25: Damping with time for the fifth mode (Fattoretto, 2012)	52
Figure 6-1: Material and thickness in the Church. Front view (upper side) and back view (low side) ..	58
Figure 6-2: CQ40S element (left) and CT30S element (right)	60
Figure 6-3: Curved shell element	60
Figure 6-4: Degrees of Freedom	60
Figure 7-1: Deformed mesh and displacement.....	63
Figure 7-2: Detailed of the reinforcement (East side)	66
Figure 7-3: Crack pattern in the model: front (left) and back (right)	67
Figure 7-4: Frequencies and MAC values.....	69
Figure 7-5: MAC values for global model and "small" one.....	72
Figure 7-6: Comparison for 2nd global mode - 1.77 Hz (left) and the "small" model.....	72
Figure 7-7: Comparison for 4th global mode - 2.15 Hz (left) and the "small" model.....	73
Figure 7-8: Comparison for 14th global mode - 4.14 Hz (left) and the "small" model.....	73
Figure 7-9: First global model of the church (walls)	74
Figure 7-10: Fifth global mode of the church (walls)	74
Figure 7-11: ninth global mode of the church (longitudinal)	74
Figure 7-12: tenth global mode	74
Figure 7-13: Location of the seismic event considered and L'Aquila city.	75
Figure 7-14: Channels 2 and 3 records.....	76
Figure 7-15: Accelerometers stations near L'Aquila (source: INGV)	77
Figure 7-16: Rayleigh damping	78

Figure 7-17: Comparison between experimental data (blue) and numerical data (red) for Channel 4 (x direction – midheight of the bell tower) 79

Figure 7-18: Comparison between experimental data (blue) and numerical data (red) for Channel 5 (y direction – midheight of the bell tower) 79

Figure 7-19: Comparison between experimental data (blue) and numerical data (red) for Channel 6 (x direction – top of the bell tower) 80

Figure 7-20: Comparison between experimental data (blue) and numerical data (red) for Channel 7 (x direction – top of the bell tower) 80

Figure 7-21: Comparison between experimental data (blue) and numerical data (red) for Channel 8 (y direction – top of the bell tower) 81

Figure 7-22: Frequencies before, during and after the seismic event 81

Figure 9-1: Tensile Principal Strain - Layer 1A

Figure 9-2: Compressive Principal Strain - Layer 1A

Figure 9-3: Tensile Principal Strain - Layer 3B

Figure 9-4: Compressive Principal Strain - Layer 3B

Figure 9-5: Tensile Principal Stress - Layer 1C

Figure 9-6: Compressive Principal Stress - Layer 1C

Figure 9-7: Tensile Principal Strain - Layer 3D

Figure 9-8: Compressive Principal Strain - Layer 3D

LIST OF TABLE

Table 1: Modal shapes of St. Silvestro (EFDD)	44
Table 2: Modal shapes of St. Silvestro (pLSCF)	46
Table 3: Experimental frequencies from ARTeMIS and MACEC (data from July 2010)	47
Table 4: Suggested values for masonry by the Italian Standards – translation from table C8A.2.1 (Nuova Circolare della Norme Tecniche per le Costruzioni, 2009)	56
Table 5: Material's parameters	57
Table 6: Material, thickness and associated part in the model	59
Table 7: Roof Weight.....	61
Table 8: Truss central nave	61
Table 9: Truss lateral naves	61
Table 10: Overview of Principal Strains (compressive and tensile)	64
Table 11: Overview of Principal Stresses (compressive and tensile)	65
Table 12: Strengthening Material's parameters	66
Table 13: Springs' stiffness	67
Table 14: Overview of the materials parameters after calibration.....	68
Table 15: Overview of errors and MAC values before and after calibration	69
Table 16: Mode I – Flexional (MAC= 0.705; ϵ = 2.72 %)	70
Table 17: Mode II – Flexional (MAC= 0.44; ϵ = 0.08 %)	70
Table 18: Mode II – Flexional (MAC= 0.44; ϵ = 0.08 %)	71
Table 19: Overview of errors and MAC values before and after calibration	72
Table 20: Channels	76

1 INTRODUCTION

1.1 Motivation

The earthquake that took place in the city of L'Aquila during the night of the 6th of April 2009 destroyed and damaged a lot of structure. The Church of St. Silvestro (Figure 1-1) is one of the churches severely damaged, but not collapsed.

Right after the seismic event, the church was temporary strengthened in order to stop the evolution of the damage, but a more suitable intervention that involves the entire structure has still to be designed.

The aim of this thesis is to build a model of the structure that can be used in the future to assess the reliability of the strengthening proposed.



Figure 1-1: The Church of St. Silvestro (actual state - May 2012)

1.2 Objectives

The Church of St. Silvestro has already been studied after the earthquake but a dynamic identification of the whole structure has still to be performed.

A description of the damage together with the history of the building process of St. Silvestro was published just after the earthquake. The report proposes also a possible intervention that was not carried out. (Borri, et al. 2010)

The Department of Civil Engineer¹ of the University of Padova together with the University of Nagoya (Japan) performed a dynamic identification on the bell tower. Moreover static and dynamic monitoring is still active in the Church especially on the bell tower that seems to be the most vulnerable part of the building

1.3 Outline

The thesis is organized in several chapters:

Chapter 1 – Introduction: it's a description of the motivation of the work and organization of the thesis;

Chapter 2 – Investigation: state of the art: it's a brief report on the state of the art of inspection regarding Historical Constructions. A step procedure is also described with several (but not all) techniques available and used to gather information on the structures;

Chapter 3 – Modelling: state of the art: this chapter describes the different techniques available in literature for modelling Historical Constructions especially when dealing with masonry;

Chapter 4 – The Church of St. Silvestro: here the history of the Church can be found. Also the geometry and the materials of the structure are described. Moreover the damage caused by the earthquake is included in this section;

Chapter 5 – Structural control: Monitoring: on the Church a static and dynamic structural monitoring has been installed on the bell tower since July 2010. Here a brief description on the post-processing of the data and how frequencies can be found is presented;

Chapter 6 – Structural analysis: Modelling: it is a description of the process of building the model of the Church with the assumptions made;

Chapter 7 – Analyses and Calibration of the model: it includes the process of calibration of the material parameters and the results obtained during the analyses performed;

Chapter 8 – Conclusions and future works: here what can be done in the future with all the information gathered on the Church can be found.

¹ Dipartimento di Ingegneria Civile, Edile ed Ambientale – Università degli Studi di Padova.

2 INVESTIGATION: STATE OF THE ART

The importance given to Historical Buildings has always played an important role in many fields. The fact that these buildings have been seen as a living memory of past cultures led to a continuous discussion on what can be good and what can harm not only the structure but also what they may have inside. Moreover, dramatic events together with time and lack of maintenance cause degradation of these structures, which may lead to their collapse. For these reasons, one of the most important things that has to be pursued when dealing with Historical Construction is the preservation of the buildings through their conservation.

The conservation and protection of Historical Buildings is a multi-disciplinary topic that gathers expertise from history, social sciences, architecture, engineering, archaeology, economy, and politics and so on. Italy is one of the most advanced countries for what regards this subject, in particular when dealing with protection of these structures from natural disasters such as earthquakes. This is mainly due to the large number of earthquakes that occurred in the last few years in the central part of the Country.

One of the most important seismic sequences (in terms of research) took place in 1997 in the regions of Umbria and Marche. Starting from then, researchers began to look at the “seismic vulnerability” in a different way especially when referring to Historical Building and a new building code was developed. Researchers’ main observations are listed below:

- the retrofitting done in previous years was not adequate and a new philosophy has to be studied;
- old masonry building showed recurring patterns of collapse.

Generally, the reason for collapse has to deal with the lack of knowledge of the structure, regarding the materials used and construction techniques. This led to the choice of incompatible interventions and then to the possibility of damage and collapse during an earthquake.

Starting from 1997, it was possible to create a database of the typical and recurring layout of damage in Historical Monuments whatever they are Churches (Figure 2-1) or general buildings (Figure 2-2).

The new building codes try to give Engineers the proper tools to design the best reinforcement, however, the conservation of Historical Buildings is hard to regulate due to its multidisciplinary approach that includes social, historic, aesthetic, technical and economic aspects. Thus, when dealing with Historical Buildings, the process of structural assessment needs to follow an integrated knowledge-base procedure.

The evaluation of a Historical Building is not a simple task due to the complexity of the structure itself and its history. The structural analysis of a Monument requires several input data that can be obtained through a studied experimental investigation program. Figure 2-3 shows the information that can be collected with both in-situ and lab tests in order to define the capacity of the structure and then model

its behaviour. For each piece of information required, the corresponding investigation technique is described in Figure 2-4.

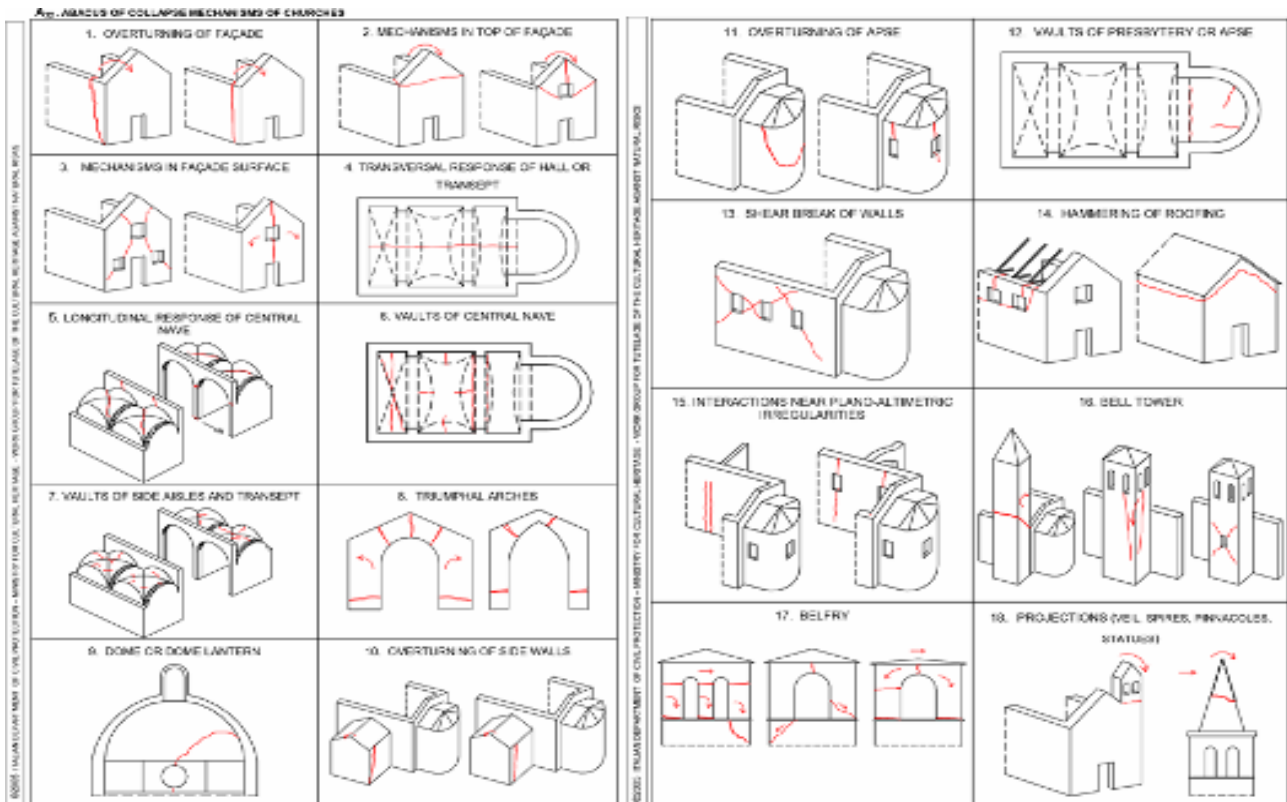


Figure 2-1: The most important crack pattern after earthquakes in churches (Linee Guida per la valutazione e riduzione del rischio sismico del patrimonio culturale (in Italian), 2010)

A	B1	B2	C	D	E	F
VERTICAL OVERTURNING	OVERTURNING WITH 1 SIDE WING	OVERTURNING WITH 2 SIDE WINGS	CORNER FAILURE	PARTIAL OVERTURNING	VERTICAL STRIP OVERTURNING	VERTICAL ARCH
			FURTHER PARTIAL FAILURES		ASSOCIATED FAILURES	
G	H	I	L	ROOF/FLOORS COLLAPSE	MASONRY FAILURE	
HORIZONTAL ARCH	IN PLANE FAILURE	VERTICAL ADDITION	GABLE OVERTURNING			
					Insufficient cohesion in the fabric	

Figure 2-2: Out of plane mechanisms for general buildings (D'Ayala & Speranza, 2002)

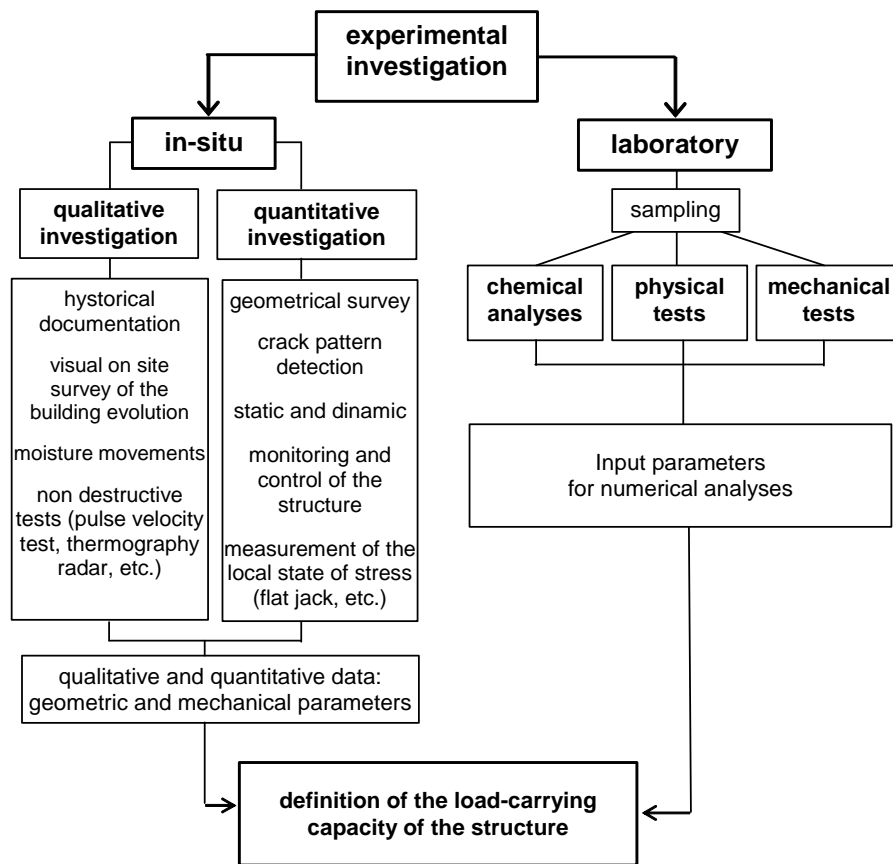


Figure 2-3: Experimental survey (Binda, Mirabella, & Abbaneo, 1994)

Before starting, the building under exam has to be included in one of the typologies listed below:

- Isolated buildings,
- Building in a row,
- Complex buildings,
- Towers,
- Palaces,
- Churches,
- Arenas.

This classification is the starting point for the investigation that must be carefully designed and optimized in order to obtain the desired results with the lowest cost.

The following sections describe the steps required during an experimental investigation, starting from the geometrical survey and the historical evolution of the building and arriving at the description of the most common on site tests that can be carried out.

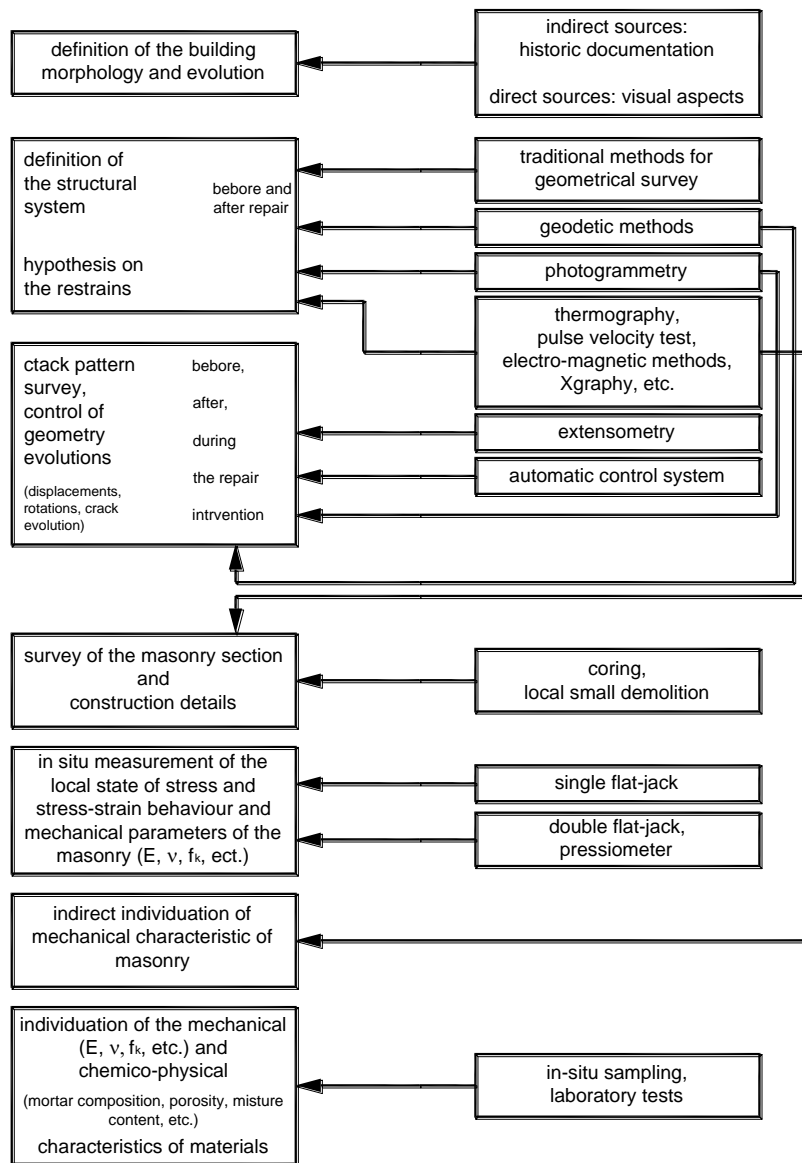


Figure 2-4: Information required and corresponding investigation (Binda, Saisi, & Tiraboschi, 2000)

2.1 Step 1: Historical Evolution

The first step is to study and analyse the history of the structure, paying particular attention to its evolution throughout time and gathering all existing data available on it.

The aim of the historical research is to identify the building process and the evolution of the structure with its change in use that lead to the current aspect. This means that the chronological succession of the construction of the building (or the aggregate) has to be known. This step also allows understanding which elements are the most vulnerable.

2.2 Step 2: Geometrical Survey

The following step is the geometrical survey, which must describe all the elements needed to represent the development in plan and height of the building (or aggregate). It should show the position and the thickness of the load-bearing walls at each floor and compare it among the different floors.

Starting from the geometrical survey, the structural model of the building will be developed, thus also information regarding the elevation of the Monument has to be recorded.

The most common tools to carry out the geometrical survey are:

- **Topographic survey**, which is not only the simplest but also the cheapest way;
- **Photogrammetry**, which can be aerial or from the ground. It is made through two cameras on a fixed support. Pictures are taken from a fixed distance. Then a software has to be used to postprocess results;
- **Laser scanning**, which is a powerful tool used to create 3D models of complex buildings and structures.

2.3 Step 3: Damage Survey

Another important step in experimental investigation is the damage survey of the structure. When looking at the crack pattern of the building, a preliminary understanding of the vulnerability is possible.

Chemical and biological decay of materials has also to be studied and recorded in maps. In fact these can be potential points of damage under seismic actions.

The damage survey importance increases in case of earthquakes (or any catastrophic event such as floods or fire) as it allows the understanding on how the structure behaved and thus it can be useful when designing proper interventions.

2.4 Step 4: On Site Investigation

It is important to plan on site investigation for a better knowledge of the structures. This can be done taking advantage of available Non Destructive Tests (NDT), Minor Destructive Tests (MDT) and Destructive Tests (DT) when allowed.

2.4.1 Non Destructive Tests - NDT

NDT can be used to obtain information regarding hidden dimensions like wall thickness that can vary internal spandrels or ribs, internal voids, foundation's condition, etc. Moreover they allow the

identification and the mapping of the damage such as cracks, voids, deterioration, and thus evaluating the masonry and other materials. They also allow checking the moisture content of the structure.

Several NDTs are described in the literature, here only the most used are briefly explained together with the information that they allow to collect and their pros and cons.

Thermovision

Thermographic analysis is a very common NDT method applied mostly to art works and monuments. It is used to identify irregularities hidden under plasters, renders, or frescoes. It can detect cavities and addition of different materials. Nevertheless, the penetration depth of this method is limited to the surface (Figure 2-5). For this reason it is not able to detect any hidden part inside the thickness of the masonry wall.

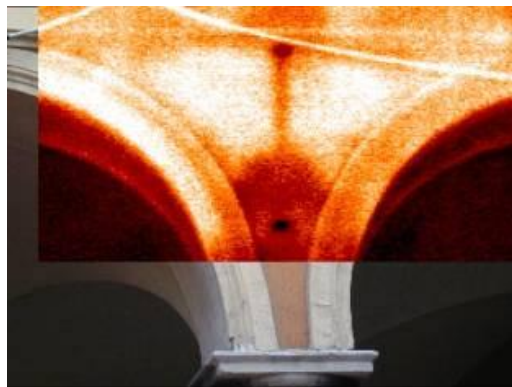


Figure 2-5: Thermovision: detection of a vertical rod behind the plaster, (Binda, Saisi, Zanzi, Gianinetto, & Roche, 2003b)

Moreover, it can be used to identify the presence of water, moisture and heating systems, as the content of moisture in walls can influence their mechanical properties. Moisture inside a structure can be stable or changeable. The latter is the most dangerous when dealing with Historical Buildings. But non-destructive tests can give relative or indirect moisture reading, thus calibration is required. Moisture content can be analysed with destructive method, which requires powder sample of the material.

Sonic Pulse Velocity

Sonic tests (together with Ultrasonic tests) are the most used Non Destructive Tests available. The test starts with the generation of a signal by a transmitter. This signal is then collected by a receiver and the time taken to cover the distance between them is recorded (Figure 2-6 left). The velocity of propagation depends on mechanical parameters of the structure, but a correlation between sonic parameters and mechanical characteristics of the material is still an open topic.

Three different layouts for the placement of the hammer (transmitter) and the receiver sensor are possible and are shown in Figure 2-6 (right).

The principal aims of this type of tests are to detect voids or cracks and check if the reparation through injection repair was done in a proper way. Moreover it allows the qualification of the morphology of the wall. The sonic transmission method records the propagation of waves on a spectrum between 500 Hz and 10 MHz through a material.

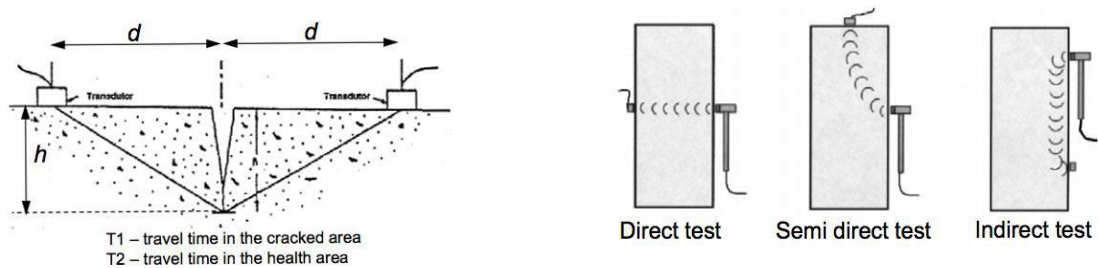


Figure 2-6: Sonic Test (left) and Possible layouts hammer-receiver (right)

Starting from the output data gathered from the sonic test, an image of the velocity distribution within the solid material can be obtained and a picture of the material's interior can be provided. This technique is called tomography and it was developed in medicine and used to reproduce the internal structure of an object from measurements collected on its external surface. This computational technique take advantage of an iterative method for processing a large quantity of data: its accuracy depends on several parameters such as the hammer-source (sonic or electromagnetic), the number and the position of measurements, the equipment settings, and the reconstruction algorithms.

Nevertheless, it is essential to stress out that the resolution capabilities of tomography are related to the diffraction phenomena, which is a limits related to the wavelength.

In Figure 5.20 shows an example of a sonic tomography done in the Church of St. Nicolò L'Arena in Catania.

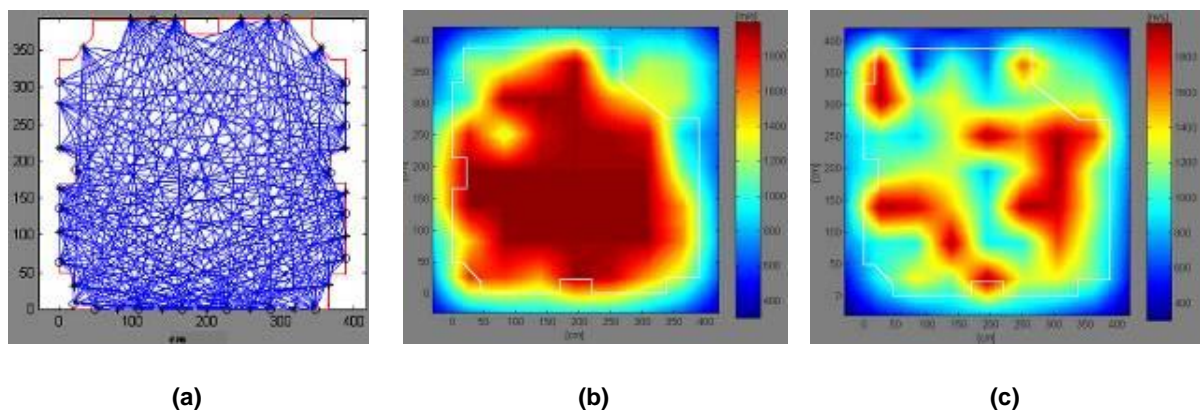


Figure 2-7: Sonic tomography of the hor. section of two pillars, (Binda, Saisi, & Zanzi, 2003)
(a) Testing points and directions. (b) Pillar 1 at 5.8m height. (c) Pillar 2 at 5.8m height.

Radar tests

Radar technique seems to be really promising in masonry investigation. Nevertheless, a lot has still to be done and the output given needs a technician to be read in a proper way.

The method is based on the use of radar pulses to image the subsurface and identify changes in the electrical properties of materials under the ground. It is a non-destructive test that detects objects, changes in material, and voids and cracks from the reflected signals.

When interpreting the output coming from a Radar test, there may be some problems related to multiple echoes due to layers and joints. Also the break-through effect² can hide partially the wall characteristics.

Also when dealing with Radar tests, the tomography technique can be applied.

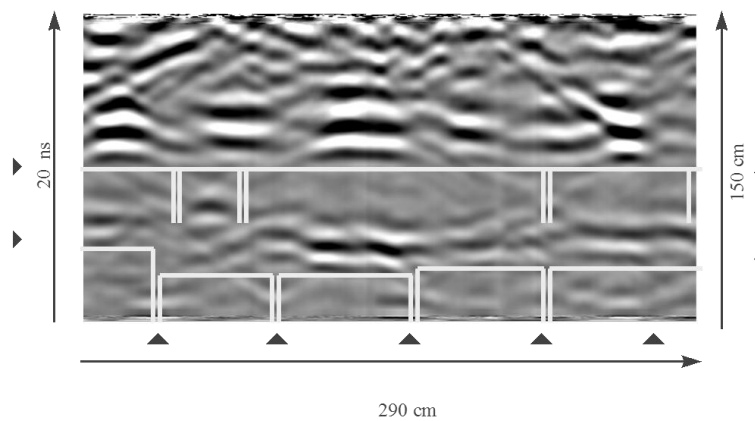


**Figure 2-8: Radargrams of the walls sections of Fontanella Church Bergamo, Italy.
(Binda, Saisi, & Tiraboschi, 2000)**

Pendulum Hammer Testing

The determination of the mechanical properties of masonry in Cultural Heritage building is a hard task. This is due to the fact that coring and the extraction of material is usually not allowed.

Compressive strength can be obtained through a superficial and non-destructive test: the Schmidt hammer. The hardness of the surface is measured by means of the rebound of a pendulum; the readings must be calibrated taking into account the type of material tested. Results are usually scattered but by using the average of a large number of readings a good approximation can be achieved.

² The break-through effect is caused by the reaction of the antenna with the waves transmitted.

The calibration equation that relates the rebound of the hammer with the compressive strength has to be known before, but it is usually found with a destructive test on the material.



Figure 2-9: Schmidt Hammer

2.4.2 Minor Destructive Tests - MDT

Single flat jack

The single flat jack test is used to assess the stress level of the masonry and detect the deformability of the material. The test is carried out by introducing a thin flat-jack into the mortar layer. When the test is completed, the flat-jack can be removed and the mortar layer restored to its original condition.

The single flat-jack tests are based on the following assumptions:

- the stress where the test is carried out is compressive;
- the masonry surrounding the slot is homogenous;
- the masonry deforms symmetrically around the slot;
- the state of stresses in the place of the measurement is uniform;
- the stress applied to the masonry by the flat-jack is uniform;
- the value of stresses (compared to compressive strength) allows the masonry to work in an elastic regime.

The single flat-jack test is based on the principle of partial stress release and involves the local elimination of stresses, followed by controlled stress compensation.

First of all, the reference field of displacements is determined by measuring the distances between the gauge's points fixed to the surface of the masonry. After that, a slot is cut, local stresses are released

and a thin flat jack is introduced into the slot. With the aid of this device, pressure (compressive stress) is applied to the masonry. This causes a partial restoration of the initial displacement field, which at some point reaches (approximately) the previously pressure values. (See Figure 2-10)

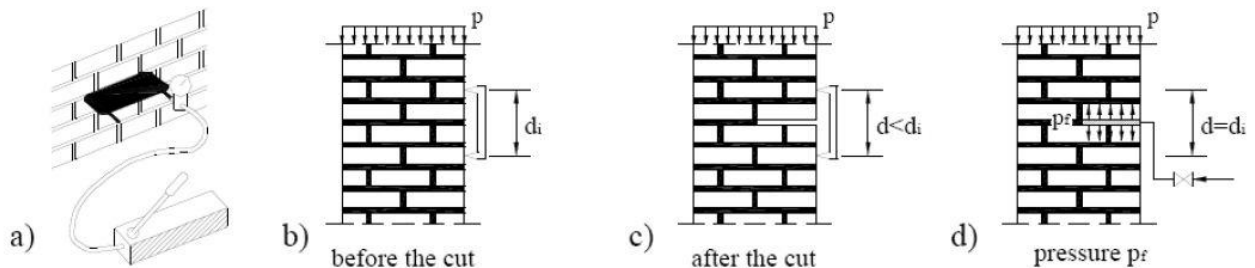


Figure 2-10: Single Flat jack test

The pressure level in the masonry wall is then given by:

$$\sigma_m = K_m \cdot K_a \cdot p$$

where K_m is the calibration factor ($0 < K_m < 1$), K_a is the ratio of the measured area of the flat-jack to the average measured area of the slot ($0 < K_a < 1$) and p is the flat-jack pressure.

It must be pointed out that the flat-jack test in the case of multiple-leaf walls gives results concerning only the outer leaf.

Double flat jack

The double flat-jack test is similar to a standard compressive test carried out in the laboratory. The difference is that it is performed in-situ and two flat-jacks are used to apply the load.

Two parallel slots are cut isolating part of the wall from the surrounding masonry forming a “specimen”. Masonry between the flat-jacks is assumed to be unstressed. Flat-jacks are then introduced into both slots, and the initial distances between gauge points are measured. Then, by gradually increasing the flat-jack pressure and measuring the deformation of the masonry between the flat-jacks, load-deformation (stress-strain) properties are obtained. Sometimes the maximum compressive strengths may be measured.

With low rise buildings (one or two story high) the level of stress resisting the pressure of the flat-jacks can be very low. When this happens, it's recommended to carry out a single flat-jack test in order to know the level of stress in the masonry and only after, a double-flat-jacks test can be done at a lower level of stress only to gather information about the elastic modulus.

The evaluation of the Young's modulus can be done in different ways. Following the ASTM standards (ASTM C 1197-91, 1991), two possible value of E can be evaluated, the tangent modulus ((1) and the secant modulus (2).

The tangent modulus is given by:

$$E_t = \frac{\delta\sigma_{mi}}{\delta\varepsilon_{mi}} \quad (1)$$

where $\delta\sigma_{mi}$ is the increment of the stress at each step of loading and $\delta\varepsilon_{mi}$ is the increment of strain at each step. This means that E is calculated following the loading curve.

The secant modulus is given by:

$$E_s = \frac{\delta\sigma_{mi}}{\delta\varepsilon_{mi}} \quad (2)$$

where $\delta\sigma_{mi}$ and $\delta\varepsilon_{mi}$ are respectively the value of stress and strain reached at step i . This second procedure becomes harder when a locking phase occurs. Another possibility to evaluate the secant modulus is to take advantage of the unloading phase, which is the elastic response of the masonry during unloading. (Figure 2-11)

Note that the evaluation of the Young's modulus with the double flat-jacks test is still under study and the formula used is a choice of the engineer.

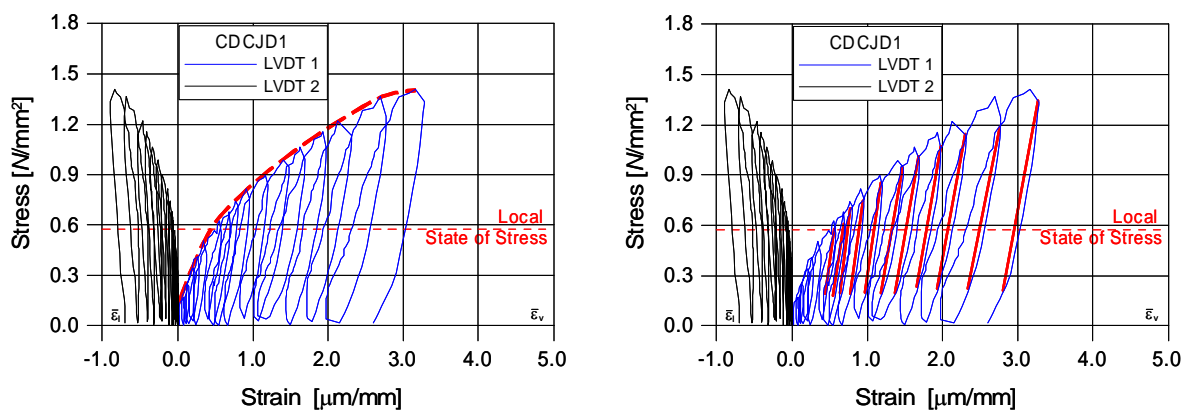


Figure 2-11: Calculation method of the tangent E modulus in the loading part (left) and of the secant E in the unloading (right). (Binda, Cantini, Saisi, & Tiraboschi, 2007)

Drilling energy and pull out tests

When destructive tests are allowed, the penetration tests can show the correlation between the depth of penetration and the material mechanical properties. But this correlation is impossible to determine with the real strength of ancient mortars and calibration tests are required. Furthermore the depth of penetration is little, thus only repointing mortars can be detected.

Finally the pull-out tests can be used on bricks and stones (and sometimes on mortar joints if they are thick enough) and it correlates the pull out force with the compressive strength.

Core drilling, boroscopy and videoboroscopy

Besides all the method of inspection already described, to understand the morphology of the specimen analysed, a direct inspection can be the solution. Sometimes it is enough to remove some bricks and look at the interior part of the wall, otherwise boreholes are needed. Through them, the morphology of the wall can be surveyed in an exhaustive way.

The core is usually performed with a rotary driller using a diamond cutting edge. Normally the specimens obtained from the borehole are without cohesion so it's impossible to check the quality of the material, however inside the hole; a boroscopy camera can help to see the interior of the wall. Even though the process looks easy, the interpretation of the images taken inside the hole is a hard task and asks for experience

2.5 Step 5: Laboratory tests

Laboratory tests are usually carried out when destructive tests are allowed and samples of the material can be collected and then used to study the mechanical, chemical and physical properties of the specimen. Sometimes optical and mineralogical analysis may be useful.

In order to represent statistically the situation of the existing masonry, the number of sampling has to be high. Usually, the information that can be gathered from laboratory tests concerns the chemical and physical composition of the existing mortars and checks the amount of salts. This can help when mortars and grouts are needed to repair the existing masonry.

2.6 Step 6: Structural control with monitoring

The last step in the inspection process is the possibility to install a monitoring system in the structure in order to evaluate its behaviour during the time and then design a proper intervention if needed. Two type of monitoring can be performed: static and dynamic.

The aim of the static monitoring is to characterize the variation of the crack opening, displacements, and tilting. Usually also temperature and humidity are recorded. Data are collected continuously in order to capture the slow changing of the parameters with time. More than one year period of time is required so that the influence of the temperature can be separated from what is the real structural behaviour.

Together with static monitoring is the dynamic monitoring. Its aim is to measure the variation of the behaviour of the structure when subjected to vibrations caused by wind or traffic. To avoid the

collection of too much data, a threshold can be set in order to activate the system only when inside the trigger is reached.

The dynamic monitoring allows the global analysis of the structure. This is really a powerful tool when dealing with Historical Constructions. The dynamic analysis it's an easy, sustainable, and non-destructive way of testing. Moreover it's the only way to study the global behaviour of the building. Starting from the dynamic identification, the modal shapes and the correspondent modal damping of a structure are collected. Then the analysis of the modal shapes is carried out and damaged areas are localized. Two criterions are mentioned here to analyse the modal shapes:

- the MAC criterion (where MAC stands for "Modal Assurance Criterion") measures the correspondence of two vectors of modal shapes. When the MAC value is equal to 1 the correlation is perfect, while when is equal to 0 no correlation is found;
- in the "Coordinate Modal Assurance Criterion" (COMAC), the correspondence between the modes is evaluated in a defined position. Thus the correlation is evaluated in a point for all the modes. Values of COMAC equal to 1 indicate a good agreement of the modal shapes in the chosen point.

3 MODELING: STATE OF THE ART

Masonry has been used as a building technique since ancient times, in all types of construction, from simple houses to big structures, like cathedrals, with a high cultural and social importance. However, only recently researchers have tried to divide the building technique from the rule of trial and error.

In literature it is possible to find different types of analysis methods and modelling strategies for masonry. The choice for one or another, first of all, is based on the objectives of the study. The selection should be done taking into account the information searched (serviceability, damage, collapse...), the accuracy required (local or global behaviour), the input data needed (information about material) and finally, costs (that include, also the time needed to complete the analysis).

Chronologically, after following the rules of thumb, designers started to apply the static graphic methods, which are very simple and fast to use. Later, limit analysis started being used and only recently, thanks also to the high capacity of computers, Finite Element Methods (FEM) started to be applied. But masonry can be modelled also with other methods such as the Structural Element Models (SEM) and the Discrete Element Method (DEM).

3.1 Rigid Block Analysis

Looking at the buildings that overcame an earthquake, it has been noted that generally if the structure did not collapse as whole, there are two types of failure modes. In particular:

- the **First Damage Mode** is caused by actions perpendicular to the wall and that starts an out of plane behaviour causing collapse;
- the **Second Damage Mode** occurs only when the First doesn't take place and causes cracks of the wind-brace walls.

These observations led Giuffrè and Carocci ((Giuffrè & Carocci, 1993) (Giuffrè, 1993)) to propose an innovative approach to study the vulnerability of masonry buildings under seismic action and based on the decomposition of the structure into a chain of rigid blocks. Then by applying the kinematic limit analysis, the collapse mechanism is studied.

The assumptions of this method include no tensile strength of the material and rigid behaviour until the establishment of the linkage. Then it is possible to evaluate a coefficient that represents the seismic masses multiplier characterizing the threshold of the equilibrium conditions for the considered element. The smaller the multiplier, the most probable is the failure of the element.

At the beginning, the principal aim of this method was to compare the vulnerability of different buildings in order to establish the priorities in the strengthening process. Recently different authors (among which Gambarotta and Lagomarsino are cited (Gambarotta & Lagomarsino, 1996)) suggest the combination of the aforementioned block analysis with the capacity spectrum method in order to

perform the seismic assessment of masonry structures. The method can be applied not only to regular buildings, but also to churches and non-regular monuments.

This approach was at the end included in the updated version of the Italian Seismic Code (Nuove Norme Tecniche per le Costruzioni, 2008) that now takes into account the high vulnerability of existing masonry buildings which do not satisfy any assumptions used for the design of new structures.

3.2 Structural Element Models (SEM)

Another technique described the building with structural elements such as column, piers, arches, vaults and walls. The material in this case is assumed to have a homogeneous behaviour.

3.2.1 Equivalent Strut

The equivalent strut approach considers deformations in the elastic range possibly followed by inelastic deformation. (Calderone, Marone, & Pagano, 1987)

Models which belong to this class may be bi-dimensional or mono-dimensional. Bi-dimensional approaches see masonry panels as equivalent elements with two main dimensions, while in a mono-dimensional approach, the masonry panel is divided into piers and lintels, regarded as equivalent struts. The connecting rod (strut) corresponds to the reactive part of the masonry panel, thus its inclination and its stiffness must reproduce the average behaviour of the wall (Figure 3-1). Each panel can be in crisis if the equilibrium is not respected or cracks occur.

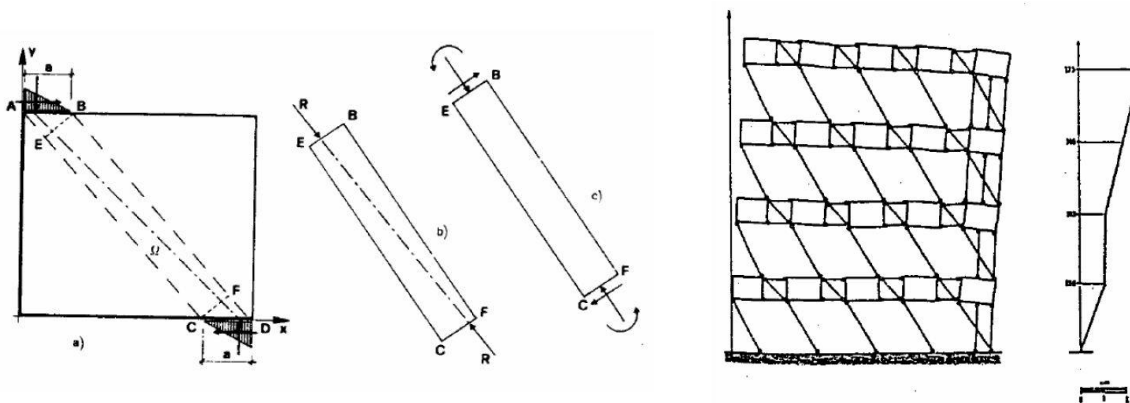


Figure 3-1: Modelling of a masonry panel (left) and a masonry building (right).

(Calderone, Marone, & Pagano, 1987)

3.2.2 POR method

The POR method was proposed in 1978 by Tomažević (Tomažević, 1978). The first aim of the method was to allow manual calculations in order to assess masonry structures. But its simplicity stresses out more than one disadvantage, such as:

- the only part where deformations and cracks can occur are the piers; other parts (lintels) are not considered places for possible damage;
- the only possible failure mode is the shear one with diagonal crack. There is no presence of rocking and sliding;
- floors are considered rigid.

Nevertheless, despite all the limitations mentioned before, the POR method has been greatly useful and it is still a fundamental reference for what concern the design of new buildings and the upgrading of old structures.

3.2.3 Macro-elements and Frame Models

When using the macro-elements approach, masonry panels are represented as a combination of structural elements (piers and lintels), Figure 3-2. Its advantage consists in the fact that it needs low computational efforts because of the reduction of the degrees of freedom, but on the other hand it gives a very rough description of the masonry elements. Usually this approach is chosen when the object of the analysis is the global behaviour of an entire structure (usually under cyclic loading).

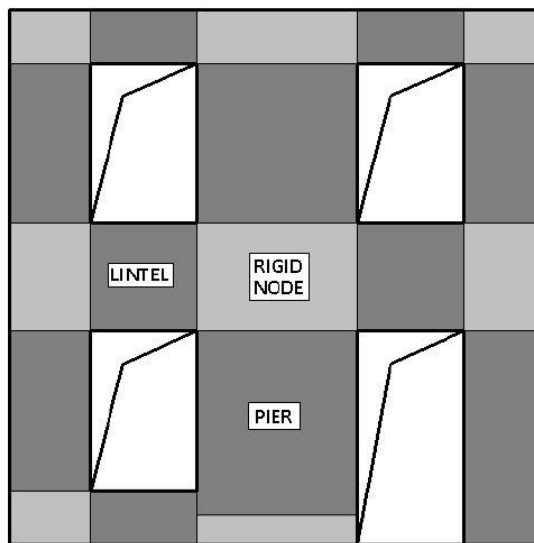


Figure 3-2: Macro elements approach

An example of macro-element is the model proposed by Gambarotta, Lagomarsino and Brencich (Gambarotta & Lagomarsino, 1997a) (Gambarotta & Lagomarsino, 1997b) (Brencich & Lagomarsino, 1998), which is able to catch both overturning and hysteretic mechanism. This approach has two degrees of freedom and was built for rectangular masonry panels. Also a nonlinear macro-element model was proposed. The macro-element is divided into three parts: the inferior and the superior part are where bending and axial effects are concentrate, while shear deformation take place only in the central part. The element static and kinematic behaviour is described with displacements, nodal rotations and resulting actions. It looks like a mono-dimensional method, but the introduction of an

internal degree of freedom gives to the element the ability to reproduce the behaviour of masonry under cyclic load. For this reason, besides the need of a calibration of the material parameters, the method was very useful in research field as in practical applications.

Another example is SAM, proposed by Magenes (Magenes, Bolognini, & Braggio, 2000). Its main aim was to analyse multi-storey walls with in-plane load and then it was improved for 3D problems. The macro-elements pier or lintel are connected by means of rigid nodes and their behaviour is linear elastic up to the strength limit (Figure 3-3). Moreover, lintels and piers are modelled as Timoshenko beam and the frame strength is determined with the minimum strength criterion. Then the displacement capacity of the frame depends on the expected failure mode. For this reason SAM is valid and reliable to perform the push-over analysis of walls in 3D problems.

Recently Casolo and Peña (Casolo & Peña, 2007) proposed a rigid body spring model (RBSM) able to simulate the behaviour of in-plane dynamic analysis of masonry walls. The springs are two for normal stresses and one for shear at each side. Specific separate hysteretic laws are assigned to the axial and shear deformation between elements. Shear spring and the vertical load are related through a Coulomb-like law. The approach gives good results also for the modelling of large masonry constructions.

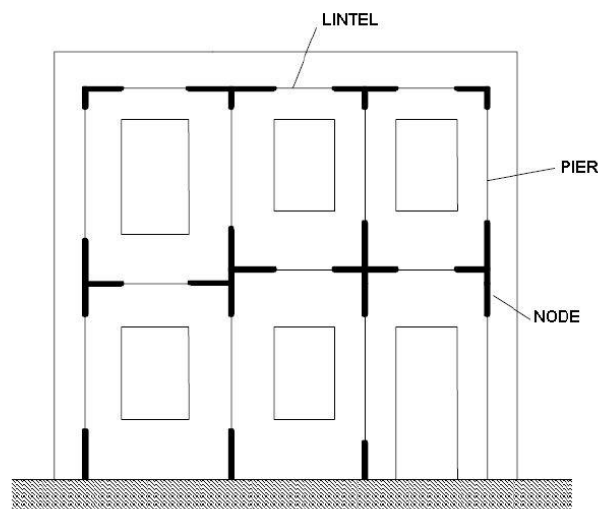


Figure 3-3: SAM method (Magenes, Bolognini, & Braggio, 2000)

3.3 Finite Element Methods (FEM)

The FEM solution is the most common and used among researchers. This class of methods offers a widespread variety of possibilities for the description of the structures made of masonry. Two main approaches are pursued: masonry can be modelled at a micro level (focusing on each component, units and mortar) or at a macro level (looking at the material as a composite).

The aforementioned strategies refer to different fields of application: micro-models are applicable when the object of the study is the local behaviour of the masonry, while macro-models are used when there must be a compromise between accuracy and efficiency. But, for both strategies the material needs to be described in detail through an experimental program on masonry specimens.

Figure 3-4 shows the three different ways of describing the material.

There are two different kinds of micro-model for masonry:

- Detailed micro-model, (among which (Silva, Costa, Guedes, Arêde, & Costa, 2008) is cited) where continuum elements are used to describe units and mortar and discontinuous elements are used to represent the unit-mortar interface. The behaviour of both units and mortar is taken into account and the interface is a plane of potential crack. This is the most accurate way for describing masonry behaviour, but requires a high computational effort.
- Simplified micro-modelling, where units are “expanded” and modelled with continuum elements, while joints and unit-mortar interface are concentrated in discontinuous elements. In this way, units are directly bounded by potential fracture planes, (Lourenço, 1996).

Both strategies have been developed for studying small elements with not homogeneous state of stress and strain. For this reason, input data comes from experimental laboratory tests on small samples.

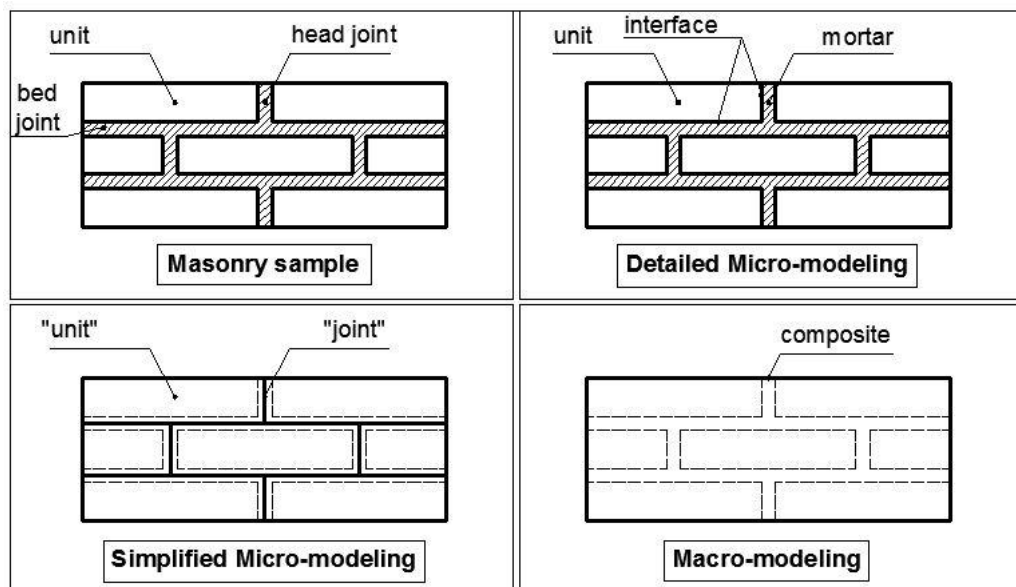


Figure 3-4: FEM modelling of Masonry (adapted from (Lourenço, 1996))

When using macro-modelling, everything (unit, mortar and their interface) is represented as a homogeneous anisotropic continuum. This approach is less computationally demanding and for this reason the most practice-oriented. Moreover with this approach meshes are simpler, since the internal structure of the masonry is not described, and may not reproduce the masonry pattern. Macro-models

are used when the purpose of the research is the seismic behaviour of old, complex, huge structures (i.e. bridges, cathedrals, historical buildings...).

The most used macro-model is the smeared crack scalar damage approach, where the damage in a given point is defined by a scalar value, which defines the level of degradation.

3.4 Discrete Element Methods (DEM)

Discrete Element Method is another good choice for modelling masonry. The method was originally applied to rock mechanics, but it was found very useful also for masonry modelling. DEM allows the simulation of cracks propagation and large displacement and rotation between blocks. This is possible because the method allows the elements to move more freely than in the FEM approaches. The technique then is able to recognize new contacts between blocks automatically as the calculation progresses. (Lemos, 2007)

The idea at the base of DEM is the idealization of the material as a discontinuum where joints are contact surfaces between different blocks.

3.5 Modelling of Historical Constructions

When dealing with Historical Constructions the modelling part can be really time consuming. The first step is to define which type of analysis is best taking into account the advantages and limitations of the available tools. It has to be clear that it is not true that the more complex the model is, the better the results are.

Other important points regard the choice of the element (shell or volumetric), the connection between the elements of the structure and the boundary conditions. Usually is good practice to validate the model with simple calculations in order to avoid mistakes.

Usually it is better to analyse the structure with different methods and compare results in order to increase the level of confidence in the results.

4 THE CHURCH OF ST. SILVESTRO

4.1 Introduction

The city of L'Aquila is the capital of the Abruzzo region located in the centre-east of the Italian Peninsula. Its name has been associated all over the world to the earthquake that struck the city on the 6th of April 2009 causing 309 deaths and damaging its Cultural Heritage. (Figure 4-1)

Among the Churches damaged by the earthquake it is the St. Silvestro Church that is going to be analysed in this thesis. This study is going to be included in the Niker Project³, along with other important Historical Buildings from all over the world. This project aims to mitigate the seismic risk in cultural heritage through the use of integrated methodologies.



Figure 4-1: The Italian Peninsula and L'Aquila

³ Niker: New Integrated Knowledge-based approaches to the protection of cultural heritage from Earthquake-induced Risk

4.2 History

The Church of St. Silvestro is located in the northern part of the historical city centre of L'Aquila (Figure 4-2). It was built against the city wall (dated back to 1316), a part of which was included in the Church as a lateral chapel at the end of the XVI century.



Figure 4-2: St. Silvestro

The story of St. Silvestro is a mix of legends, which make it difficult to identify facts regarding its constructive process and evolution. According to tradition, the Church was built during the XII-XIV centuries by the people of the Castle of Collebrincioni. Among the existing theories regarding the structure evolution throughout time, the one given by Orlando Antonini (Antonini, 1999) and simplified in Figure 4-3 appears as the most accurate. According to him, only the basement of the bell tower is from the XIII century (inclined lines in Figure 4-3) together with the Branconio's Chapel (squared in Figure 4-3) which was obtained from a part of the old city wall along which the church was placed. The central body of the church has been built after the 1315 earthquake when part of the church has been destroyed, while the façade and the apses were rebuilt after the 1349 earthquake.

Between 1967 and 1969, the architect Mario Moretti⁴ carried out some intervention on the Church. He added a reinforced concrete (RC) curb under the roof and some steel ties. After the 6th April 2009 shocks it has been possible to observe that he also closed some windows.

⁴ Mario Moretti, besides being an architect, was also the head of the office in charge of the supervision of the Cultural Heritage at that time.

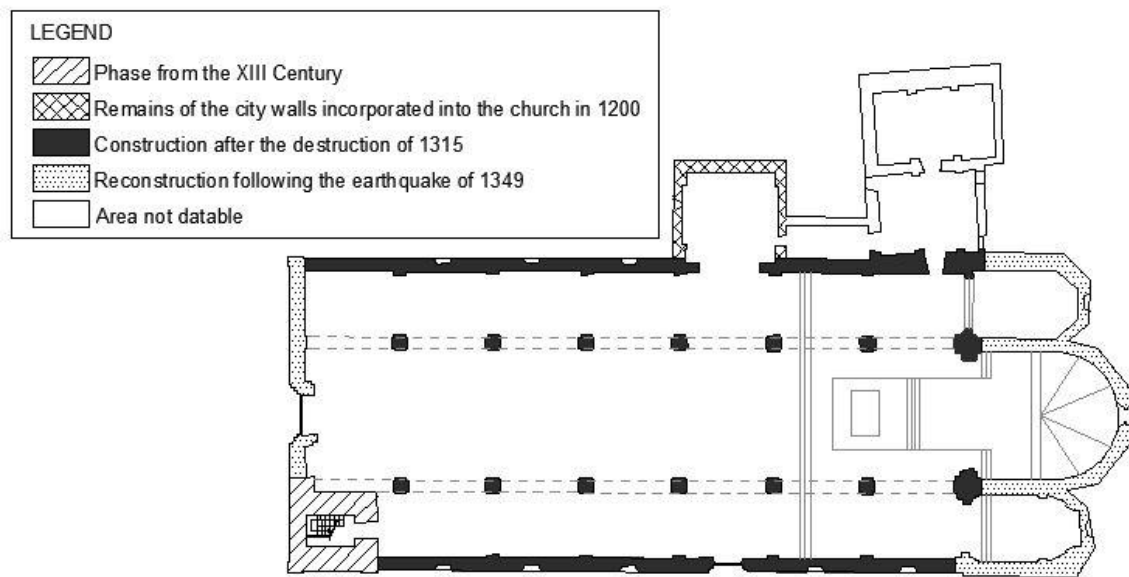


Figure 4-3: Building phases according to O. Antonini

4.3 Architectural and Structural description

The Church, as can be noted from the plan in Figure 4-3, has three naves: the central one is two times larger than to the side ones.

Looking at the organization of the space inside the church, it can be noted that the last two pillars have a different style: this can be due to the fact that the original project was supposed to include a transept that has never been built. Moreover, it is thought by looking to the structure of the other pillars that probably vaults were to be constructed, but for economic reason the project was changed to an easier and cheaper one. This is also confirmed by comparing St. Silvestro to the other churches in L'Aquila (like St. Giusta and the Basilica of Collemaggio). Besides that, the apses are vaulted, as well as the lateral chapel. Different views of the Church are shown in Figure 4-4 and Figure 4-5.

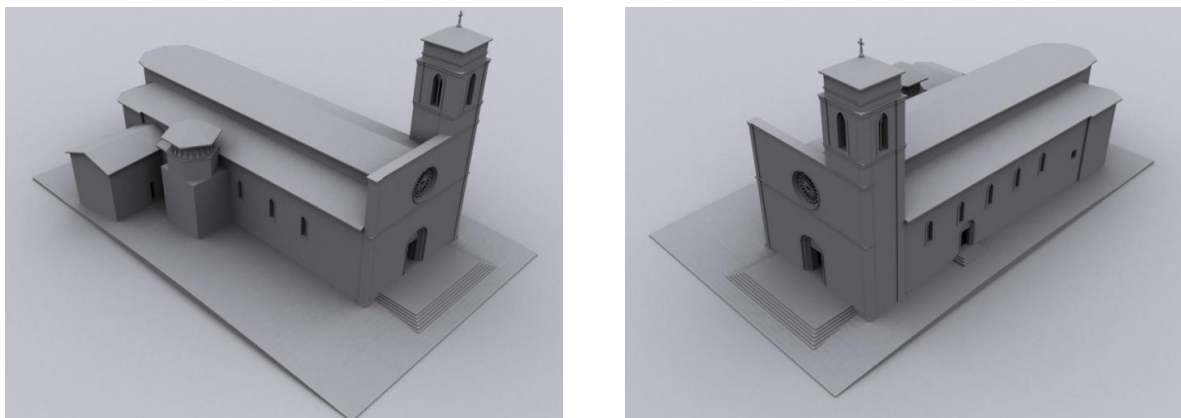


Figure 4-4: South-West (left) and South-East (right) views

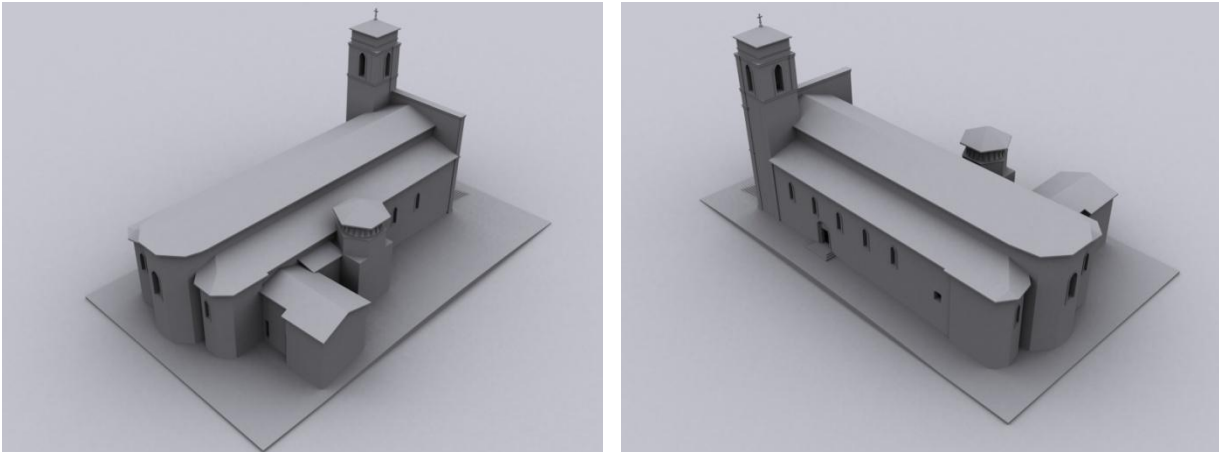


Figure 4-5: North-West (left) and North-East (right) views

Figure 4-6 shows the front façade of the building. It is characterized by a portal with the original timber doors dating back to 1539, but following the same style that can be observed in St. Giusta and St. Marco and coming from the XIV century. Just above the portal is the rose window: it is finely decorated and follows the gothic style, even if its central part seems to be from the XVI century.



Figure 4-6: St. Silvestro Façade

Just behind the façade is the bell tower, which makes the façade asymmetric. The basement is confirmed to be from the 1200 but the belfry was built more recently (but no information was found on the date of construction).

As said before, the Church of St. Silvestro has three naves. The naves are separated by two longitudinal walls characterized by pointed arches that run from the façade to the columns of the triumphal arches at the end of the Church.

The apses have a polygonal plan, similar to three semi-octagons. The central apse is almost twice in plan and height in comparison to the two lateral apses.

Along the West side is the Branconio's Chapel erected on the existing base of one of the tower's city walls, and the Sacristy.

The roof of the Church is composed of a wooden structure made of trusses along the nave and by two half-trusses along the aisles. The apses roof is characterized by vaults and the Chapel has a dome.

4.4 Materials

The central body of the Church is characterized by a type of masonry typical of this region and defined as the "apparecchio aquilano" (Figure 4-7). This type of masonry layout is built with pieces of limestone with squared section between 10 and 20cm. The "apparecchio aquilano" found in the church is different depending on when the structural elements have been built.

Other materials found in the Church are the RC curb (Figure 4-9) added in 1967 by Moretti and steel ties already described before.



Figure 4-7: The "apparecchio aquilano" layout of the east wall (left) and west wall (right)



Figure 4-8: Masonry in the interior part of the bell tower



Figure 4-9: The RC curb (Borri, et al., 2010)

4.5 Damage after the 6.4.2009 earthquake

Starting from December 2008, the Abruzzo region had been affected by a series of earthquakes. The main shock occurred during the night of the 6th of April 2009 at 3.32 am (local time). This principal shock was rated 5.8 on the Richter scale and 6.3 on the moment magnitude scale. Other seismic events rated more than 5 on the Richter scale were recorded in the days after, but the region underwent thousand of aftershocks. Figure 4-10 shows the seismic activity near L'Aquila up to the 15th of June 2009.

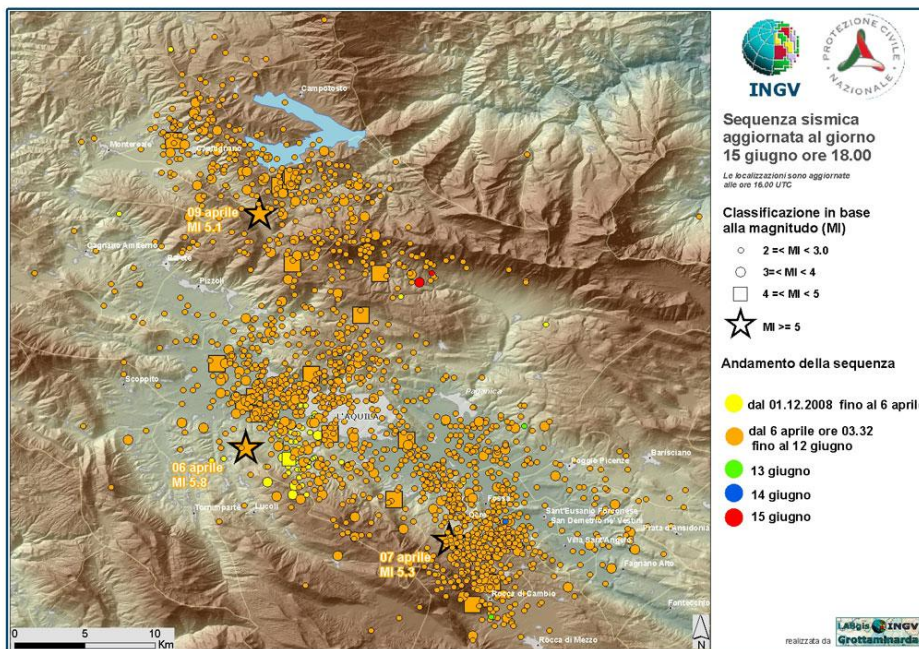


Figure 4-10: The seismic activity in L'Aquila (updated to 15th June 2009)

The epicentre of the main event (6th April 2009) was recorded near the city of L'Aquila which, together with the small town near it, was the most damaged. All the sequence of earthquakes was characterized by epicentres within the crust, between 10 and 12km depth.

Also the Church of St. Silvestro had been damaged but collapse was avoided thanks to the intervention carried out by Moretti between 1967 and 1969. Nevertheless the design looked unstable and both systems worked only partially.

For instance, the RC curb was designed to work only by friction, thus connection with the masonry of the lateral wall did not exist. Moreover it was not connected to the front façade; in this way the box behaviour was not guaranteed, so Moretti designed a steel tie in order to connect the façade to the rest of the structure, but the anchorage was done in the middle of the west side walls and this causes cracks starting from that point.

The collapsing mechanisms that took place in St. Silvestro are listed here:

1. overturning of the bell tower (Figure 4-13);
2. overturning of the all façade and part of it (Figure 4-14);
3. overturning of the side chapel (Figure 4-15);
4. overturning of the apses (Figure 4-16 and Figure 4-17)
5. shear cracks in the apses (Figure 4-16);
6. partial collapse of the roof (Figure 4-18)

Moreover inside the Church since the longitudinal wall is not connected to the bell tower, it was observed that this caused a hammering effect against the bell tower (Figure 4-19). (Borri, et al., 2010)

Figure 4-11 and Figure 4-12 show the main cracks in the bell tower, in the front façade and in the apse.

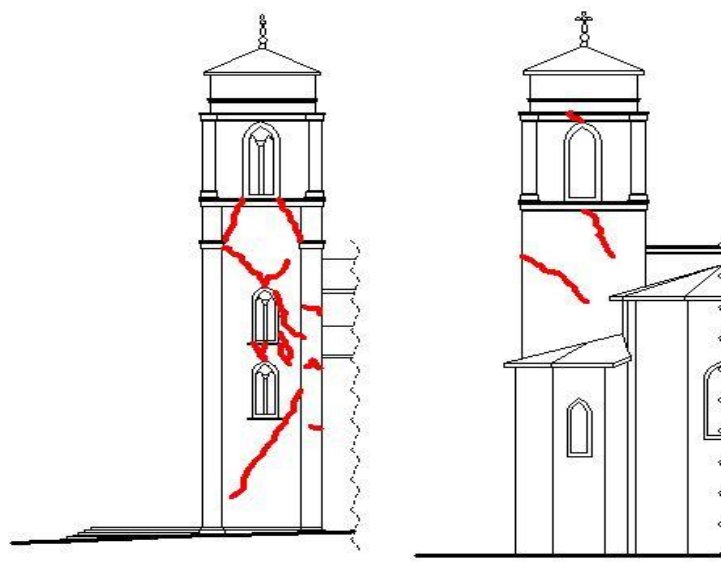


Figure 4-11: Bell tower: cracks on the North side (left) and East side (right)

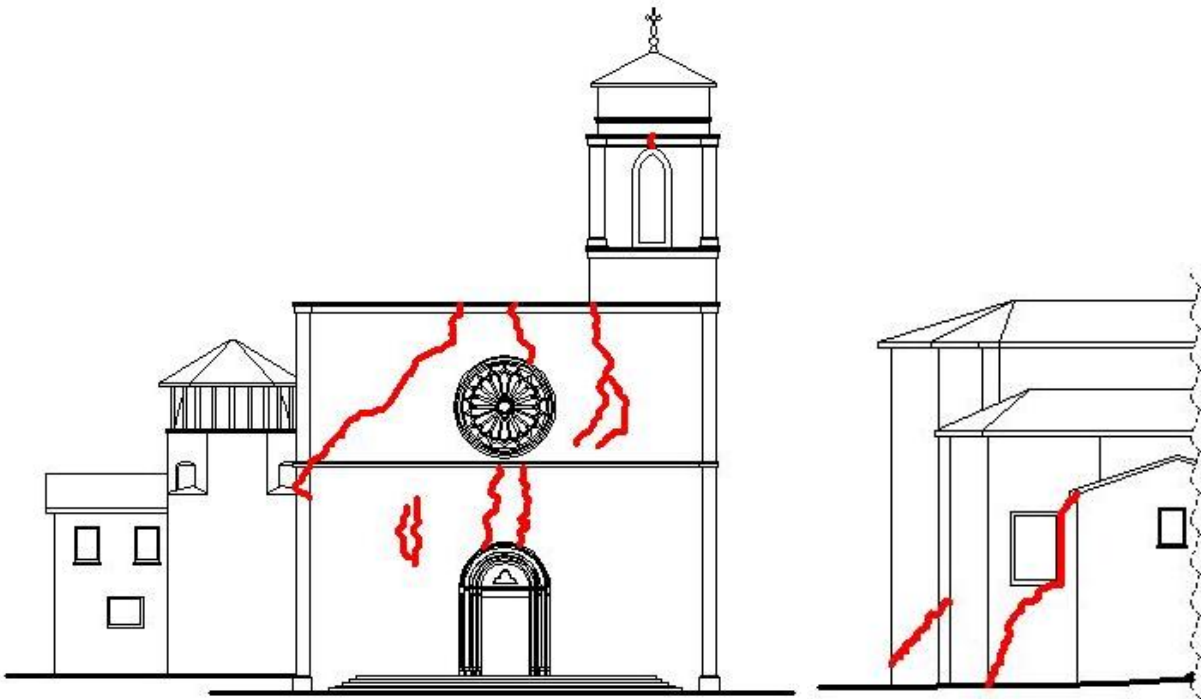


Figure 4-12: Cracks pattern on the front façade (left) and in the apse (right)



Figure 4-13: Overturning mechanisms of the bell tower (Borri, et al., 2010)

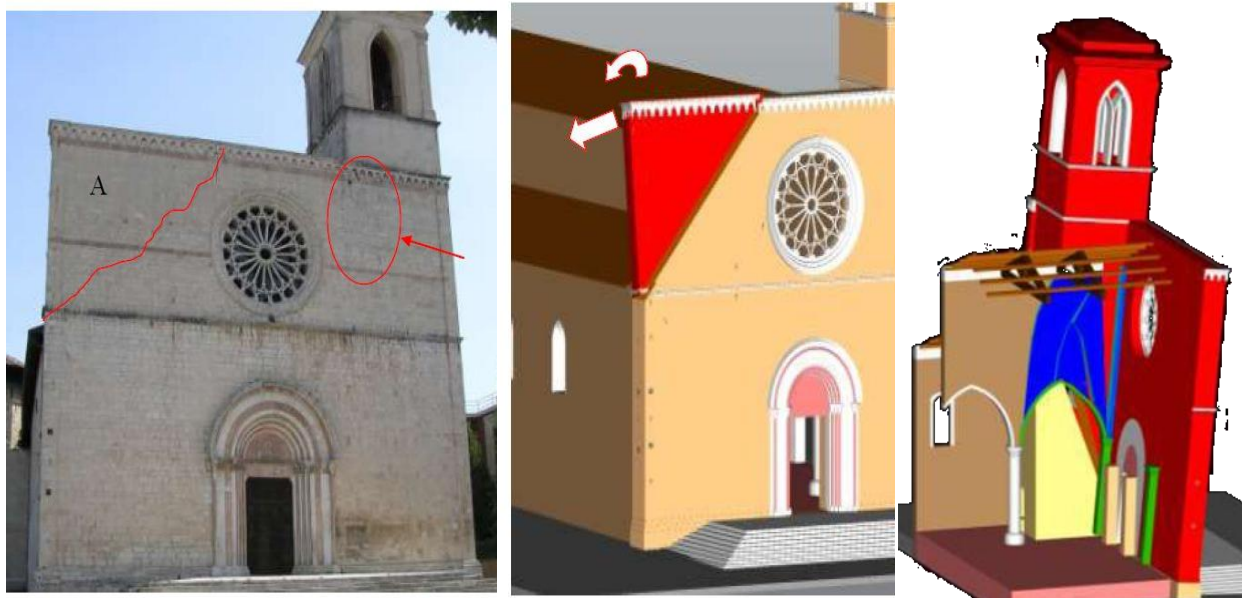


Figure 4-14: Overturning of the façade (Borri, et al., 2010)

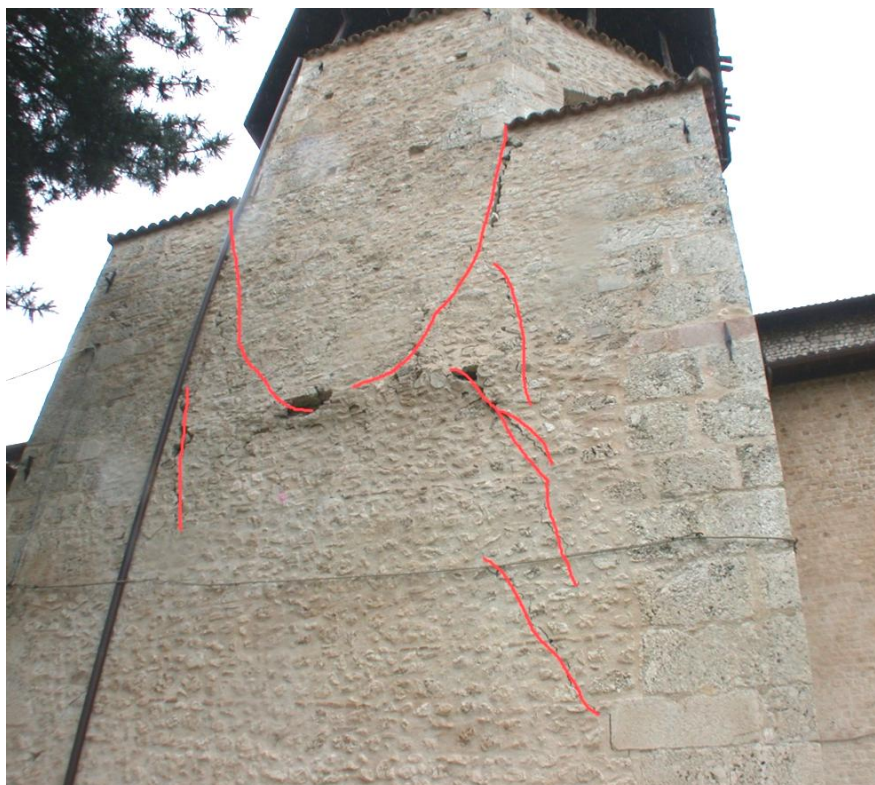


Figure 4-15: Cracks in Cappella Branconio

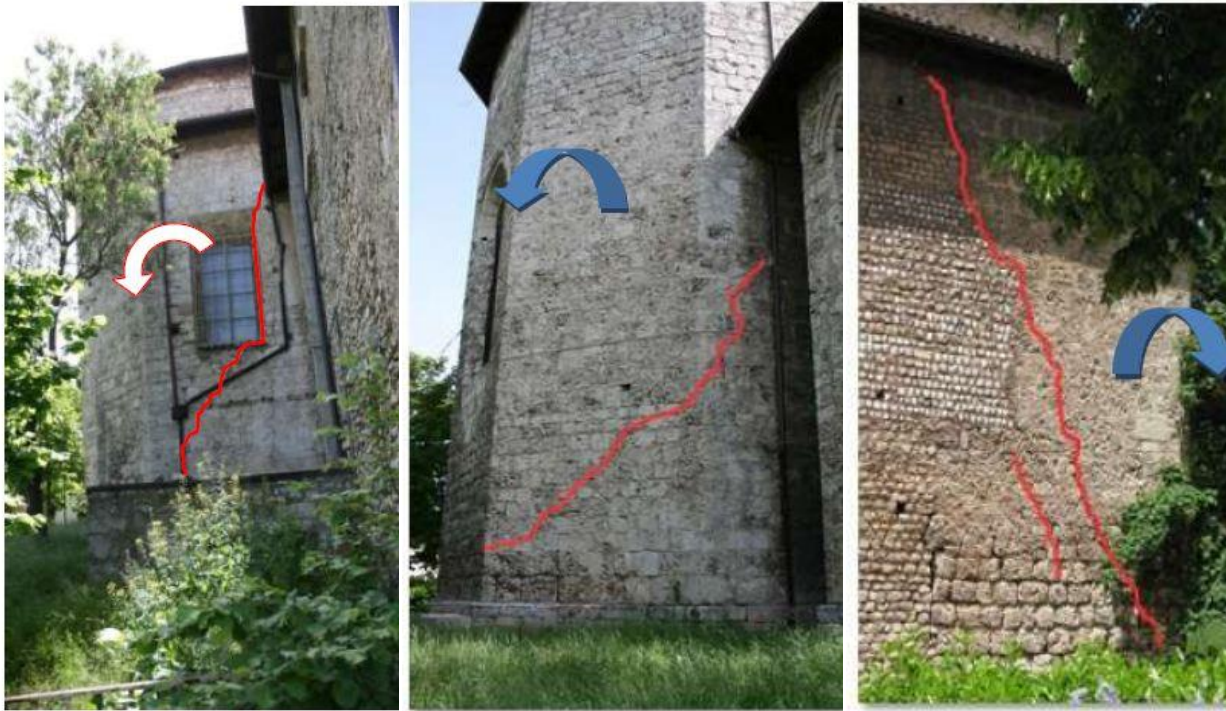


Figure 4-16: Overturning of the apses and shear cracks (Borri, et al., 2010)

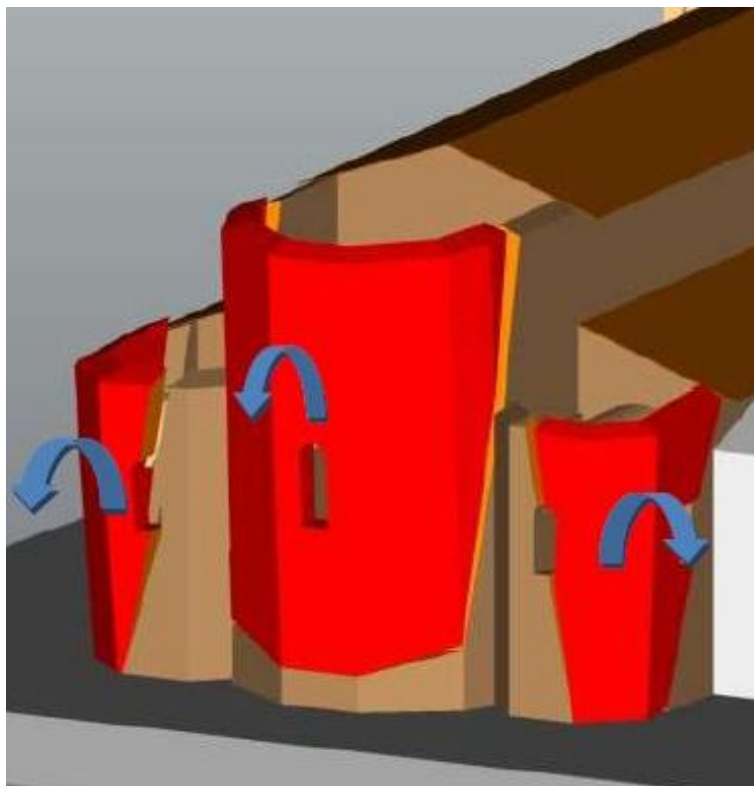


Figure 4-17: Graphic reproduction of the overturning in the apses (Borri, et al., 2010)



Figure 4-18: Roof collapse (Borri, et al., 2010)

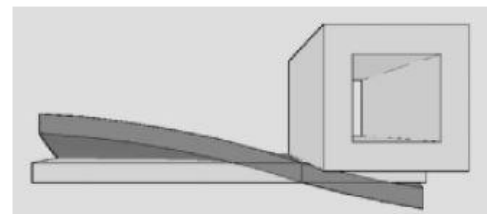
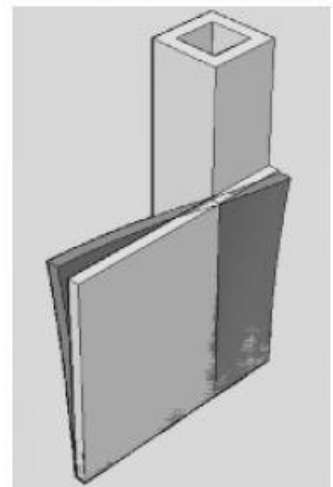


Figure 4-19: Hammering process and effects inside the Church (Borri, et al., 2010)

5 STRUCTURAL CONTROL: MONITORING

5.1 Introduction

The monitoring (static or dynamic) aims at the acquisition of data that can characterize the global behaviour of the structure. The data acquired may be acceleration, velocity or displacement of some interesting points of the structure. Records can be performed at regular intervals of time or can be activated at a level exceeding fixed threshold. In this case a continuous system has been installed.

The acquisition systems of St. Silvestro is composed of accelerometers for the acquisition of the structure's vibrations, displacement transducers, inclinometers and strain gauge, used to evaluate the damage variation. Also temperature and relative humidity are recorded.

The changing over time of all this data lead to the understanding of the global behaviour of the structure, which means that, it is possible to notice if any damage is developing after the earthquake.

Moreover when dealing with Historical Construction, the monitoring (static and dynamic) applied after an important event as the earthquake of the 6th of April 2009 is useful to:

- check the evolution of the damage;
- ensuring the security level when monitoring activity take place in the structure;
- check the effectiveness of interventions and provisional reinforcement;
- characterizing the dynamic response to the vibrations together with the environmental parameters (temperature, humidity);
- characterize the dynamic response in case of an earthquake.

In other words, the evaluation over time of the variables related to the structural behaviour of the building allows the characterization and the identification of the structural conditions with respect to the initial conditions.

The importance of monitoring in Cultural Heritage is also stress in the Italian Guidelines (Linee Guida per la valutazione e riduzione del rischio sismico del patrimonio culturale (in Italian), 2010).

The next paragraphs also describe the work of post-processing of data collected from the Church and carried out by Caccin and Fattoretto at the University of Padova for their Master thesis (Caccin, 2012), (Fattoretto, 2012).

5.2 The monitoring system in St. Silvestro

5.2.1 Static

In the bell tower of St. Silvestro a static monitoring system has been installed. The system counts 13 channels divided as follow:

- 2 tiltmeters to keep under control both the bell tower and the façade in X and Y direction (Channels: 1-2 and 8-9, Figure 5-1 (a));
- 7 displacement transducers put on the most severe cracks (Channels 3, 4, 5, 6, 10, 11, and 12, Figure 5-1 (b));
- 2 sensors for the temperatures of air and walls (Channels 7 and 13, Figure 5-1 (c))

The system acquires data and records the measurements every 30 minutes.

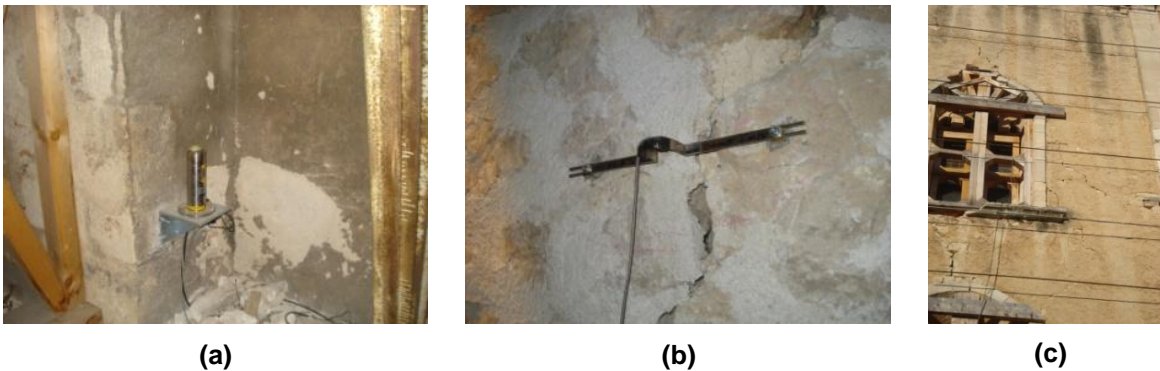


Figure 5-1: Tiltmeter (a), displacement transducer (b), and sensor for the temperature (Caccin, 2012)

Figure 5-2 and Figure 5-3 show the placement of the static monitoring system in the bell tower and façade.



Figure 5-2: Static monitoring at (starting from left): 2.5 m, 6.8 m, 8.6 m, and 26 m (Caccin, 2012)

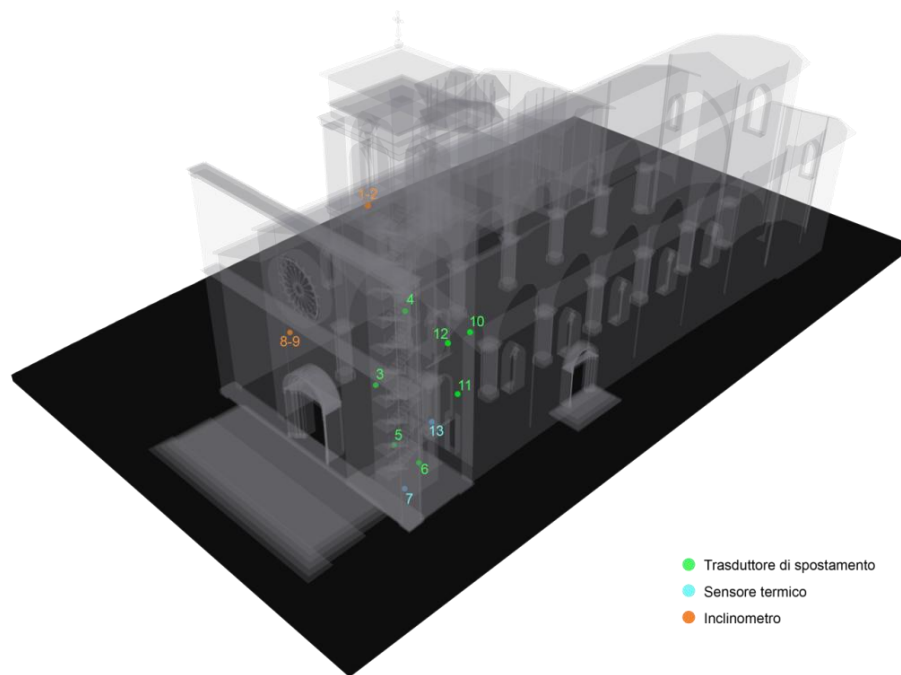


Figure 5-3: Static monitoring system (green: displacement, Ciano: temperature, orange: tiltmeter) (Caccin, 2012)

5.2.2 Dynamic

The dynamic monitoring system of St. Silvestro is composed of 8 high-sensitivity piezoelectric accelerometer (Figure 5-4) placed in the bell tower. These accelerometers are connected to the acquisition unit which sends the data through internet connection directly to the University of Padova.

Three reference sensors are fixed to the base of the bell tower to record the ground acceleration. Then two accelerometers are placed at a height of +14.50 m and three at + 26.00 m. Figure 5-5 shows disposition of the accelerometers, while Figure 5-6 gives a 3D view of the church and of the accelerometers.



Figure 5-4: The accelerometer in St. Silvestro (Fattoretto, 2012)

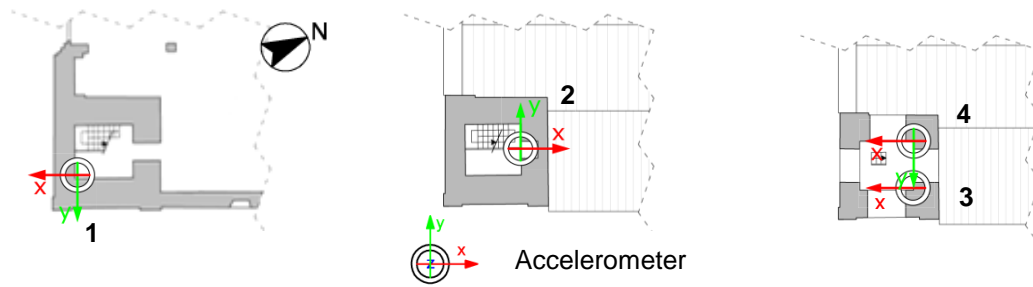


Figure 5-5: Dynamic monitoring system in the bell tower of St. Silvestro: ground level (left), +14.5m (centre), +26m (right)

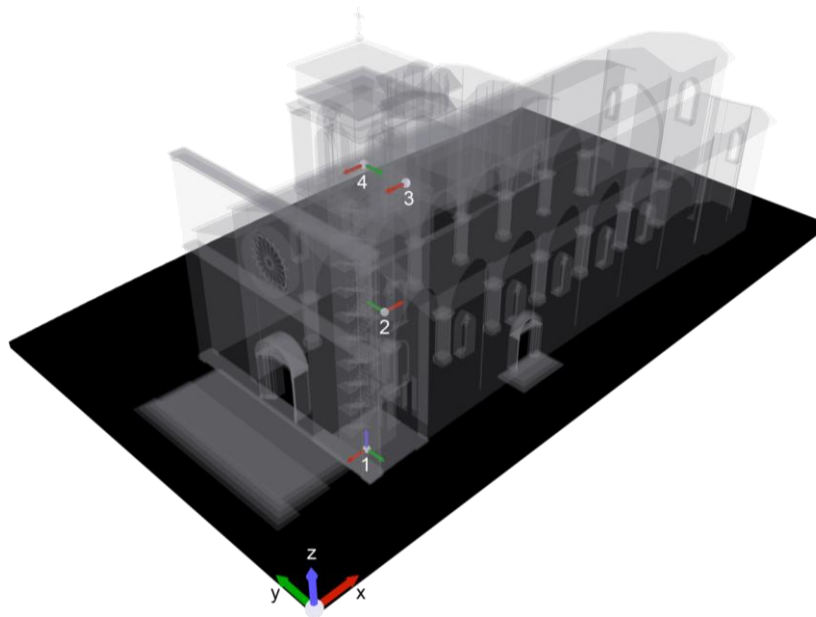


Figure 5-6: 3D view of St. Silvestro and the accelerometers (Fattoretto, 2012)

The accelerometers' location was decided after dynamic identification carried out before the installation of the system. The dynamic data are sampled at high frequency (80 samples per second) and the environmental vibrations are continuously recorded.

5.3 The static control

The data coming from static monitoring collected between the 23rd of July 2010 and the 5th of February 2012 have been analysed (Caccin, 2012). Crack openings and tilting data have been related to temperature, but it is not possible to clearly understand the behaviour of the structure as the acquisition was interrupted several times due to lack of electricity.

In Figure 5-7 the collected data are shown. Note that the opening of the crack corresponds to an increment of the value read from the system. The channel's layout is presented in Figure 5-3: channel's names correspond to the numbers in the figure.

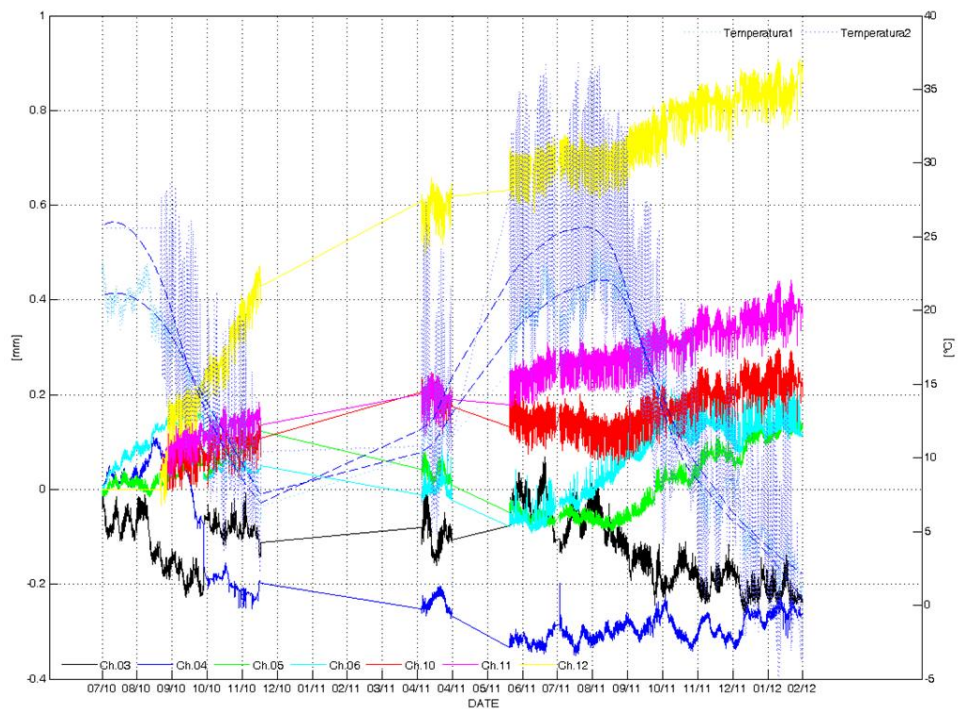


Figure 5-7: Cracks opening and time (dash lines are the temperature) (Caccin, 2012)

Looking at tiltmeters (Figure 5-8 and Figure 5-9), it can be noted that tilting is going with the temperature. This process can be direct or inverse, but in both cases shows something that is reversible and cyclic.

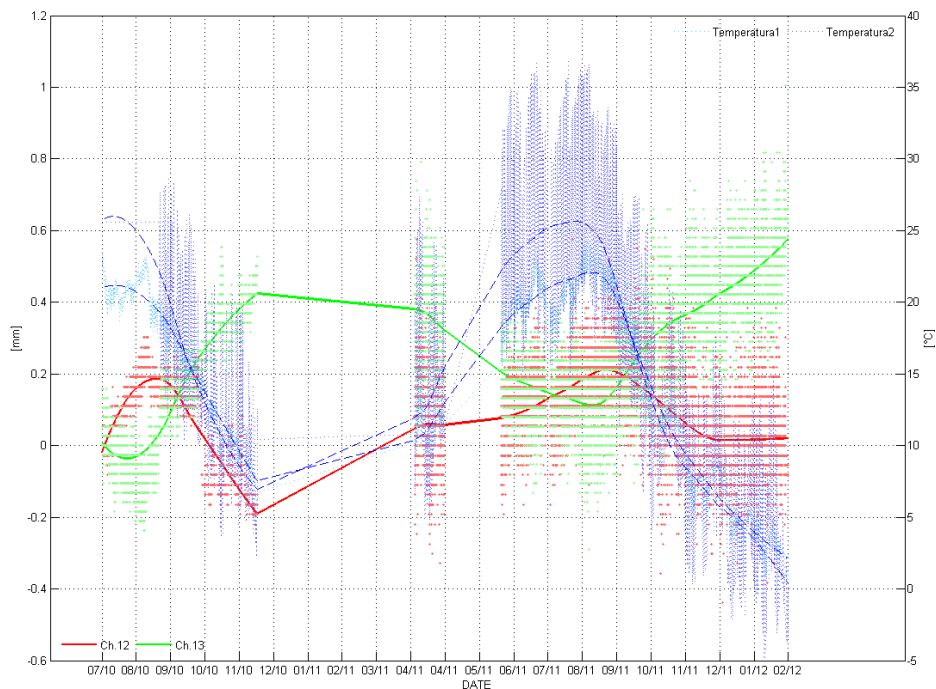


Figure 5-8: Tiltmeter data (red and green lines) (Caccin, 2012)

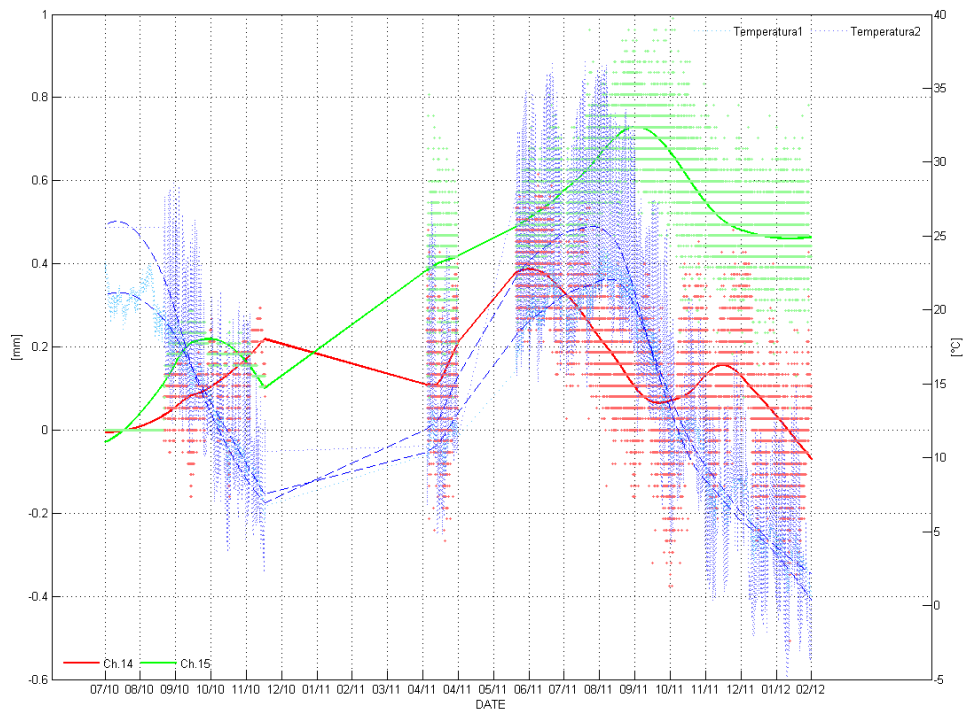


Figure 5-9: Tiltmeter data (red and green lines) (Caccin, 2012)

5.4 The dynamic identification

The dynamic identification of the Church was carried out during July 2010. To the already applied sensors used for monitoring, other sensors were applied. The layout is shown in Figure 5-10.

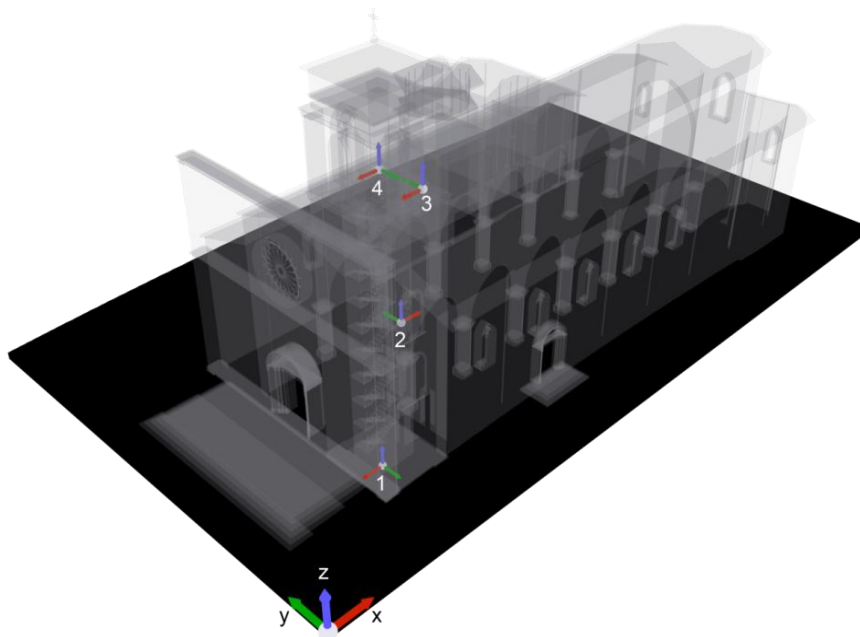


Figure 5-10: Sensors used for the dynamic identification of the structure (Fattoretto, 2012)

In order to find the natural frequencies and associated modal shapes of the bell tower, the Output-Only Identification Techniques were used. This group of techniques are based on random ambient vibrations with enough capacity to excite all the structure. This allows the measurement of the dynamic response of the structure. In particular, the excitation was the wind and the traffic. Two records have been acquired with 144'000 points each. The sampling frequency was equal to 80 SPS (samples per second), and the total duration of the record was 21'51".

The signal was then processed using two different software ARTeMIS Extractor 4.0 and MACEC 3.2. The methods used to get the modal parameters were the Frequency Domain Decomposition method (FDD), the Enhanced Frequency Domain Decomposition method (EFDD), and the poly-reference Least Squares Complex Frequency Domain method (pLSCF).

FDD and EFDD

FDD and EFDD methods belong to the Output-Only Identification Techniques. This means that the exciting input is unknown and only the output can be measured. With these techniques, the response of the structure includes the modal contributions of the ambient forces, the contribution of the structural system and the contribution of the noise signals from undesired sources

This class of technique assumes that the ambient vibration (which is the unknown excitation input) is a stationary Gaussian white noise stochastic process in the frequency range of interest. This means that its PSD (Power Density Function) is considered constant (C in the equation below) and the FRF (Frequency Response Function) $H_{(i,j)}(\omega)$ can be evaluated with equation (3).

$$|H_{(i,j)}(\omega)|^2 = \frac{S_{(i,j)}(\omega)}{C} \quad (3)$$

The FDD method evaluates the Singular Value Decomposition (SVD) of the response spectral density matrix, given by:

$$S_y(\omega_k) = \Psi_k A_k \Psi_k^H \quad (4)$$

where Ψ_k is a complex matrix where each column contains the mode shape vectors of each spectral peak and A_k is a diagonal matrix with the singular values, positive and real eigenvalues of the matrix $S_y(\omega_k)$.

The FDD is a simple method that is not able to evaluate with enough precision the modal frequencies of the system. This is due to the fact that the method is based on the Fast Fourier Transform (FFT) signal analysis. Difficulties usually arise when two close resonant frequencies exist. To increase the frequency resolution, very large time series can be used for the modal analysis.

Another way to increase the frequency resolution comes through an improvement of the FDD method: the Enhanced FDD. Both FDD and EFDD start with the Peak Picking technique which allows the identification of the frequencies of the system. But the EFDD evaluates the frequency values and damping coefficients with the application of the inverse Fourier transformation spectral density functions of each mode.

These two methods are implemented in the software ARTeMIS Extractor 4.0. The data acquired with a sampling rate of 80 SPS were processed using windows of 2048 points and an overlapping of 66.67%. In this way the main frequencies of the structure were found through the Peak Picking process which allows the identification of the singular values of the matrix of spectral density.

Figure 5-11 shows singularities of the spectral density matrix obtained with the method FDD. This method does not allow the evaluation of any damping of the structure; this possibility is given when using the EFDD.

Figure 5-12 shows the singularities of the spectral density matrix obtained with the method EFDD. This method is divided into two phases:

- The selection of the peaks with the Peak Picking method as for the analysis as FDD;
- The identification of the degrees of freedom of the spectral bells required for the estimation of frequency and damping (Figure 5-13).

Note that for both methods only the first three frequencies are shown (Table 3). These will be used later for the calibration of the material parameter of the bell tower (see Chapter 7 for more details).

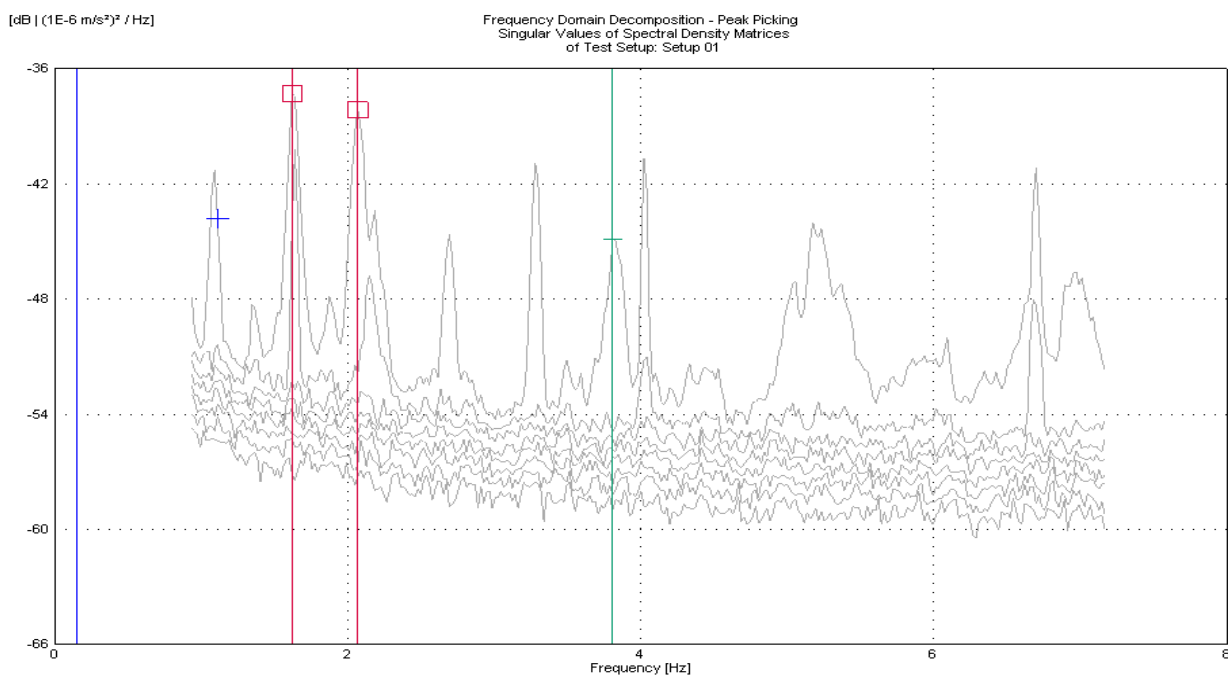


Figure 5-11: Singularities of the spectral density matrix (FDD)

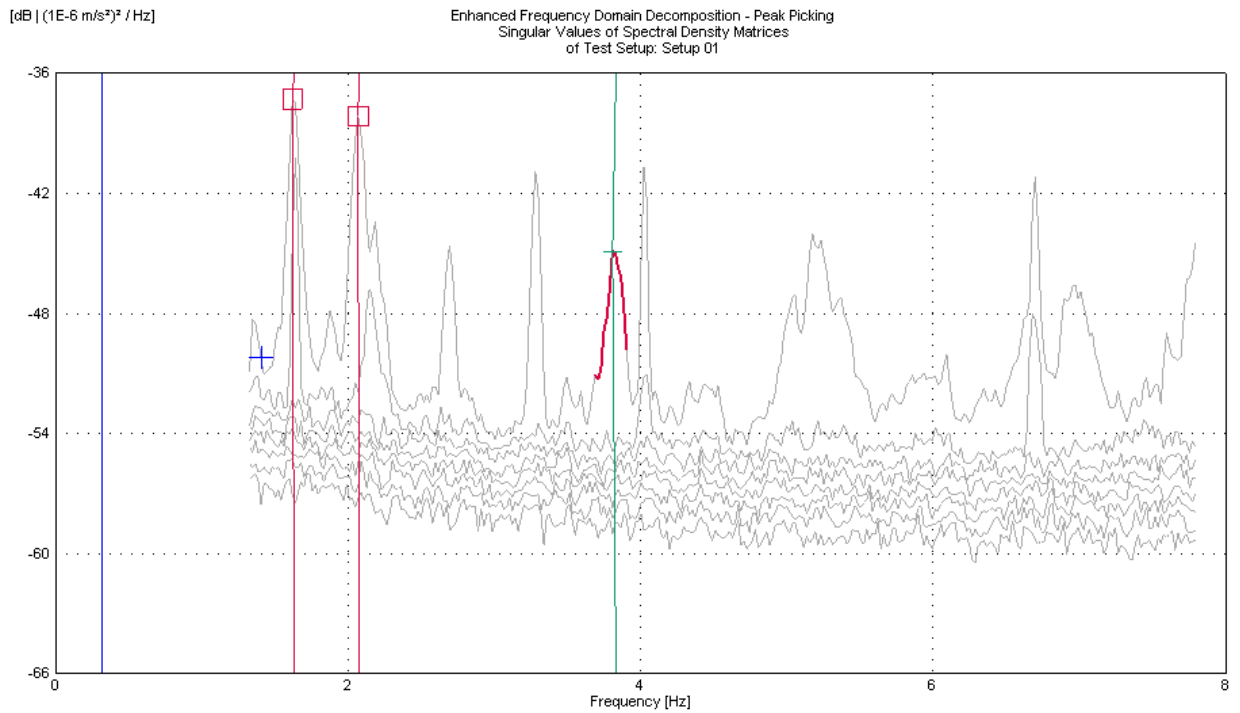


Figure 5-12: Singularities of the spectral density matrix (EFDD)

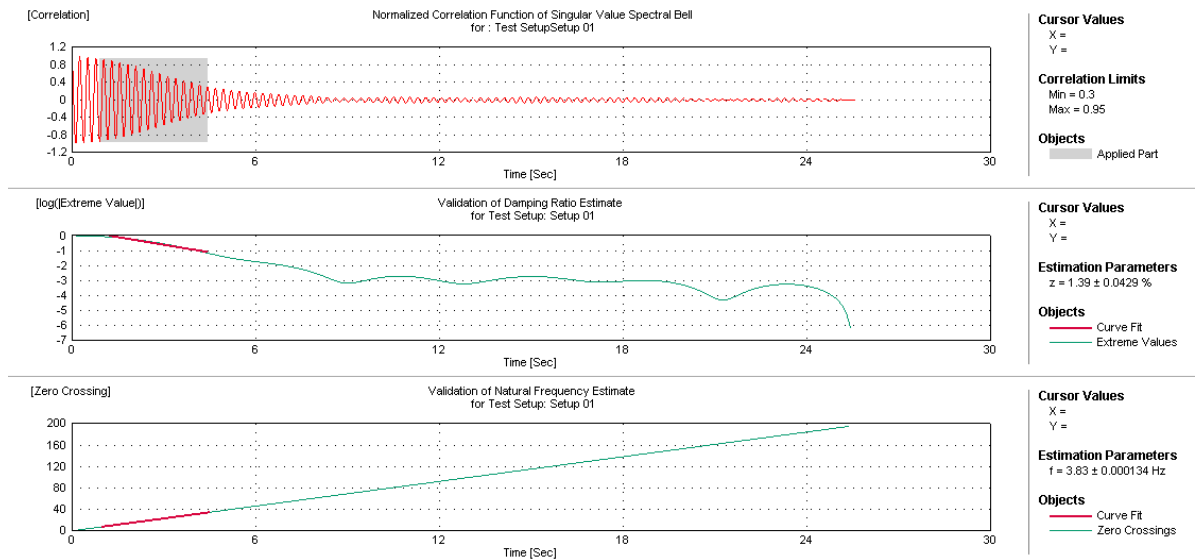
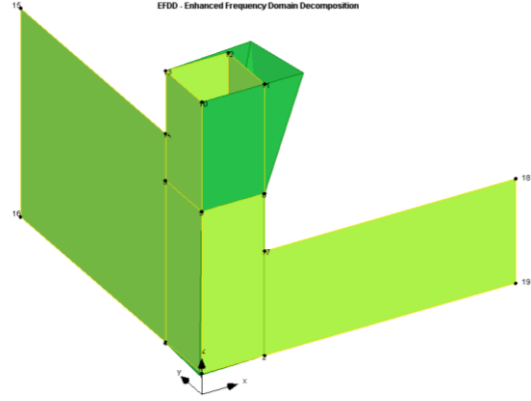
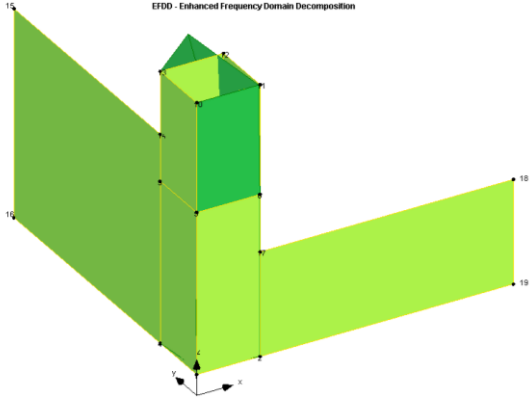
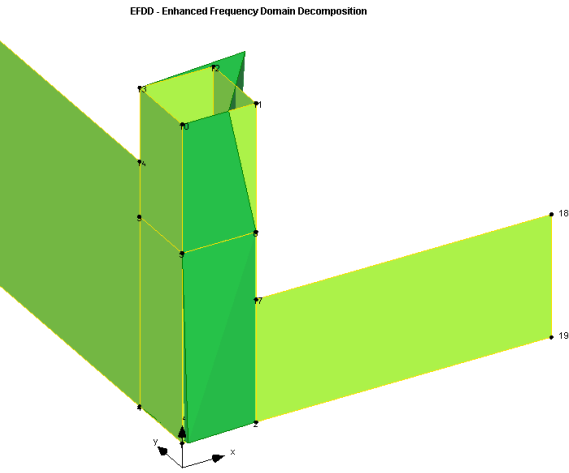
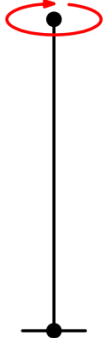


Figure 5-13: Modal estimation parameters

Table 1: Modal shapes of St. Silvestro (EFDD)

Mode and frequencies	Modal Shapes	Flexural shape
<p>I 1.632 Hz</p>		
<p>II 2.075 Hz</p>		
<p>III 3.833 Hz</p>		

pLSCF

The poly-reference Least Squares Complex Frequency Domain method is commercially known with the name PolyMAX. This method is really innovative and allows the estimation of the modal parameters through an easy process which makes straightforward the separation between fake and physical vibration modes. The physical modes usually result in a complex form which identify poles in the complex space: the pole's imaginary part relates to the resonance frequency and the real part to the damping (note that structural damping is typically a few percentage of the critical damping). The system's eigenvectors, expressed in the basis of the structural coordinates, correspond to the mode shapes.

The pLSCF algorithm is implemented in MACEC 3.2 which is a MATLAB toolbox developed at the Katolietet Universiteit of Leuven. MACEC is really powerful and provides broad functionalities for the visualization and processing of data, the identification, and finally the determination and visualization of the structure's modal parameters. In this case it was used only to extract eigenfrequencies, damping ratios, and mode shapes through the pLSCF method of the bell tower of S. Silvestro.

The first step in the analysis with MACEC is the input of the geometry of the structure. Then measured signal is converted into mcsignal so that they can be easily processed. Information about the position of the sensors and their orientation is also required.

Then the estimation of the matrix of Positive Power Spectral Densities (PSD+) is carried out. The windows are set of 2048 points. Once this procedure is concluded, the experimental determination of the modal parameters is the modal analysis of the identified system. A stabilization diagram (Figure 5-14) is calculated and from this diagram, the selection of the stable (thus, physical) modes is possible.

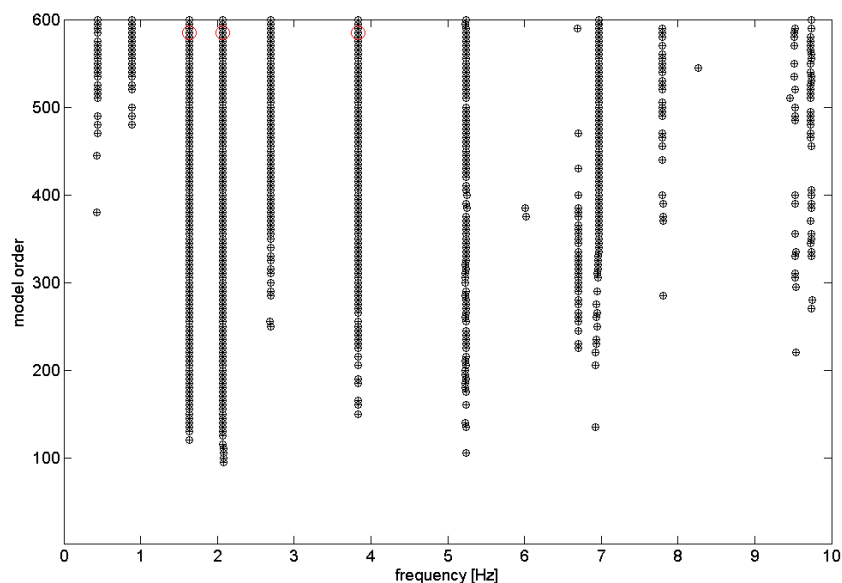


Figure 5-14: Stabilization diagram

Table 2 shows the modal shapes found with MACEC.

The program also allows the saving of the displacement of the nodes where the sensors are placed. This information will be used during the calibration process in order to get the MAC values of the modal shapes. (For a description of the MAC value evaluation see paragraph 0)

Table 2: Modal shapes of St. Silvestro (pLSCF)

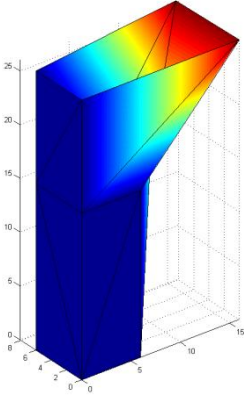
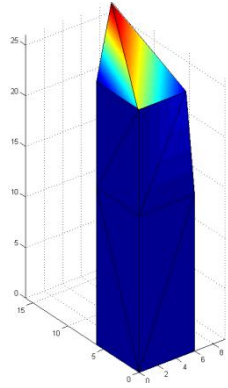
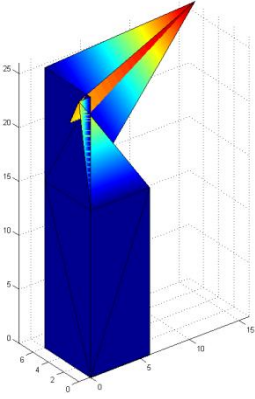
Mode and frequencies	Modal Shapes	Flexural shape
<p>I 1.6314 Hz</p>		
<p>II 2.069 Hz</p>		
<p>III 3.8318 Hz</p>		

Table 3 summarizes the frequencies obtained with the software used.

Table 3: Experimental frequencies from ARTeMIS and MACEC (data from July 2010)

	FDD	EFDD		pLSCF		Description
	Frequency [Hz]	Frequency [Hz]	Damping Ratio [%]	Frequency [Hz]	Damping Ratio [%]	
Mode 1	1.621	1.632	1.646	1.6314	1.3738	flexional north - south
Mode 2	2.07	2.075	1.641	2.069	1.4273	flexional east - west
Mode 3	3.809	3.833	1.394	3.8318	1.168	torsion

Also dynamic data collected between the 23rd of July 2010 and the 6th of February 2012 have been analysed, (Fattoretto, 2012). Data coming from the accelerometers allow a global evaluation of the structure with time and temperature. The relationship between acceleration and ambient parameters is asses through the evaluation of the modal frequencies, MAC values and damping. Figure 5-15, Figure 5-16, Figure 5-17, Figure 5-18, Figure 5-19, and Figure 5-20 show the relationship for each mode with time. Also the MAC value for each value is shown.

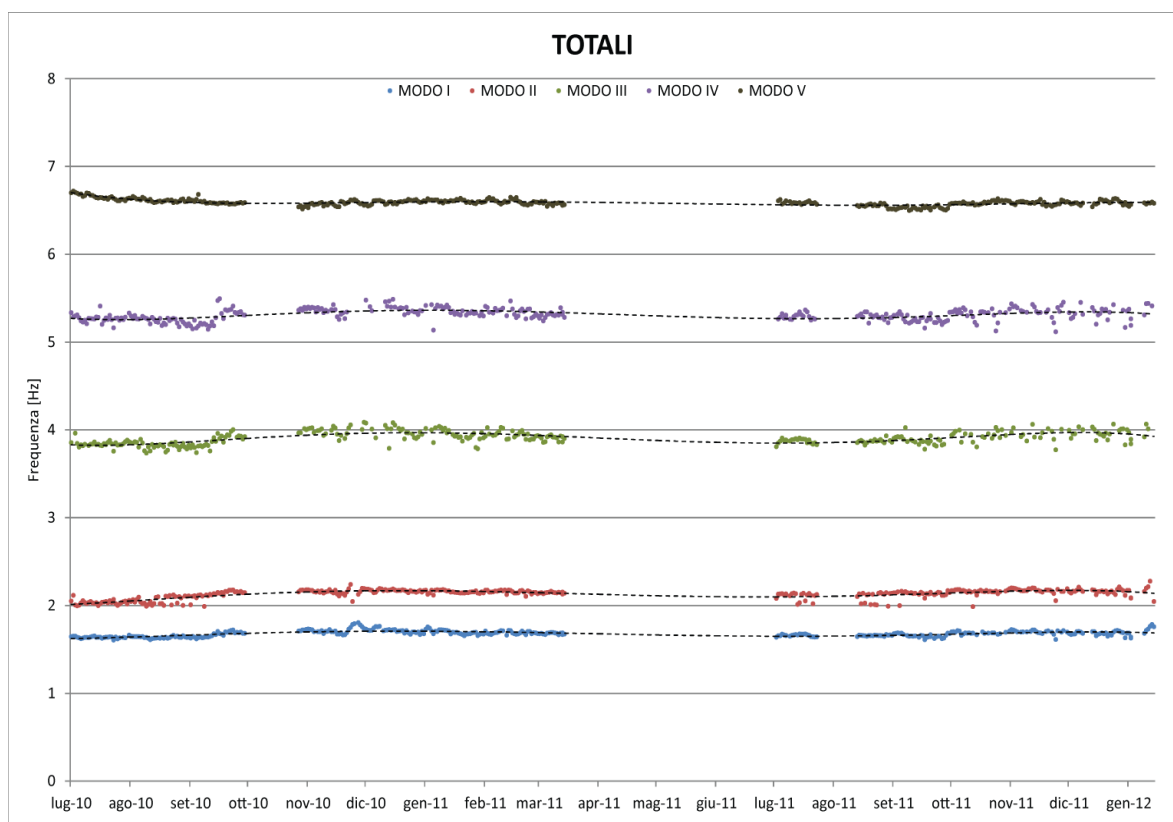


Figure 5-15: First five modal frequencies of St. Silvestro (Fattoretto, 2012)

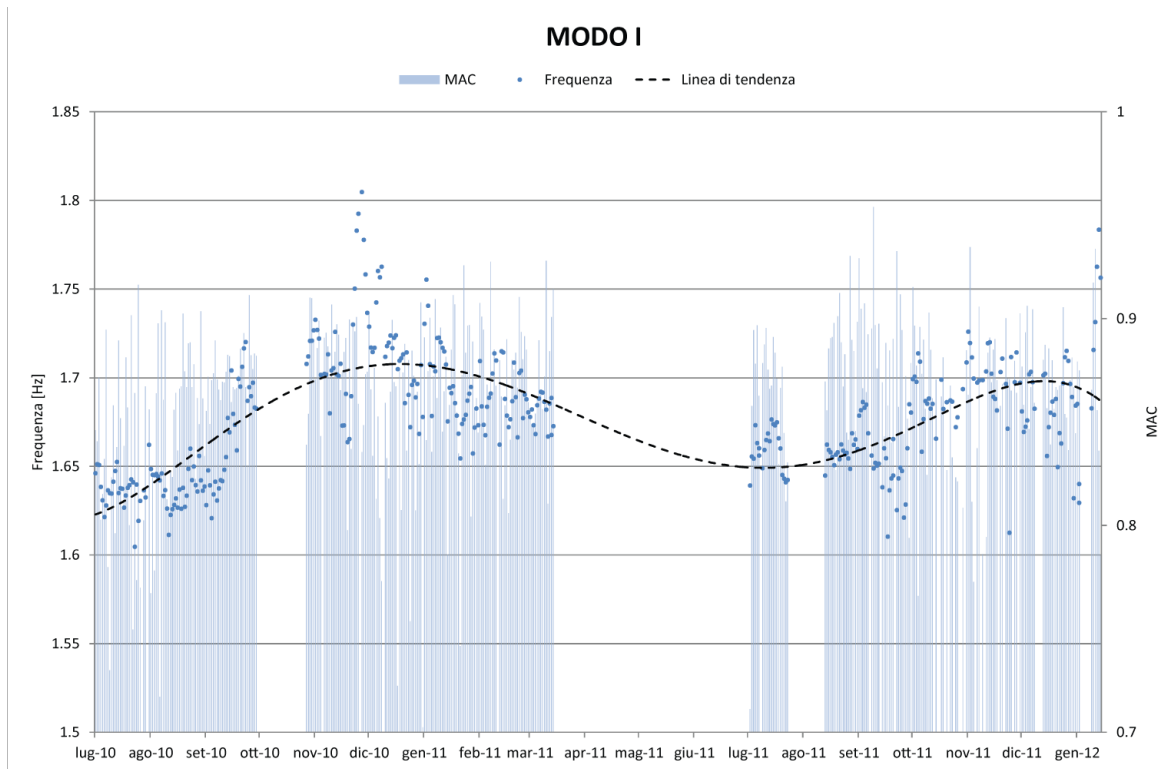


Figure 5-16: Modal frequencies and MAC value of the first mode (Fattoretto, 2012)

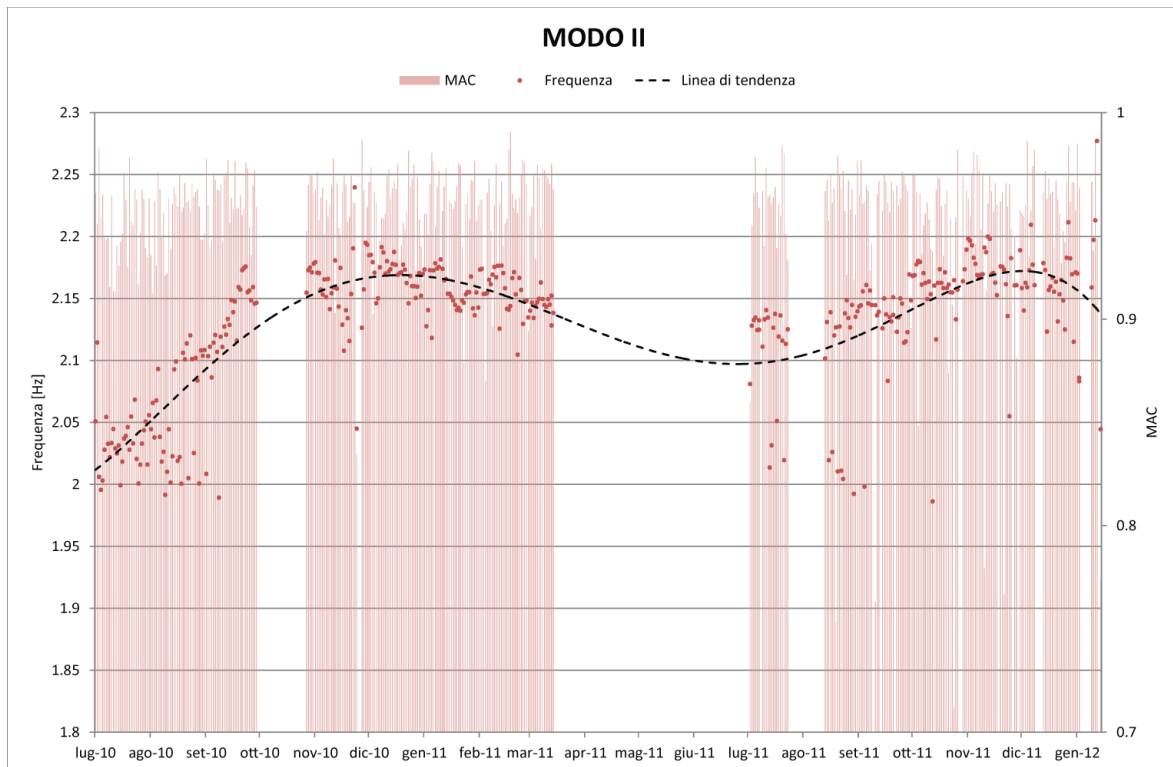


Figure 5-17: Modal frequencies and MAC value of the second mode (Fattoretto, 2012)

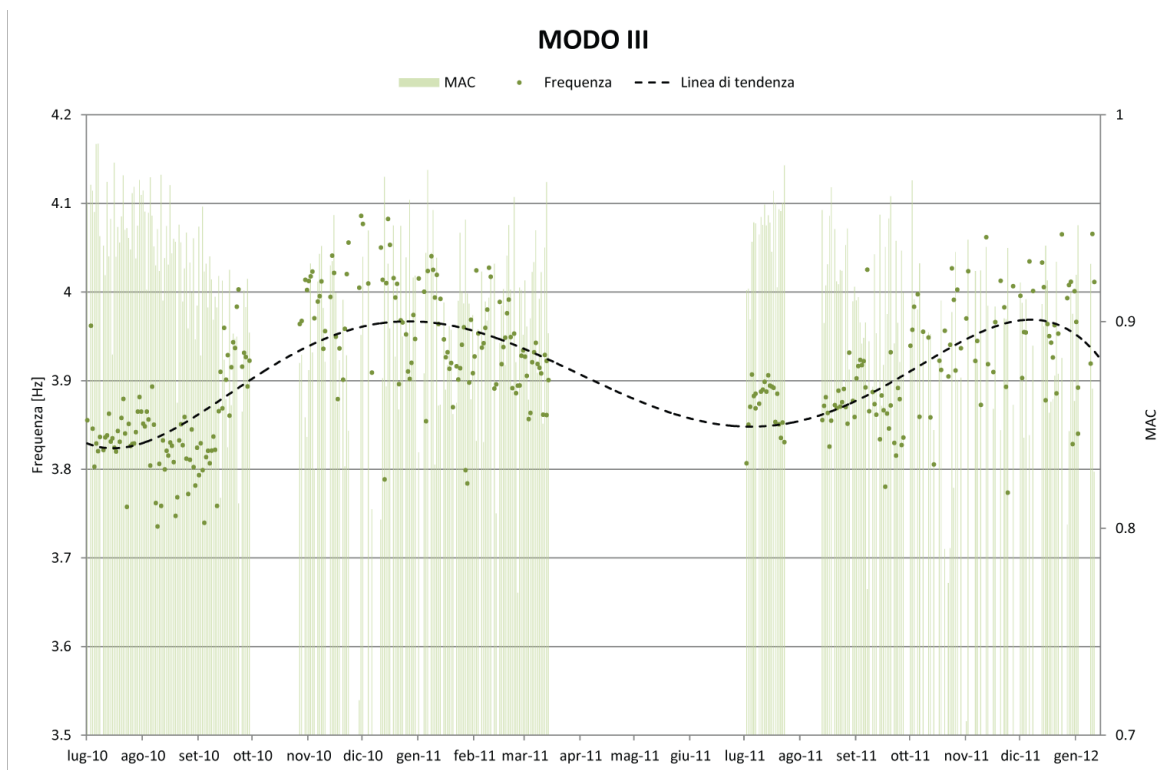


Figure 5-18: Modal frequencies and MAC value of the third mode (Fattoretto, 2012)

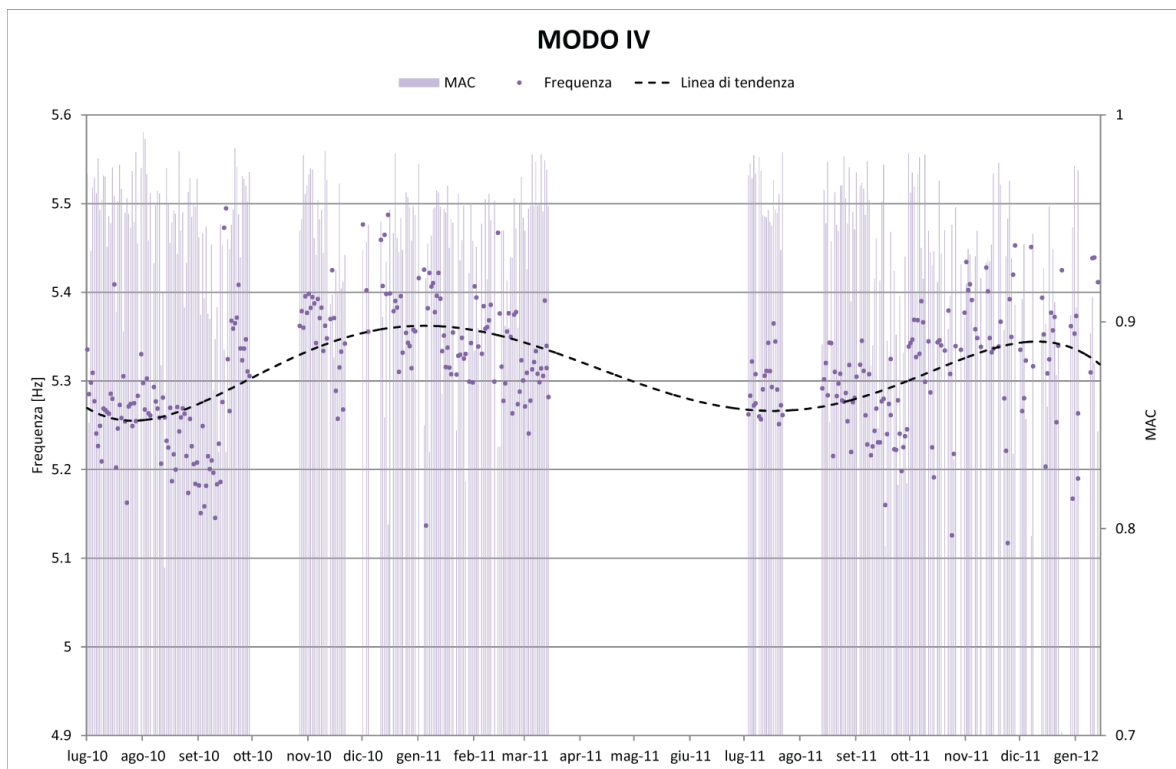


Figure 5-19: Modal frequencies and MAC value of the fourth mode (Fattoretto, 2012)

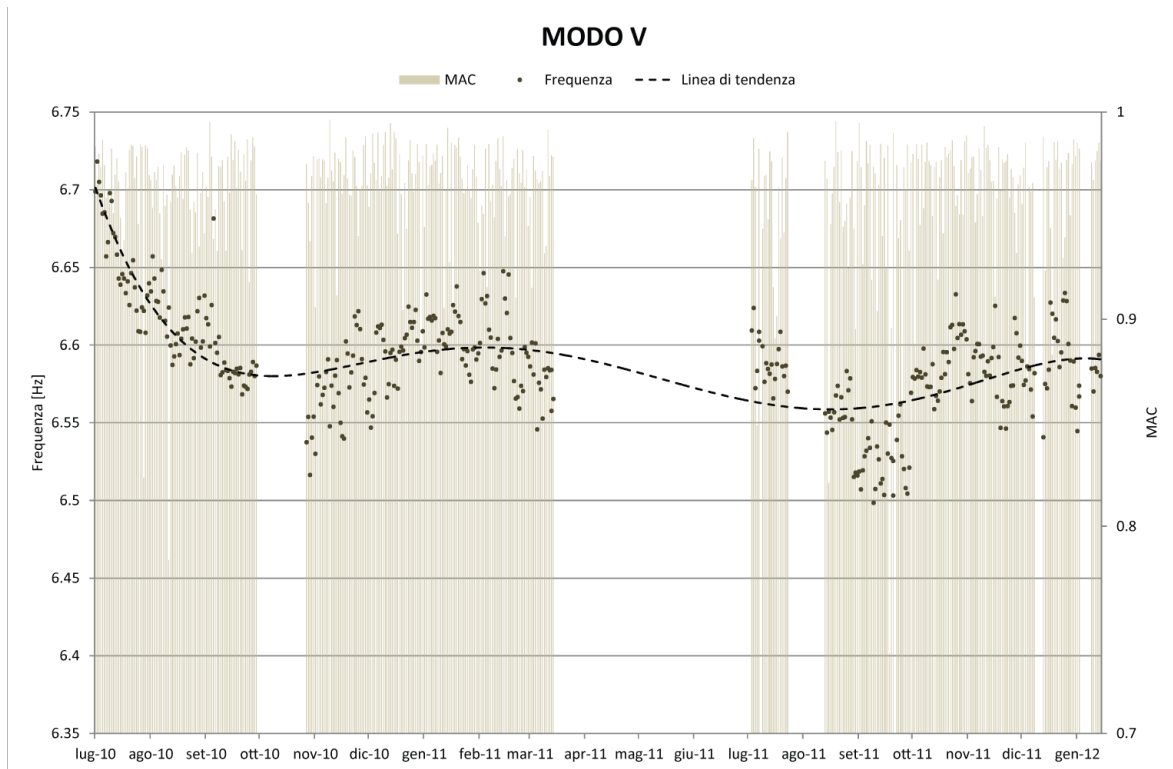


Figure 5-20: Modal frequencies and MAC value of the fifth mode (Fattoretto, 2012)

Also the damping can be related to temperature. Figure 5-21, Figure 5-22, Figure 5-23, Figure 5-24, and Figure 5-25 graph this behaviour.

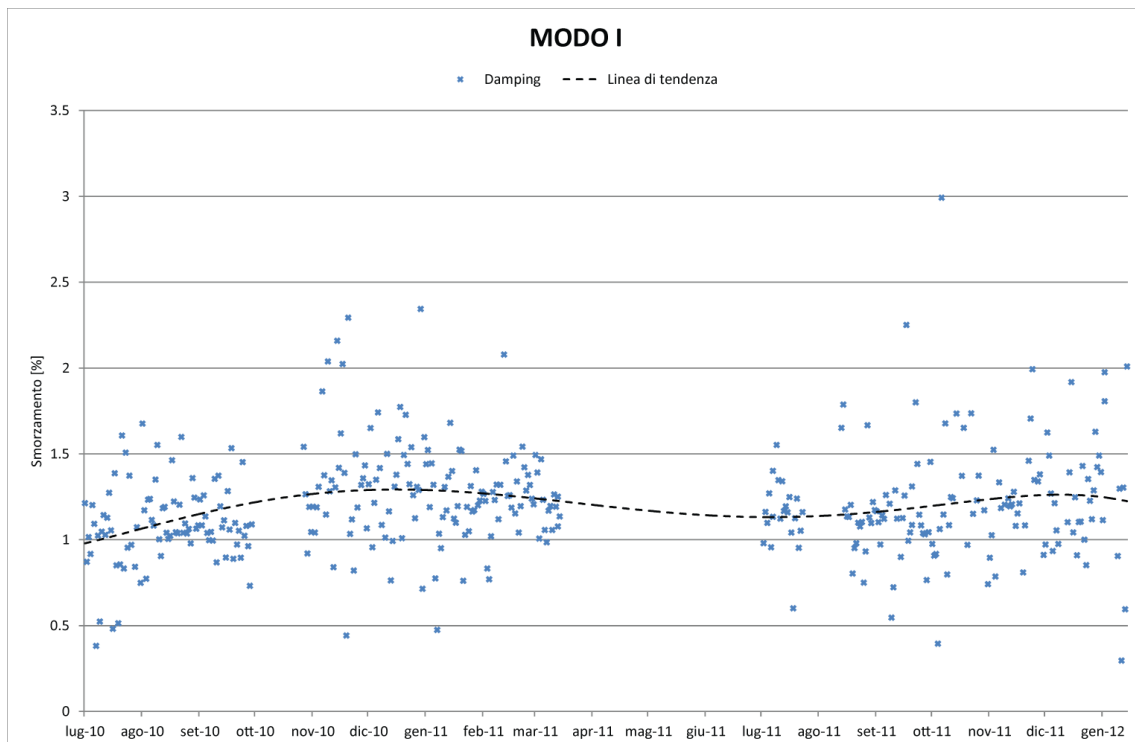


Figure 5-21: Damping with time for the first mode (Fattoretto, 2012)

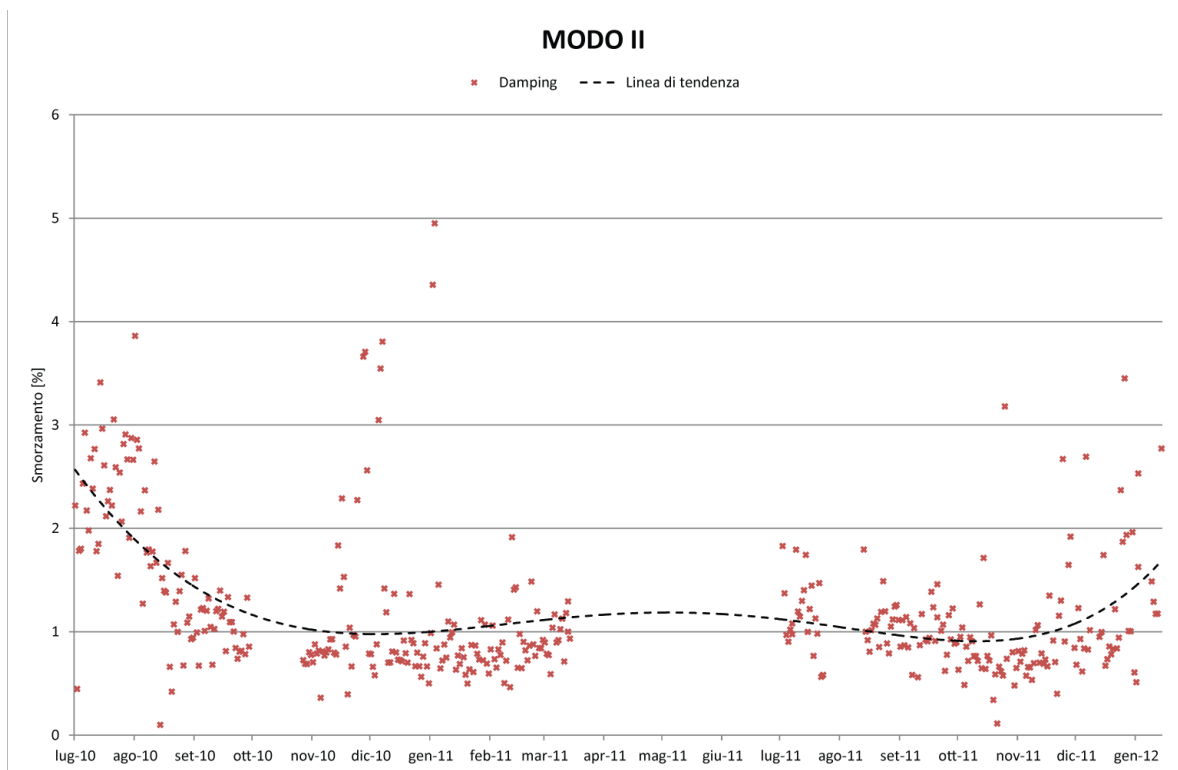


Figure 5-22: Damping with time for the second mode (Fattoretto, 2012)

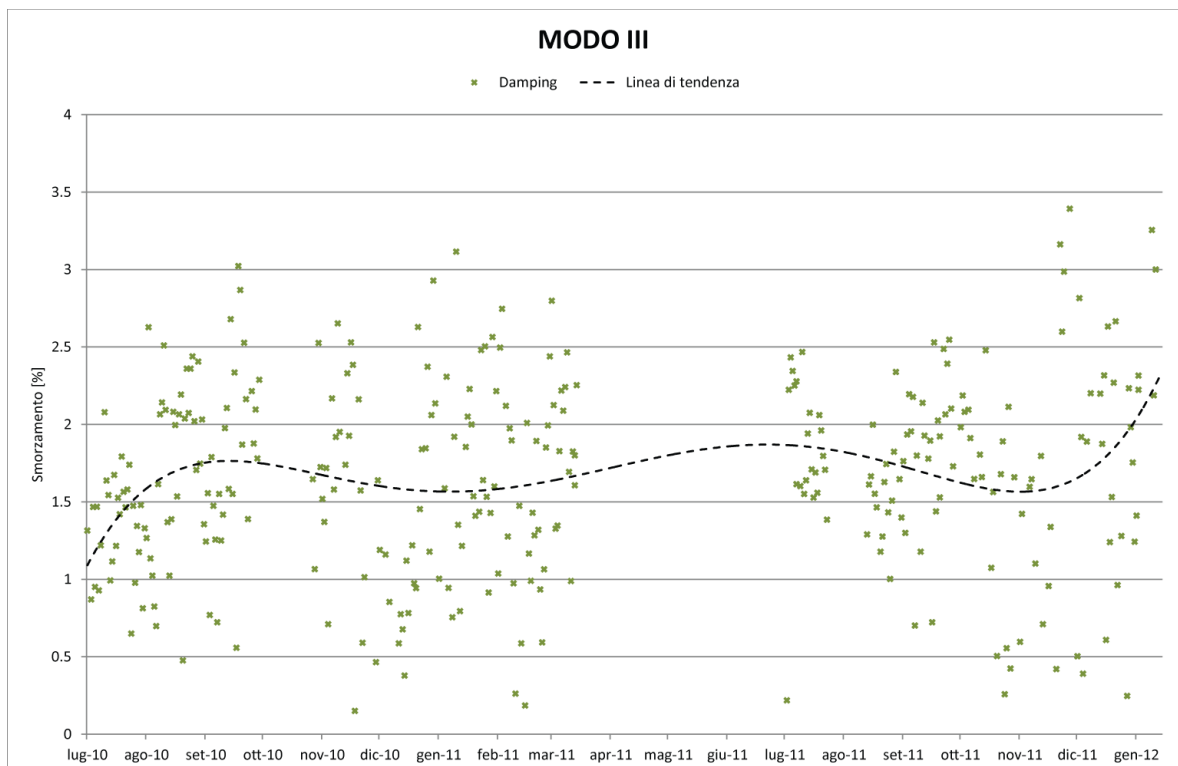


Figure 5-23: Damping with time for the third mode (Fattoretto, 2012)

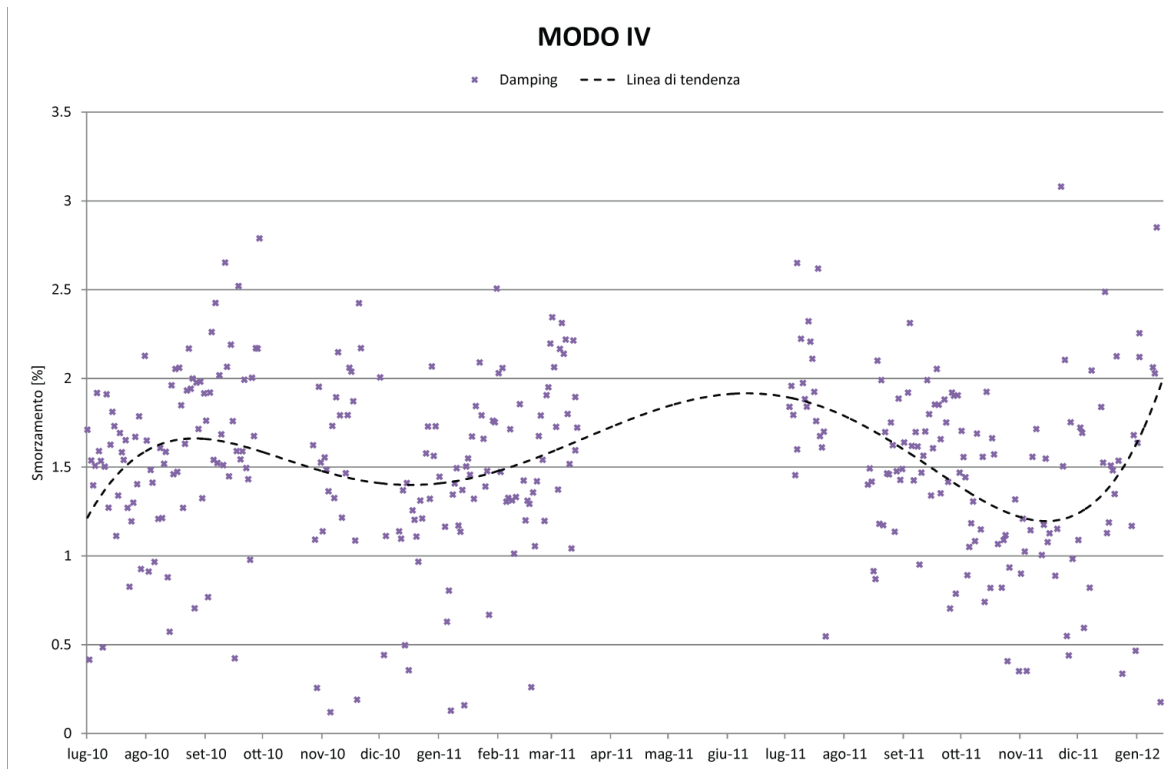


Figure 5-24: Damping with time for the fourth mode (Fattoretto, 2012)

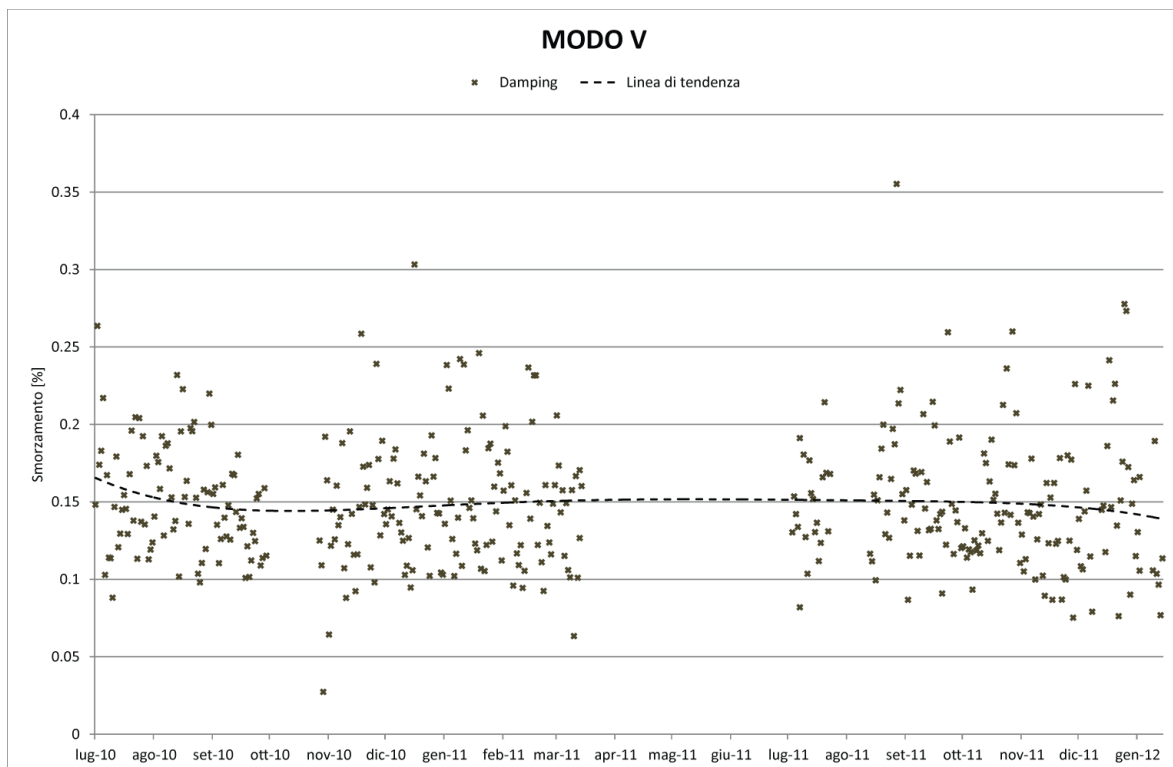


Figure 5-25: Damping with time for the fifth mode (Fattoretto, 2012)

Looking at the graphs presented above, it can be noted that the behaviour of the Church does not present irregularities in its behaviour. Infact, the modal frequencies follow the variation of the temperature due to seasonal changing. Also the damping (especially for the first and fourth mode) follows the climatic changes. For the others, a more accurate method is required.

6 STRUCTURAL ANALYSIS: MODELING

6.1 Introduction

The objectives of the structural analysis performed to St. Silvestro Church are:

- The calibration of the church model in order to reproduce the collapse mechanisms that were activated in the church during the earthquake;
- to use both static and dynamic monitoring systems applied to the bell tower to study the church model under damaged conditions;
- to assess the effectiveness of the temporary interventions that have been already designed and applied to the structure.

6.2 Geometry

The geometry of the church was built with the software AutoCAD 2011 (from Autodesk). The plans and the elevations were already given. For the 3D model it was planned to use shell elements (see Chapter 6.4 for more details on the mesh), thus the midline of the walls and pillars considered. The structure was modelled with 2D regions and considering different layers for the different materials and properties of the Church's structural elements.

Some assumptions and simplifications were made while creating the church geometry, in particular related to the ground level and boundary conditions, which do not interfere on the global structural behaviour of the church.

The final 3D drawing was saved as *.igs and imported in FX+ for Diana in order to mesh it and add loads and boundary conditions

6.3 Materials, Properties, and Boundary Conditions

In St. Silvestro Church different materials were found and identified through a visual inspection and considering the structure constructive process (see paragraph 4.2).

Since no laboratory information on materials was available, the mechanical properties of the different material observed were estimated following the Italian Standards (Nuova Circolare della Norme Tecniche per le Costruzioni, 2009). Table 4 is a translation of Table C8A.2.1 of the code; it summarizes the range between which the listed value may vary. The mechanical properties collected in the table are:

- f_m : average compressive strength of masonry;

- τ_0 : average shear strength of masonry;
- E: average value of the normal elastic modulus;
- G: average value of the shear modulus;
- w: average specific weight of the masonry.

Table 4: Suggested values for masonry by the Italian Standards – translation from table C8A.2.1 (Nuova Circolare della Norme Tecniche per le Costruzioni, 2009)

Masonry typology	f_m	τ_0	E	G	w
	N/cm ²	N/cm ²	N/mm ²	N/cm ²	kN/m ³
	min-max	min-max	min-max	min-max	
Irregular stone masonry (pebbles, erratic and irregular stone)	100	2	690	230	19
	180	3.2	1050	350	
Uncut stone masonry with facing walls of limited thickness and infill core	200	3.5	1020	340	20
	300	5.1	1440	480	
Cut stone masonry with good bonding	260	5.6	1500	500	21
	380	7.4	1980	660	
Soft stone masonry (tuff, limestone, etc.)	140	2.8	900	300	16
	240	4.2	1260	420	
Dressed rectangular stone masonry	600	9	2400	780	22
	800	12	3200	940	
Full brick masonry with lime mortar	240	6	1200	400	18
	400	9.2	1800	600	
Masonry in half-filled brick blocks with cement mortar (e.g. double UNI)	500	24	3500	875	15
	800	32	5600	1400	
Hollow brick masonry (percentage of perforations < 45%)	400	30	3600	1080	12
	600	40	5400	1620	
Hollow brick masonry with dry perpendicular joints (percentage of perforations < 45%)	300	10	2700	810	11
	400	13	3600	1080	
Concrete block masonry (percentage of perforations between 45% and 65%)	150	9.5	1200	300	12
	200	12.5	1600	400	
Masonry in half-filled concrete blocks 300	300	18	2400	600	14
	440	24	3520	880	

The materials found in the church belong to the third and fifth class. The values found in these classes will be used as initial values for the model calibration.

Three more parameters have to be taken into account in order to add the uncertainties related to the materials used. All these parameter are here briefly described.

The first coefficient is the Corrective Coefficient (CC). It is applied when the masonry is good and has good mortar, through stones, or some kind of reinforcement was applied in the past. Since no quantitative information was obtained on the materials, this coefficient will be considered equal to 1.

The Confidence Factor (FC) depends on how much information on the structure is available. The existing information is not much: a dynamic identification was carried out on the bell tower of the Church, but everything (except for the geometry) regarding the rest of the building is unknown. For this reason for what concern the bell tower a category 2 (FC=1.2) is considered, while the rest of the Church is classified as category 1 (FC=1.35). The structure is a Cultural Heritage building and thus the most suitable code to use when evaluating the Confidence Factor would have been the Guidelines for the Evaluation and Mitigation of Seismic Risk to Cultural Heritage (Linee Guida per la valutazione e riduzione del rischio sismico del patrimonio culturale (in Italian), 2010), but since the material parameters that are going to be used are just the starting point for the calibration process, the Italian Code (Nuove Norme Tecniche per le Costruzioni, 2008) was followed.

The last factor γ_m is the partial factor used with material properties in case of seismic assessment of new building. For this reason it is taken equal to 1.

Depending on the level of knowledge, the code gives suggestion on how to obtain the mechanical properties of the materials from the values in Table 4. For the linear and modal analyses only E , w and ν are needed. The Young's Modulus is obtained as the average of the minimum and maximum values proposed in Table 4 and divided by the Confidence Factor, thus:

$$E = \frac{\text{mean value}}{FC} \quad (5)$$

The values used for the first run of the model are summarized in Table 5.

Table 5: Material's parameters

	Knowledge level	E N/mm ²	w kN/m ³ /g	ν
Masonry 1	LC1	1289	2.14	0.2
Masonry 2	LC2	1450	2.14	0.2
Good Masonry	LC1	2074	2.24	0.2

The materials included in the class "masonry 1" are: the Branconio Chapel, the internal and external walls, and the Apses. In "masonry 2" only the bell tower is included, while "good masonry" takes into account the better quality found in the façade, the pillars of the Church and the arches just above them. Figure 6-1 shows the materials and their properties. Note that the trusses and the roof masses are applied as punctual over the RC curb. Also the roof on the Branconio chapel was added in this way.

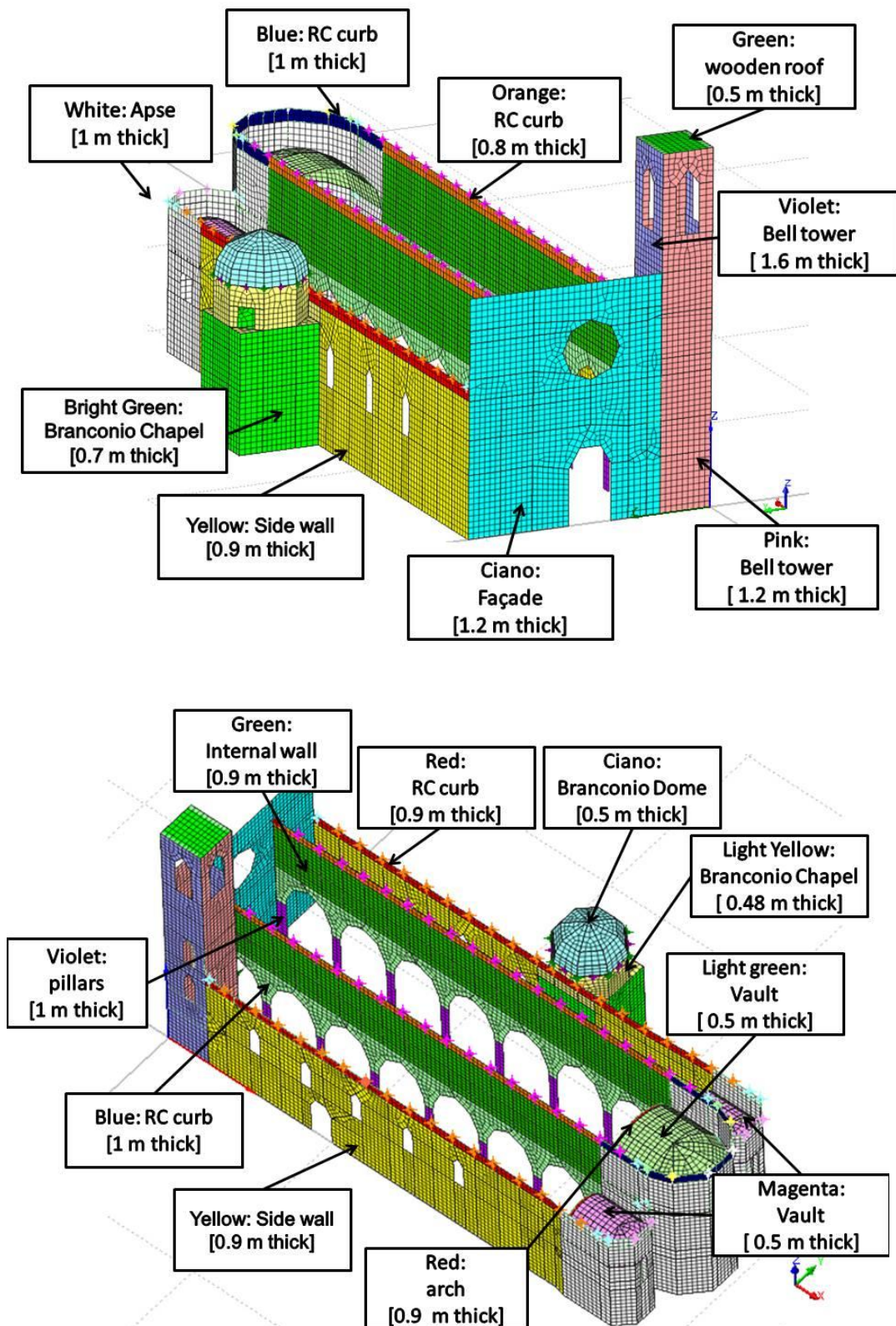


Figure 6-1: Material and thickness in the Church. Front view (upper side) and back view (low side)

Also, Table 6 shows the material together with the associated properties (in this case the thickness) of the different part of the Church.

The boundary conditions were assumed to be fixed to the zero level of the Church which was defined in Section 6.2 as the level reached with the frontal stairs. For the first analysis no other constraints were assumed: the Sacristy was assumed not to have any influence on the Church as the connections between the two different materials were supposed to be without any type of interlocking.

Table 6: Material, thickness and associated part in the model

Part	Material	Thickness m
Façade	Good Masonry	1.2
Internal wall	Masonry 1	0.8
External wall	Masonry 1	0.9
Columns	Masonry 1	0.97
Bell Tower (sides)	Masonry 2	1.6
Bell Tower (front)	Masonry 2	1.2
Bell Tower (back)	Masonry 2	1.2
Apse	Masonry 1	1
Chapel 1	Masonry 1	0.7
Chapel 2	Masonry 1	0.5
Branconio Dome	Masonry 1	0.48
Internal curb	RC	0.8
External curb	RC	0.9
Apse curb	RC	1
Arches	Good Masonry	0.5
Side Vaults	Masonry 1	0.4
Central Vault	Masonry 1	0.5

6.4 Mesh: quadrilateral and triangular curved shell elements (Diana User's Manual, 2012)

The element chosen for the analysis is a curved shell element with mid-side nodes. The quadrilateral or triangular elements available with this characteristic are: CQ40S (Figure 6-2 - left) and CT30S (Figure 6-2 - right). By default, a local element axis points from the first to the second node of the element.

Curved shell elements (Figure 6-3) are based on two hypotheses:

- **Straight normals:** The normals of the element plane remain straight after the deformation but they don't have to be perpendicular to the element plane. Transverse shear deformation is included according to the Mindlin-Reissner theory.

- **Zero-normal-stress:** the normal stress component in the normal direction is forced to be zero.

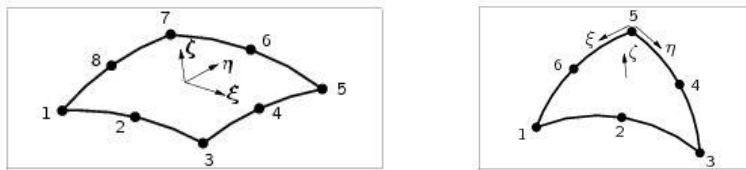


Figure 6-2: CQ40S element (left) and CT30S element (right)

Another characteristic is that curved shell elements must be thin. This means that the thickness t of the element must be small when compared to the dimensions b in the plane of the element. The loads F can act in any direction between perpendicular to the surface and in the surface, while moment loads M should act around an axis which is in the element face, as seen in Figure 6-3.

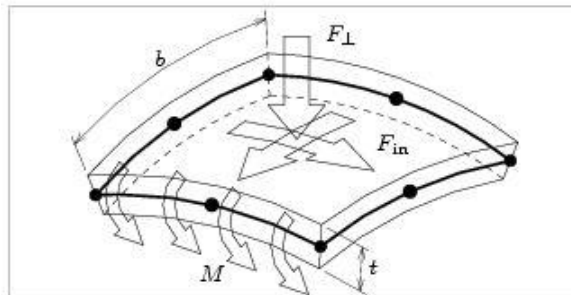


Figure 6-3: Curved shell element

In each node 5 DOF are defined (Figure 6-4): 3 translations (u_x, u_y, u_z), and 2 rotations (ϕ_x, ϕ_y)

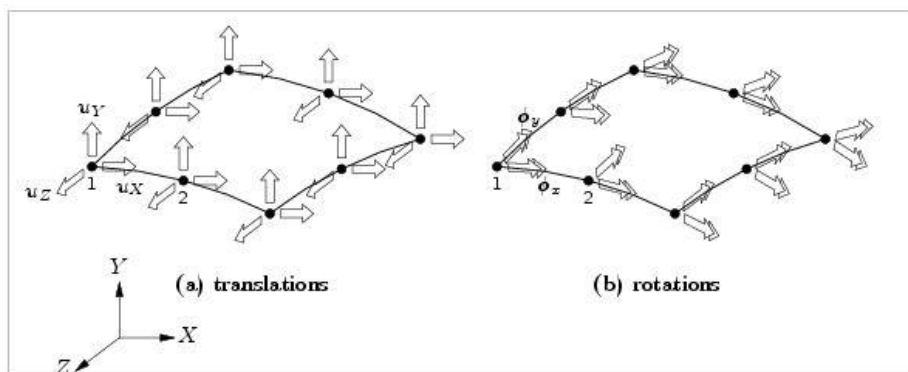


Figure 6-4: Degrees of Freedom

The in-plane lamina strains ϵ_{xx} , ϵ_{yy} , and γ_{xy} vary linearly in the thickness direction. The transverse shear strains γ_{xz} , γ_{yz} are forced to be constant in the thickness direction. This means that they are not varying parabolically over the thickness, but they are constant on a corresponding area with an equivalent value.

The final model counts 54 036 nodes and 17 696 elements.

6.5 Loads

6.5.1 Roof weight

The model built is not considering the mass of the roof. To do this, punctual masses were added where the trusses are located. The masses values were determined taking into account the roof (tiles and wooden elements) and the trusses themselves.

The wood weight is assumed 6 kN/m^2 and the dimension of the elements are obtained from the autoCAD drawings already available. It was not possible to inspect the roof and check the real dimensions of the elements. Table 7 summarizes the loads of the roof. It was assumed a wooden board 3 cm thick, purlins' section of $0.14 \times 0.19 \text{ m}^2$ and 1.6 m of spacing, while the contribution of the wooden beams was assumed to be 0.16 kN/m^2 . Moreover, the spacing between trusses is 2.7 m. Thus the value considered is: 2.8 kN/m

Table 7: Roof Weight

Roof	
Tiles	0.6 kN/m^2
Wooden board	0.18 kN/m^2
Purlins	0.10 kN/m^2
wooden beams	0.16 kN/m^2

Table 8 and Table 9 show the load coming from the trusses of the central nave and the lateral naves.

Table 8: Truss central nave

Central Nave			
	section [m]	length [m]	Weight [kN]
Tie Beam	0.25 x 0.25	10	3.8
Principal Rafter	0.25 x 0.25	5.4	2.0
Principal Rafter	0.25 x 0.25	5.4	2.0
King post	0.25 x 0.3	1.6	0.7
TOTAL			4.3 kN

Table 9: Truss lateral naves

Lateral Nave			
	section [m]	length [m]	Weight [kN]
Tie Beam	0.25 x 0.25	5.7	2.1
Principal Rafter	0.25 x 0.25	5	1.9
King post	0.25 x 0.3	3.1	1.4
TOTAL			5.4 kN

These loads are summed up and then converted into mass in order to perform the analyses planned. The masses considered for each supports in the central nave is 2.0 kN/g , while for the lateral nave the

external support is assumed to carry two thirds of the total weight (1.3 kN/g) while the internal support is carrying the remaining third (0.7kN/g).

6.5.2 Other loads

Following the Italian Standards [Chapter 3 (Nuove Norme Tecniche per le Costruzioni, 2008)] the accidental load for roof category H1 is considered to be 0.5 kN/m².

The load due to snow is evaluated always following the Italian Standards [Chapter 3, (Nuove Norme Tecniche per le Costruzioni, 2008)] and it is given by:

$$q_s = \mu_i q_{sk} C_E C_t \quad (6)$$

where:

- C_E takes into account the exposition of the place and considered equal to 1.
- C_t is a coefficient that takes into account the fact that the snow can be melted if under the roof the place it is heated up and considered equal to 1.
- μ_i is a coefficient that depends on the slope of the roof. For St. Silvestro it is equal to 0.8 for both the central nave and the laterals.
- q_{sk} depends on the height of the place. For L'Aquila (which is more or less 700m over the sea level) this value is 1.63 kN/m².

Thus, the snow load is 1.3 kN/m².

6.5.3 Load Combination

The Combination of load that is going to be used in the modal analysis is the seismic combination given by the Italian Standards (Nuove Norme Tecniche per le Costruzioni, 2008) in Chapter 2:

$$E + G_1 + G_2 + \sum_j \Psi_{2j} Q_{kj} \quad (7)$$

Since Ψ_{2j} for category H roof, wind and snow under 1000 m over the sea level is zero, the load considered will be only the weight of the structure and the earthquake:

$$E + G_1 + G_2 \quad (8)$$

For the same reason, the masses associated to the structure for the seismic analysis will be given only by the structural, G_1 and non structural weight, G_2 in the Church.

7 ANALYSES AND CALIBRATION OF THE MODEL

7.1 Introduction

The properties defined in the previous section need to be calibrated. The aim of the calibration is to find the mechanical properties of the materials that best simulate the behaviour of the Church, bearing in mind that the reference starting point is composed by the modal shapes and frequencies of the bell tower (Chapter 5.4).

The first analysis run is a linear static analysis. The Church is subjected to the gravity load: only the body forces are considered. This run is used to check the model and see if the mesh deforms properly. The material values used are the one described in Chapter 6.3.

Figure 7-1 shows the displacement and the deformed mesh of the entire Church. The analysis shows the most deformed element of the church is the arch and vault over the central apses, with a maximum displacement in the mid around 1.12 cm.

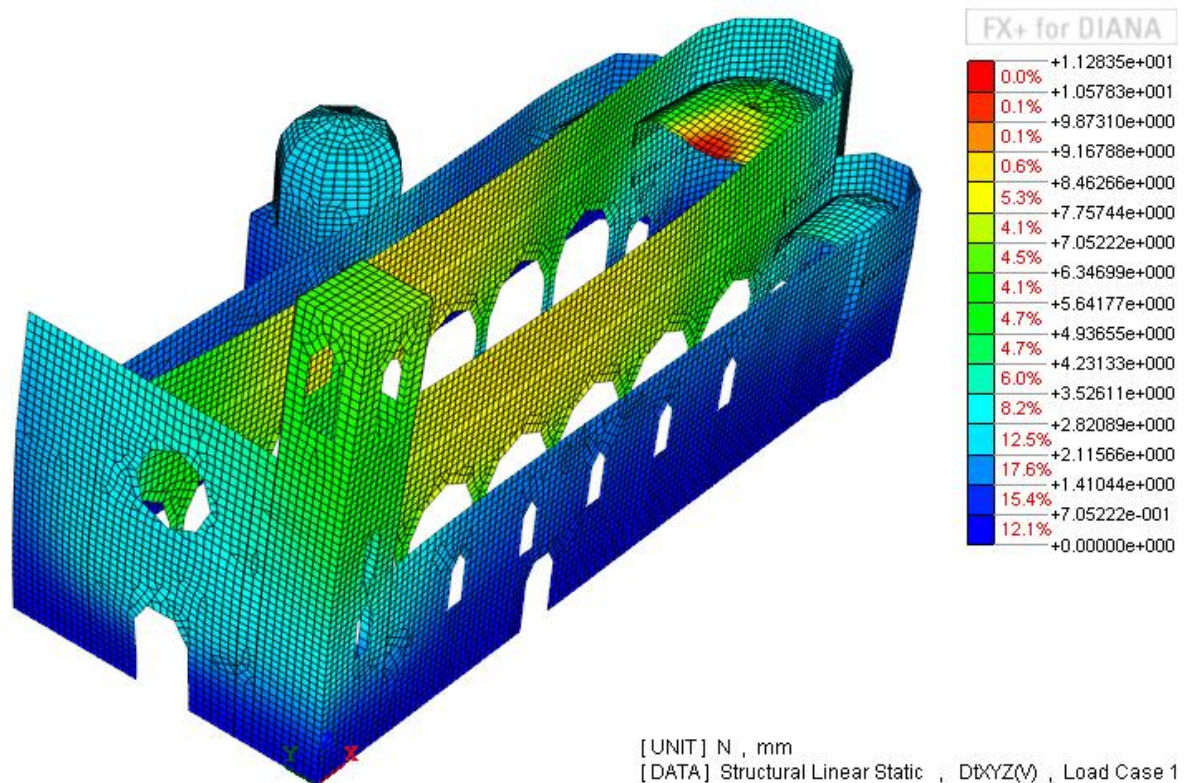


Figure 7-1: Deformed mesh and displacement

Table 10 shows an overview of the principal strain in compression and tension for the two external layers (Layer 1 and 2). With the type of element chosen there is also integration in the thickness of the

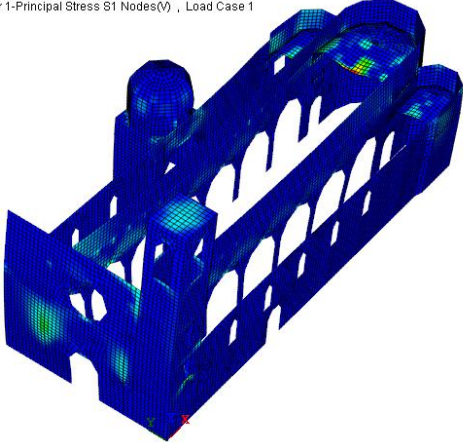
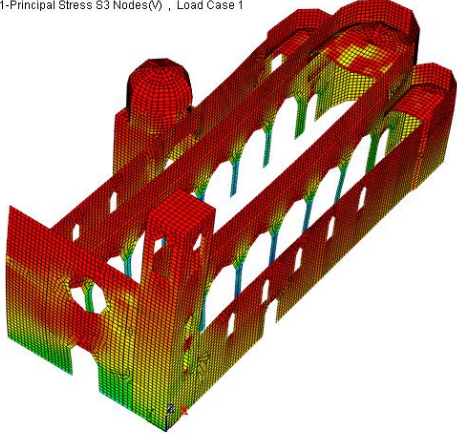
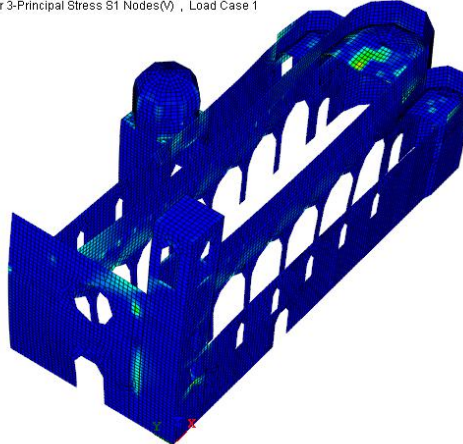
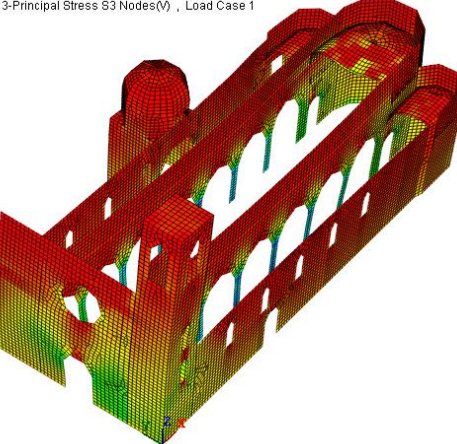
element itself; for this reason two layers are shown both in tension and compression. (For better resolutions figures see Annex - Strains 9.1)

The principal stresses are presented in Table 11. The RC curb is not considered in the evaluation as it is considered of interest the values reached in the masonry. It is possible to see (for better resolutions figures see Annex - Stresses 9.2) that the maximum tensile stresses appear in the keystone of the central vault, while the maximum compression is reached in the pillars of the nave and is about 1.5 MPa, which are acceptable compressive resistance values for the masonry that compose the arches, although some tests should be performed to the pillars material in order to accurately characterize them.

Table 10: Overview of Principal Strains (compressive and tensile)

	E1 - Compression	E3 - Tension
Layer 1		
Layer 3		

Table 11: Overview of Principal Stresses (compressive and tensile)

	S1 - Compression	S3 - Tension
Layer 1	<p>Layer 1-Principal Stress S1 Nodes(V) , Load Case 1</p> 	<p>Layer 1-Principal Stress S3 Nodes(V) , Load Case 1</p> 
Layer 3	<p>Layer 3-Principal Stress S1 Nodes(V) , Load Case 1</p> 	<p>Layer 3-Principal Stress S3 Nodes(V) , Load Case 1</p> 

The same model was also used for a first modal analysis. Results are not shown in this thesis; but looking at the behaviour of the Church several observations were made:

- the large number of materials of the church does not allow a proper calibration since there is no reference not only for what concern the material parameters of each type of masonry, but also the global behaviour of the Church has not been studied. Only the modal shapes of the bell tower elaborated from dynamic identification tests and monitoring system, are available. For this reason a smaller model was considering the bell tower and frontal façade in order to calibrate the material properties in this part of the church.
- the roof is more rigid than expected, thus once the materials of the bell tower and façade will be calibrated, it is recommended to consider the rigidity given by the trusses.
- since the dynamic identification was carried out after the bell tower was strengthened, the model has to take into account also the influence of the ties around the tower and the vertical

elements on the edges. Only the parameters related to the bell tower and the façade will be updated. This step is referred in this thesis as a “first level of calibration”.

- it is thought that to further assess the validity of the calibration on the partial model a linear dynamic analysis was carried out considering seismic events registered in L'Aquila⁵ since the monitoring system was installed (“second level of calibration”).

7.2 The Calibration Process: first level

7.2.1 Bell Tower & façade

The first set of analyses is aimed at the calibration of the materials of the bell tower and façade. The geometry considered includes only the bell tower, the façade, and part of the walls of the naves. In order to consider the influence of the strengthening (Figure 7-2) applied to the structure, vertical beam elements and horizontal beam were added with the aim of simulate the job done by the wooden vertical elements and the steel ties that confine the entire bell tower. Table 12 summarizes the parameters used.



Figure 7-2: Detailed of the reinforcement (East side)

Table 12: Strengthening Material's parameters

	E N/mm ²	w kN/m ³ /g	v
Wood	1000	0.72	0.35
Steel Cables	21000	21	0.3

⁵ iside.rm.ingv.it

The influence of the rest of the Church is taken into account through the use of equivalent spring evaluated with the following equation:

$$K = \left(\frac{h^3}{3 \cdot EJ} + \frac{1.2 \cdot h}{GA} \right)^{-1} \quad (9)$$

While evaluating the stiffness of the spring, the influence of the RC curb was not considered as it is known that this concrete element is not connected with the rest of the Church and it only works by friction. The springs' stiffness found for San Silvestro through equation (9) are summarised in Table 13.

After running several modal analyses, the model was modified in order to reach a good MAC value for the considered experimental frequencies. In particular, it was tried to reproduce the cracks found in the part of the Church considered. The areas that are damage on the church were considered in this model with poorer properties in respect to the rest of the church (Young's modulus was decreased by a factor of 10 and thickness of the elements kept constant to 0.9 m). Figure 7-3 shows (in black) the damaged elements of the final model. (The crack pattern of the Church is shown in paragraph 4.5)

Table 13: Springs' stiffness

Spring	Stiffness for each node [N/m]
SPRING east	25 000
SPRING centr	92 000
SPRING west	24 000

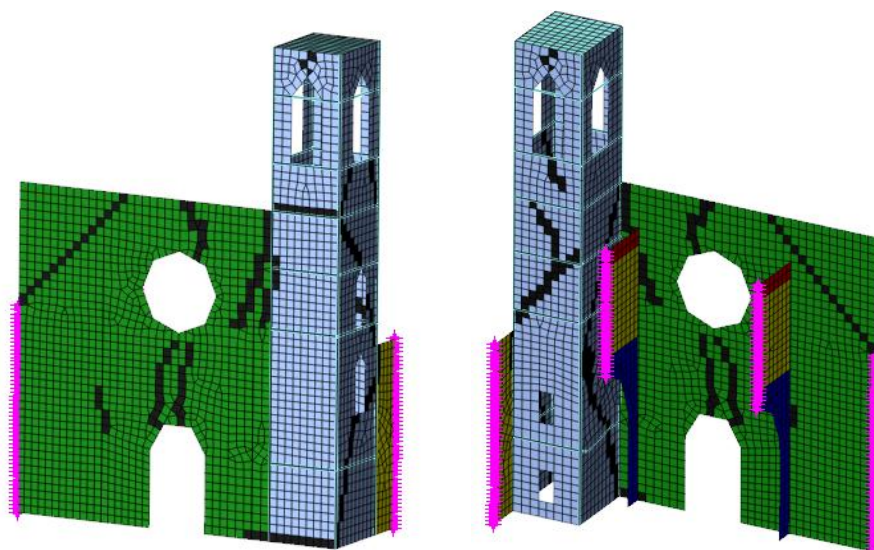


Figure 7-3: Crack pattern in the model: front (left) and back (right)

To better fit the material parameters to the structure's global behaviour several analyses were performed and a double check was performed.

The first check regards the frequencies. The first three numerical frequencies have to be fitted to the experimental ones. To do this the average percentage error is evaluated with equation (10).

$$\varepsilon = \frac{f_{num} - f_{exp}}{f_{num}} \cdot 100 \quad (10)$$

where f_{num} is the numerical frequency (found with DIANA) and f_{exp} is the mean value of the experimentals.

Then the modal shapes are checked with the evaluation of the MAC (Modal Assurance Criterion) value through expression (11):

$$MAC_{e,n} = \frac{|\sum_{i=1}^n \varphi_i^e \varphi_i^n|^2}{\sum_{i=1}^n (\varphi_i^e)^2 \sum_{i=1}^n (\varphi_i^n)^2} \quad (11)$$

where the subscript e refers to experimental values and n refers to the numericals. φ_i in general, is the component of the eigenvector. Expression (11) leads to a scalar value between 0 and 1, associated with low and high correlation between the experimental and numerical vectors.

At the end of the calibration, the material values picked as a reference for the future analyses are listed in Table 14.

Table 14: Overview of the materials parameters after calibration

Material	Young's Modulus [MPa]	Poisson's Ratio	Density [kN/m ³ /g]
Façade	2600	0.2	2.3
Bell tower	2400	0.2	1.85

It has to be remembered that no investigation was carried out on the materials of St. Silvestro and that the values used were suggested by the Italian Code (Nuova Circolare della Norme Tecniche per le Costruzioni, 2009) for the type of masonry found in the church.

For the first mode a MAC value of 0.7 was obtained with an error near 3%. The second mode has a MAC of 0.44 and an error less than 0.5%. Finally the third mode has a MAC of 0.3 and an error near 6%. As can be noted, even if frequencies are well calibrated, MAC values do not go over 0.7. To better calibrate the model a more thorough experimental campaign has to be conducted to the material and to the extent of the damages. (Table 15)

Table 15: Overview of errors and MAC values before and after calibration

	Mode I		Mode II		Mode III	
	ϵ	MAC	ϵ	MAC	ϵ	MAC
Before Calibration	4.75 %	0.47	7.57 %	0.24	5.73 %	0.16
After Calibration	2.72 %	0.71	0.08 %	0.44	3.84 %	0.32

Figure 7-4 shows the numerical frequencies (x axis) and the experimental ones (y axis). The dot's diameter is the MAC value. The bigger the dot, the better is the simulation of the mode. Moreover the nearer the dot to the line, the less is the error in the approximation of the frequency's value.

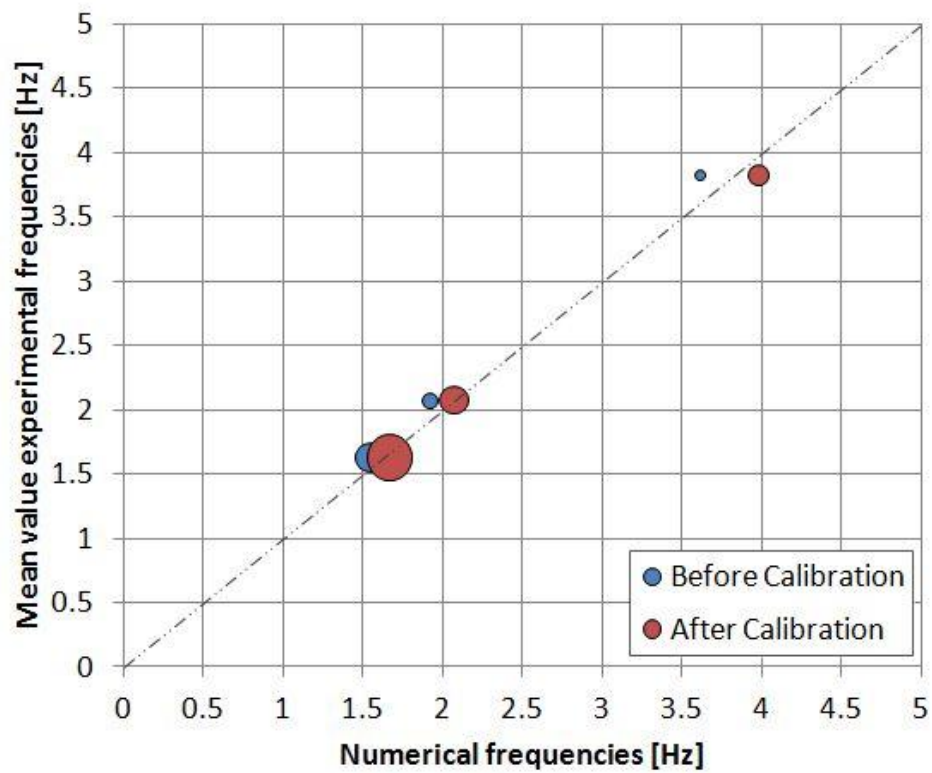


Figure 7-4: Frequencies and MAC values

Table 16, Table 17, and Table 18 show a comparison of the modal shapes obtained with MACEC and ARTeMIS with the results of DIANA.

Table 16: Mode I – Flexional (MAC= 0.705; ϵ = 2.72 %)

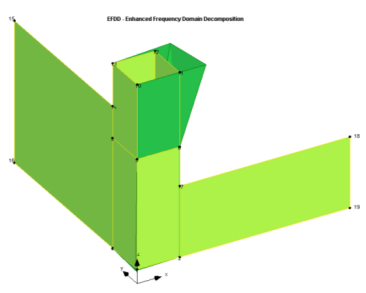
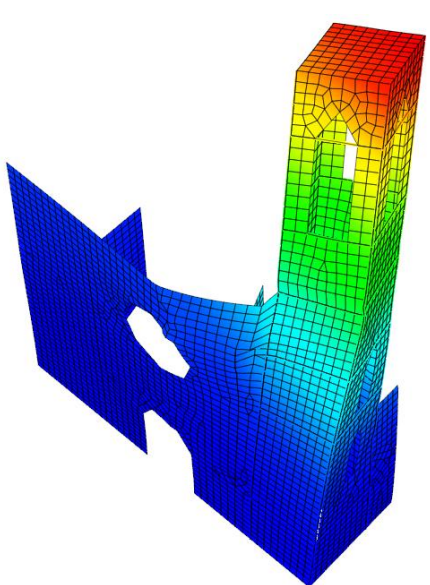
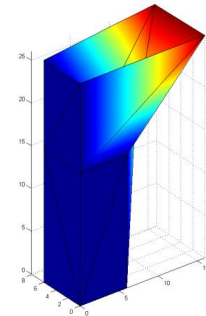
Experimental Frequency [Hz] and Modal Shape		Numerical Frequency [Hz] and Modal Shape	
EFDD			
pLSCF			
1.628		1.67358	

Table 17: Mode II – Flexional (MAC= 0.44; ϵ = 0.08 %)

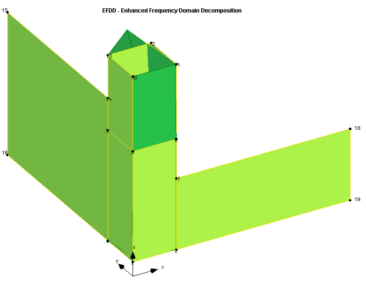
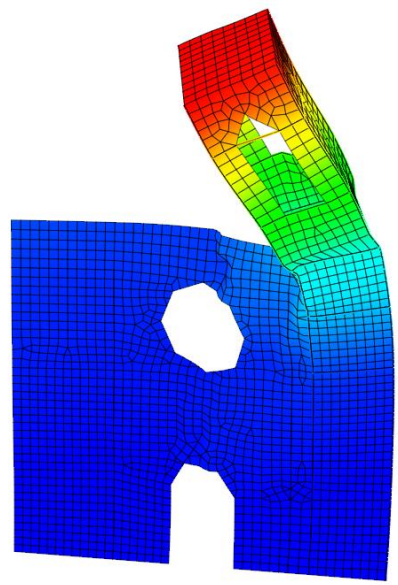
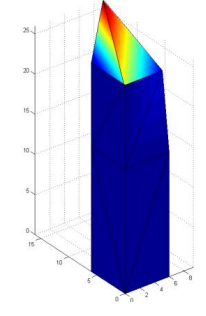
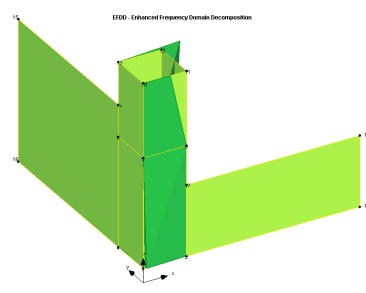
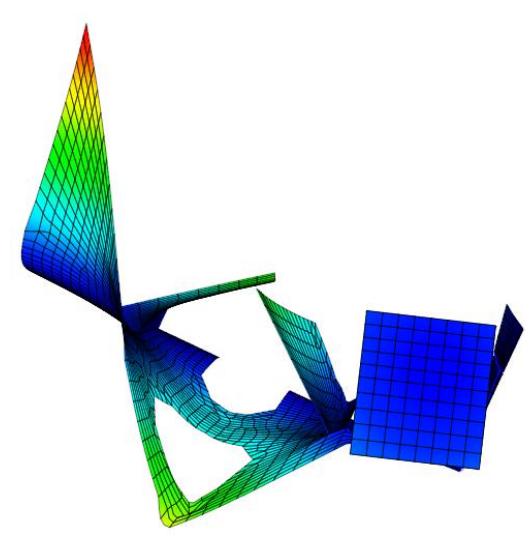
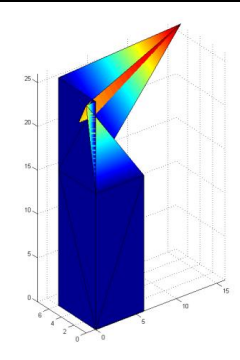
Experimental Frequency [Hz] and Modal Shape		Numerical Frequency [Hz] and Modal Shape	
EFDD			
pLSCF			
2.071		2.07295	

Table 18: Mode II – Flexional (MAC= 0.44; ϵ = 0.08 %)

Experimental Frequency [Hz] and Modal Shape		Numerical Frequency [Hz] and Modal Shape
EFDD		
pLSCF		
3.8246		3.97735

7.2.2 Global model

In order to check more deeply the behaviour of the Church, another modal analysis has been run considering the entire Church. The material parameters found in the calibration and all the considerations described in the previous chapter were kept. In addition to that, the damage found on the first arches of both internal walls have been introduced.

Moreover beam elements were added on the roof with the function of simulate the real behaviour at the top of the Church. These elements have a section of $0.25 \times 0.25 \text{ m}^2$ and a Young's Modulus of 10000 MPa.

Results confirm the values obtained with the “small” model. MAC values are almost the same, but the error on the frequencies increases.

The modes of the entire Church considered for the comparison and the evaluation of the MAC value are the second mode, the forth and the fourteenth. Figure 7-6, Figure 7-7, and Figure 7-8 show the modes that includes the bell tower. On the right it is possible to see the mode in the “small” model shown in the previous paragraph.

With the global modal analysis it is also possible to observe the modes of the entire Church. Figure 7-9, Figure 7-10, Figure 7-11, and Figure 7-12 show the most important.

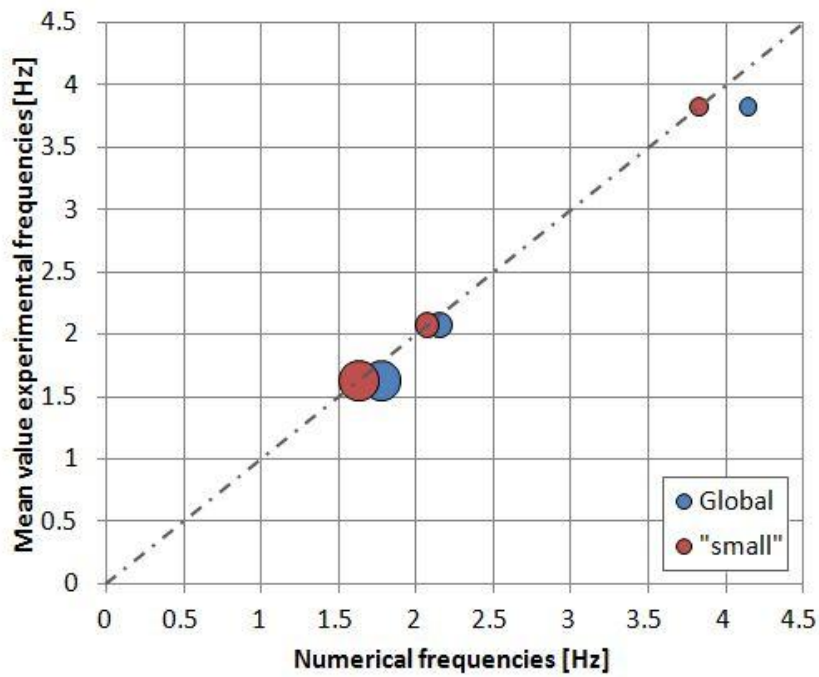


Figure 7-5: MAC values for global model and "small" one

Table 19: Overview of errors and MAC values before and after calibration

	Longitudinal (N-S)		Longitudinal (E-W)		Torsion	
	ϵ	MAC	ϵ	MAC	ϵ	MAC
"small" model	2.72 %	0.71	0.08 %	0.44	3.84 %	0.32
Global model	8.16 %	0.69	3.52 %	0.45	7.68 %	0.31

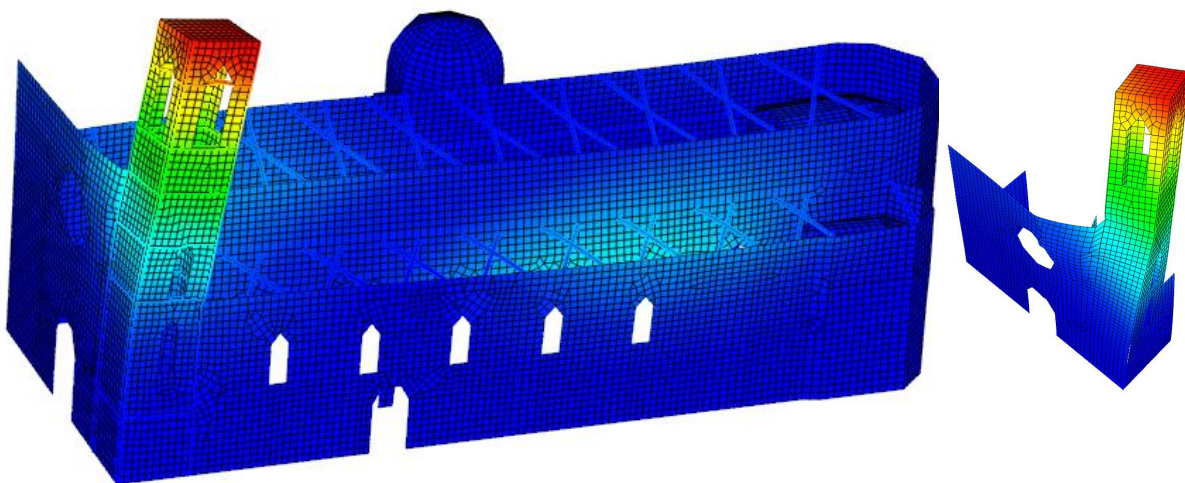


Figure 7-6: Comparison for 2nd global mode - 1.77 Hz (left) and the "small" model

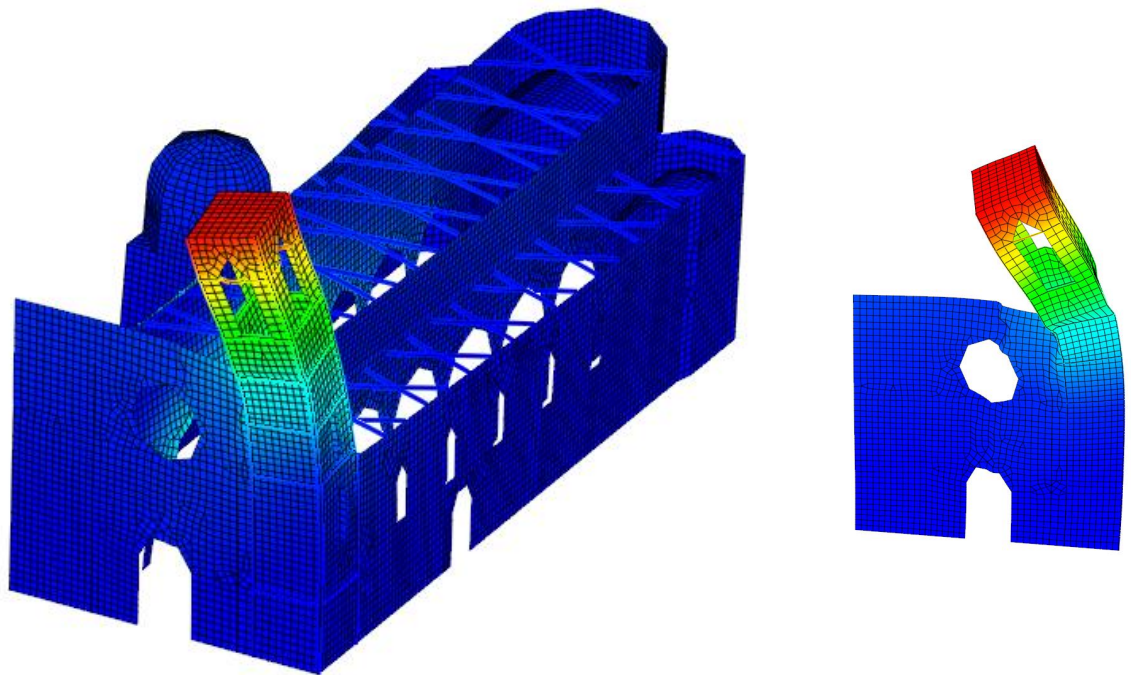


Figure 7-7: Comparison for 4th global mode - 2.15 Hz (left) and the “small” model

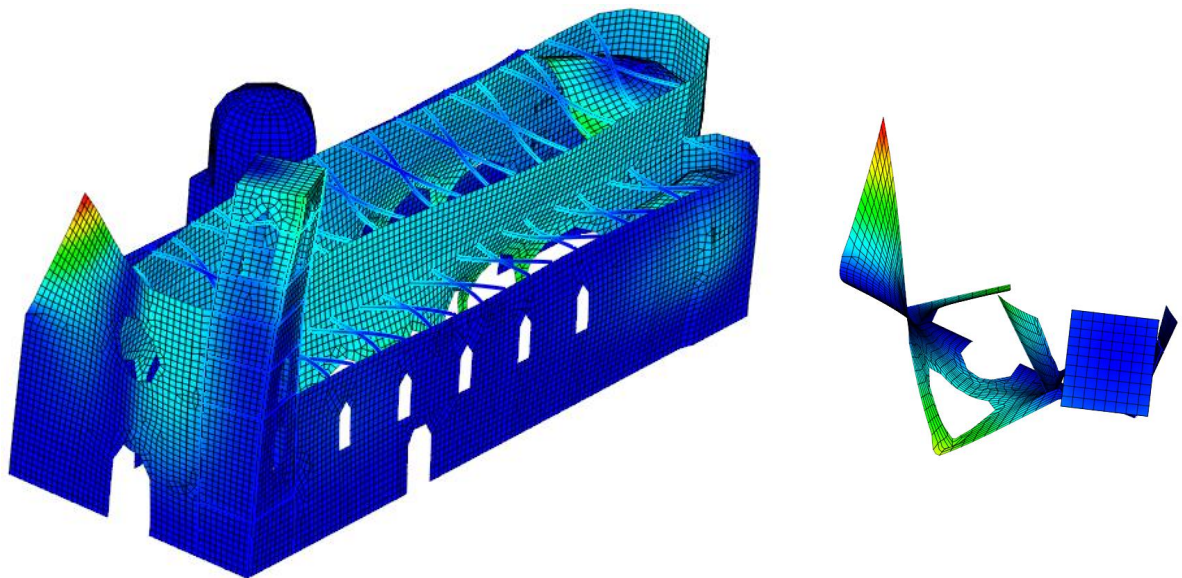


Figure 7-8: Comparison for 14th global mode - 4.14 Hz (left) and the “small” model

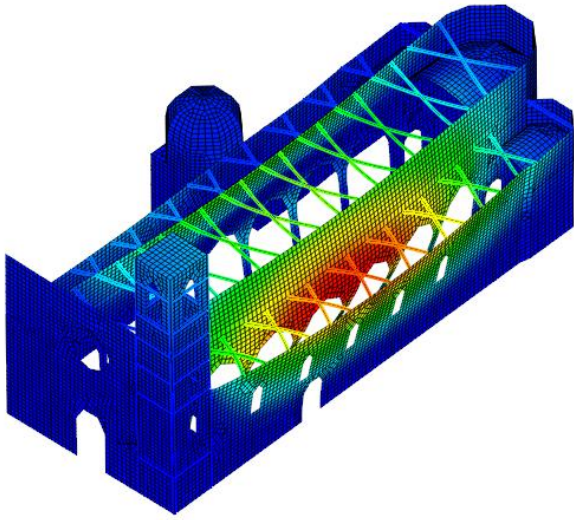


Figure 7-9: First global model of the church (walls)

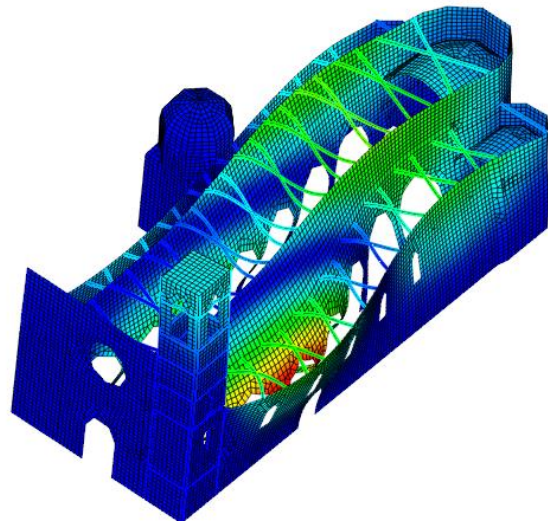


Figure 7-10: Fifth global mode of the church (walls)

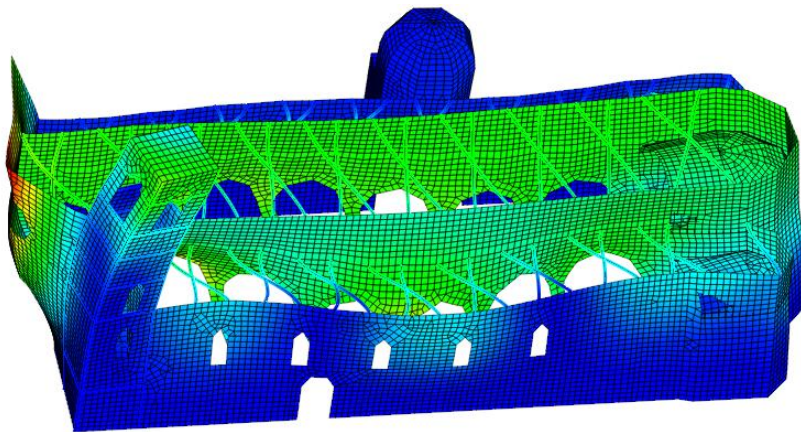


Figure 7-11: ninth global mode of the church (longitudinal)

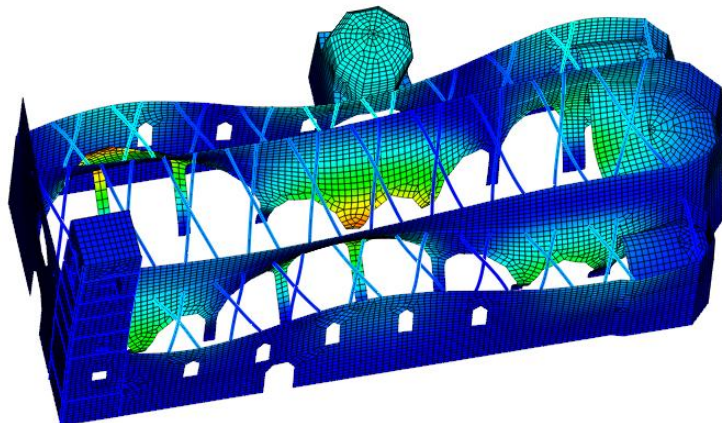


Figure 7-12: tenth global mode

7.3 The Calibration Process: second level

The second level of the calibration consists on performing a linear dynamic analysis, considering a seismic event registered in the area of L'Aquila after the installation of the monitoring system and evaluate if the calibration carried out in the previous section can give good results.

The first step is to find an earthquake that took place near L'Aquila and find in the data collected from the monitoring, the records of the event. To do this the Italian Seismological Instrumental and parametric Data-basE (ISIDe) was used.

Though ISIDe an easy research was done with the aim of finding a seismic event with magnitude more than 3 and not farther than 100 km from L'Aquila. The event that took place on October 30th, 2011 around 2:40 UTC was chosen. This event had a magnitude of 3.6 and took place at a depth of 9.7 km.

Note that since the analysis that is planned to be carried out is a linear dynamic analysis, the earthquake chose has to be not very strong. This is to avoid the structure to have a nonlinear behaviour and stay in the elastic range.

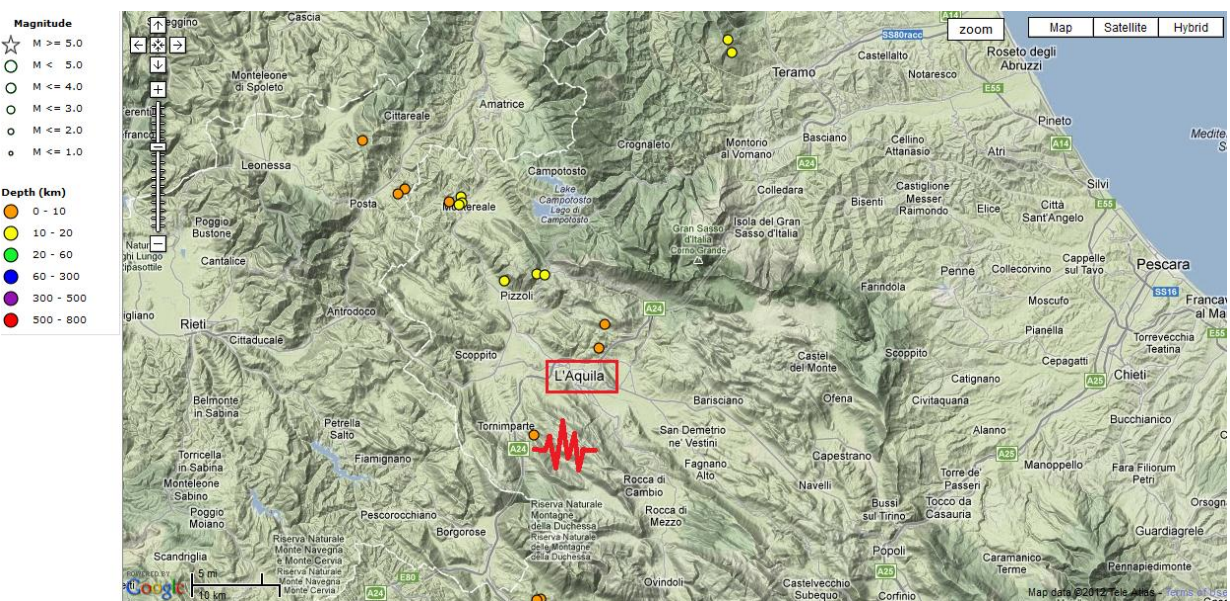


Figure 7-13: Location of the seismic event considered and L'Aquila city.

As the monitoring system (does not have any type of triggering, it were manually extracted from the register the 20 seconds of the seismic event that contained the maximum PGA and following damping of the vent. The processing of the data was carried out using the software DIAdem.

Table 20 summarizes the Channels, their rough location in the Church and the peak measured (see Chapter 5 for more details about the monitoring system installed). The input of the dynamic analysis consist of the records of the second channel and third channel, which measure the base acceleration

at the base of the bell tower in X and Y direction. The other Channels (except for Channel 1 which measures the base acceleration in Z direction) are used to check how the model behaves.

Figure 7-14 shows the records used as input. Channel 2 (red line) is the acceleration in Y direction, while Channel 3 (green line) is the acceleration in X direction.

Table 20: Channels

	Channel	Direction (without versus)	Min [m/s^2]
			Max [m/s^2]
Base	1	Z	-0.006973267
			0.008733749
	2	Y	-0.0057
Base	3	X	0.005529
			-0.00826
Base			0.009865
			4
Middle	5	Y	0.013657
			-0.01011
Middle			0.009037
			6
Top (East)			0.010191
			7
Top (West)	8	Y	0.01055
			-0.01203
Top (West)			0.008263

Channels 2 and 3 are the one used as input for the model (Figure 7-14). The records from the other channels are used to check the behaviour of the model.

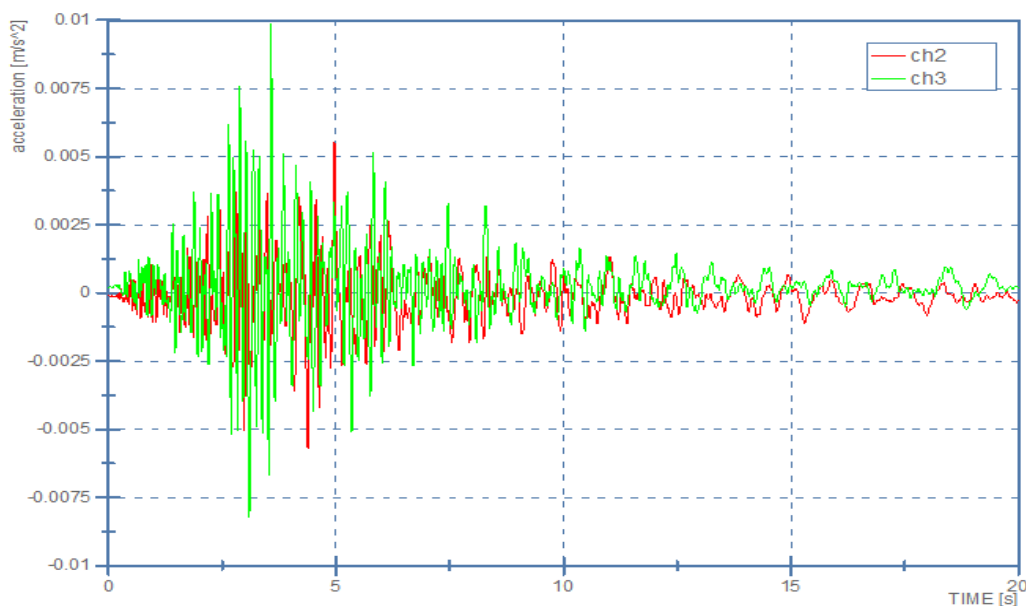


Figure 7-14: Channels 2 and 3 records

It was also checked how this seismic event was felt by the accelerometers of the strong motion network near the Church. The AQK station (Figure 7-15) records 3 cm/s^2 . This value agree with the maximum value of 1 cm/s^2 measured in St. Silvestro (which is near the AQU triangle in Figure 7-15).

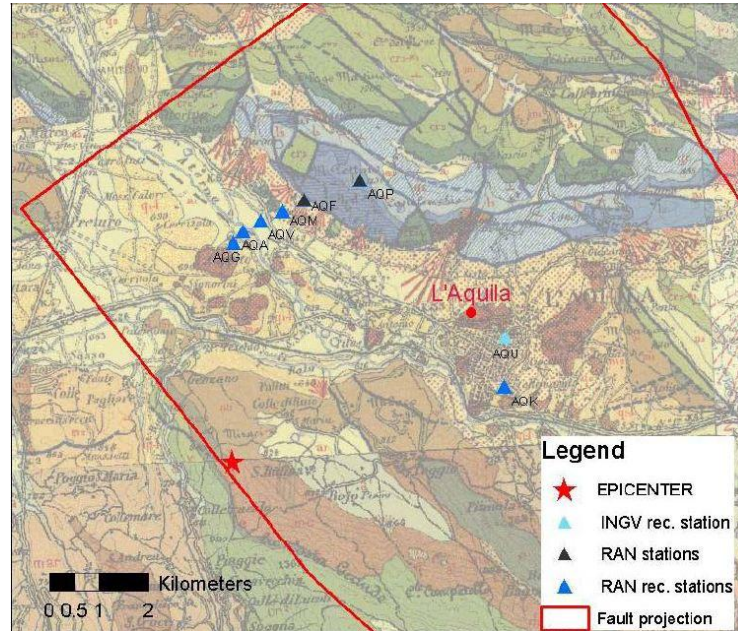


Figure 7-15: Accelerometers stations near L'Aquila (source: INGV)

The accelerometers are added in FX+ as non-spatial functions and are applied with the option “base excitation” to the structure.

The analyses run are “structural nonlinear” and need the definition of the Rayleigh damping factors. Rayleigh damping takes proportional mass and stiffness into account, equation (12), and results in a diagonal matrix. A generalized visualization of the damping can be seen in Figure 7-16.

$$\mathbf{c} = \alpha \mathbf{m} + \beta \mathbf{k} \quad (12)$$

Through mathematical passages and assumptions, the damping factor related to the n-th mode is finally given by equation (13) and it is function of ω_n .

$$\xi_n = \frac{1}{2} \left(\frac{\alpha}{\omega_n} + \beta \omega_n \right) \quad (13)$$

Assuming a damping coefficient ξ_n equal to 5%, α and β are evaluated with equations (14) and (15).

$$\alpha = \xi \frac{2\omega_i\omega_j}{\omega_i + \omega_j} \quad (14)$$

$$\beta = \xi \frac{2}{\omega_i + \omega_j} \quad (15)$$

where ω_i and ω_j are related to the first mode and the mode where the 85% of the cumulative participation mass is reached.

In the case of St. Silvestro $\omega_i = 1.67 \text{ Hz}$ and $\omega_j = 17.67 \text{ Hz}$. This last one is related to the 32nd mode where the cumulative participation mass is at least equal to 85% in both direction x and y.

For our case, $\alpha = 0.095$ and $\beta = 0.00082$.

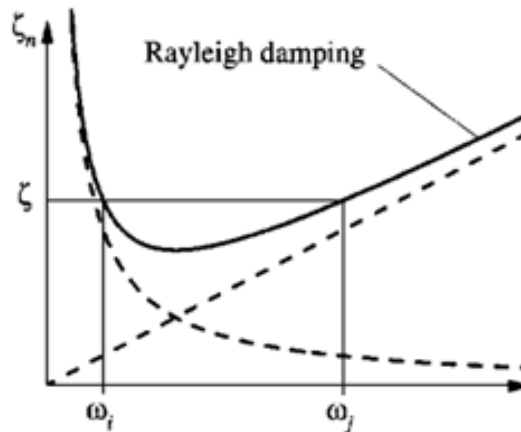


Figure 7-16: Rayleigh damping

The linear dynamic analysis's results are compared with the data available from the monitoring system. It has to be noted that the monitoring system collects data every 0.0125 s. The step of the analysis was 0.1 s (that is 8 times the experimental step).

Figure 7-17 and Figure 7-18 show the comparison between numerical and experimental data for the acceleration at mid height of the bell tower. The numerical data follow the experimental one; the shape of the graph is the same and in y direction the maximum acceleration felt is the same (0.012 for the experimental).

On the other hand, the accelerations felt on the top of the bell tower are 2 or 3 times amplified. Figure 7-19, Figure 7-20, and Figure 7-21 show the comparison of the acceleration measured and simulated on the top of the bell tower. It has to be pointed out that a more accurate analysis (also including nonlinear behaviour of the masonry) can simulate in a better way the real behaviour, however also the experimental data need to be checked. As can be seen in Table 20, the accelerations felt on the top of the tower are the same as in the middle.

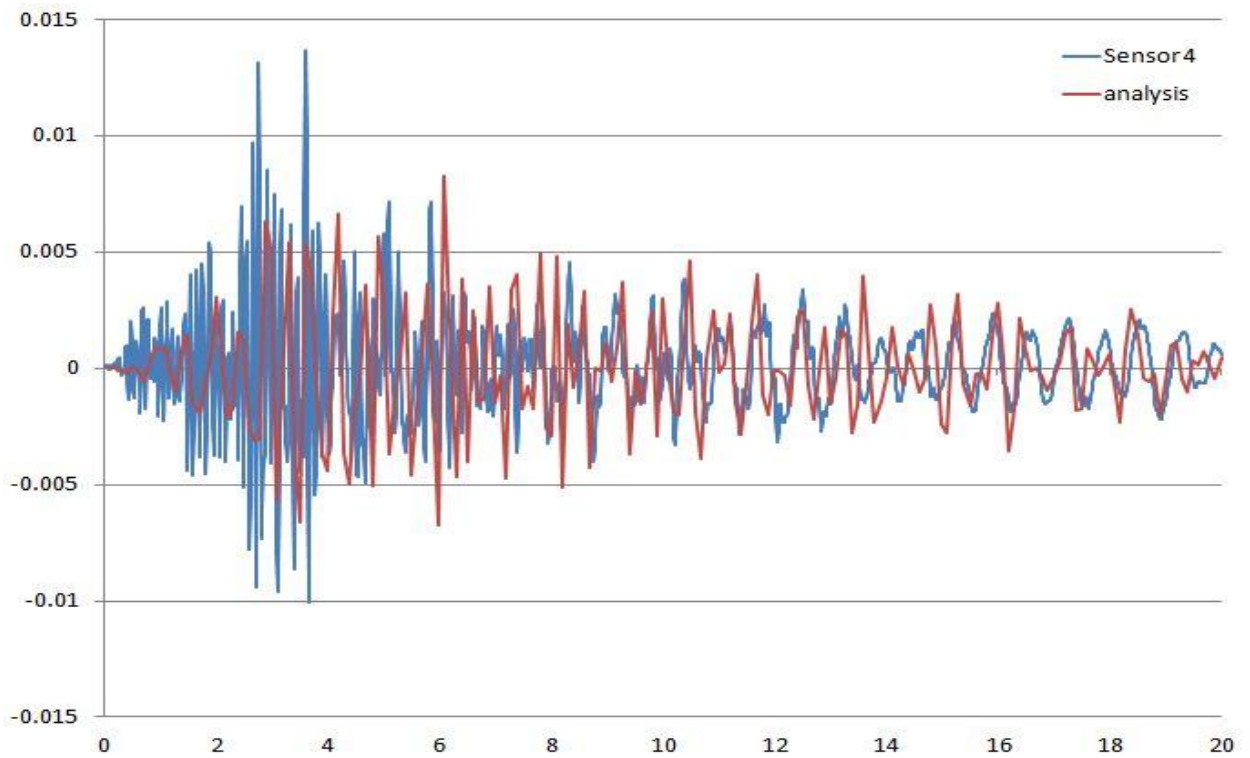


Figure 7-17: Comparison between experimental data (blue) and numerical data (red) for Channel 4 (x direction – midheight of the bell tower)



Figure 7-18: Comparison between experimental data (blue) and numerical data (red) for Channel 5 (y direction – midheight of the bell tower)

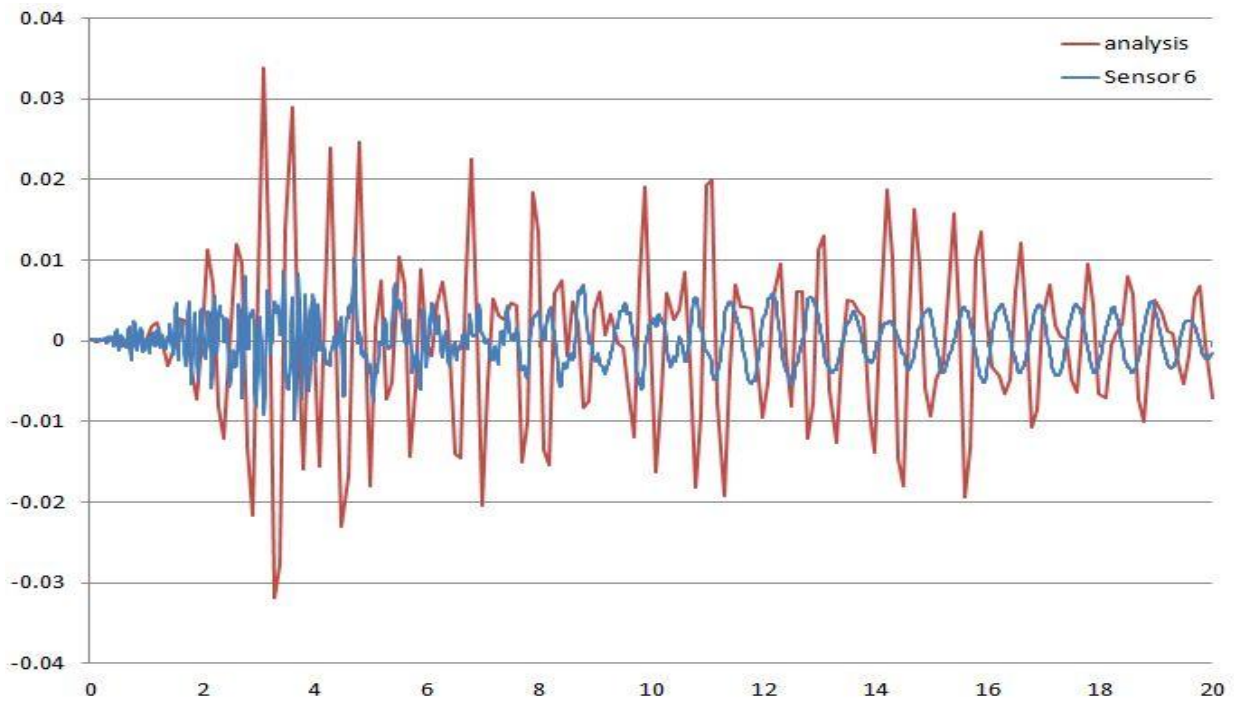


Figure 7-19: Comparison between experimental data (blue) and numerical data (red) for Channel 6 (x direction – top of the bell tower)

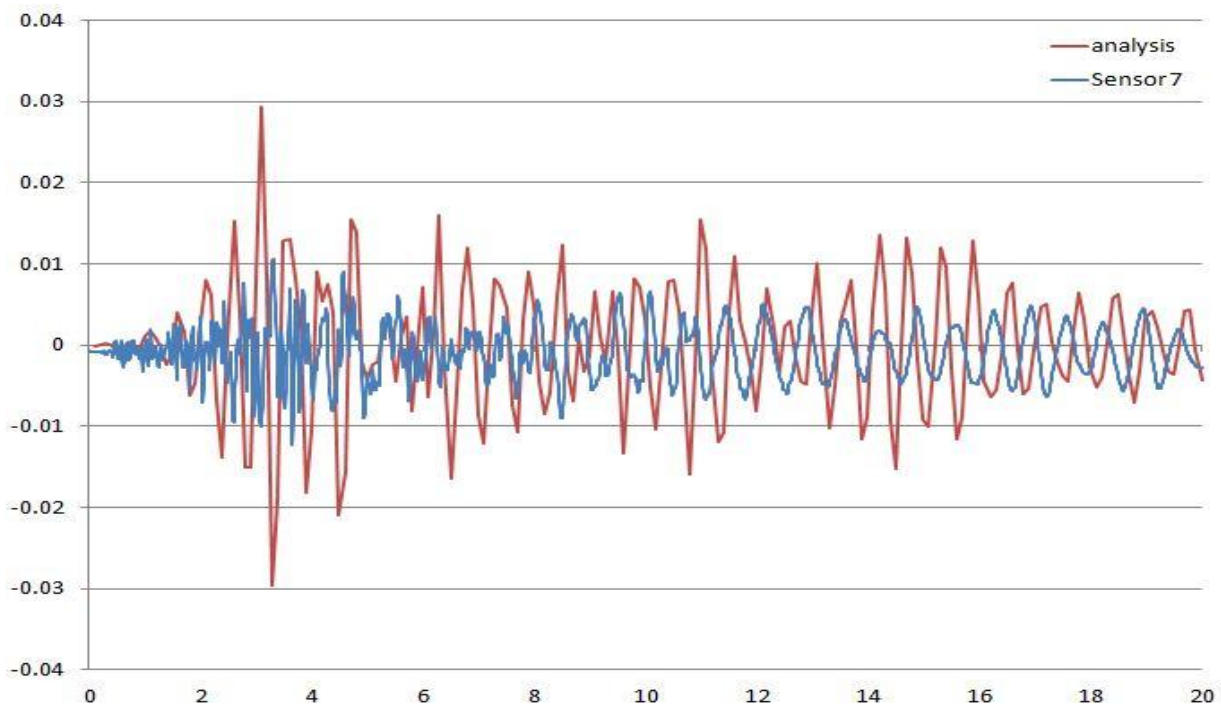


Figure 7-20: Comparison between experimental data (blue) and numerical data (red) for Channel 7 (x direction – top of the bell tower)

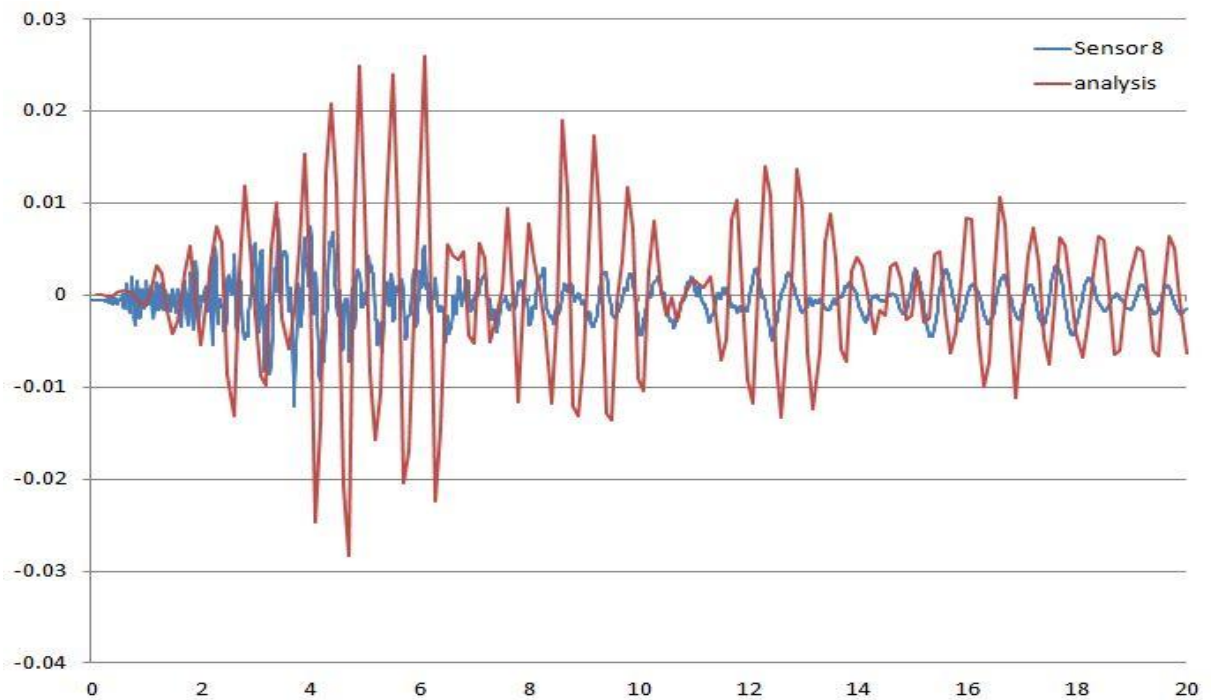


Figure 7-21: Comparison between experimental data (blue) and numerical data (red) for Channel 8 (y direction – top of the bell tower)

Also, a check on the frequencies before, during and after the seismic event was done. Using MACEC, the frequencies of the first three modes are evaluated. As expected, the frequencies decrease during the seismic event and then return at their normal values just after.

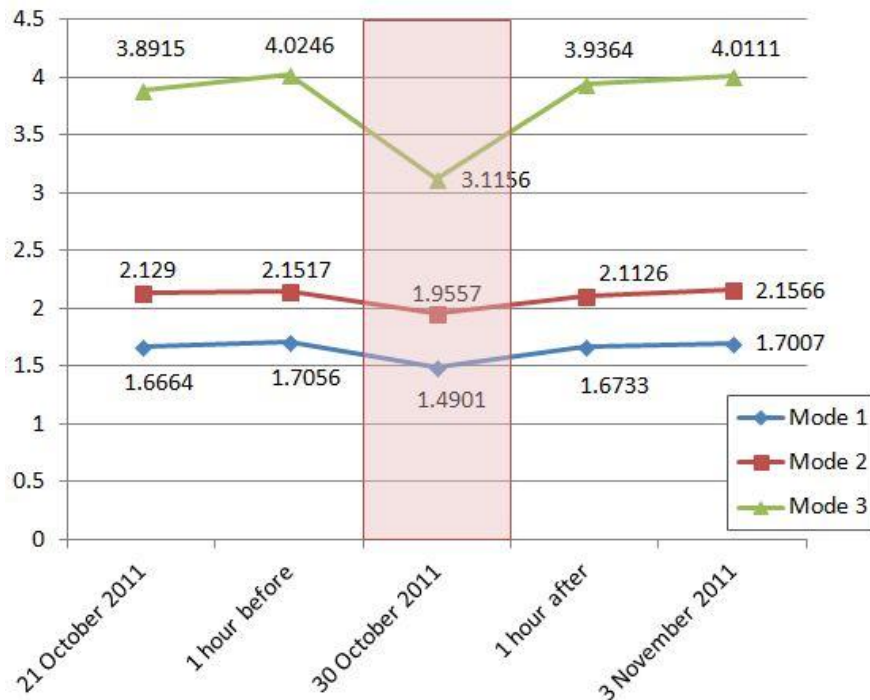


Figure 7-22: Frequencies before, during and after the seismic event

8 CONCLUSIONS AND FUTURE WORKS

This work of thesis aimed at the building and calibration of a finite element model of the Church of San Silvestro. The model is going to be used in future assessment works for the strengthening on the Church.

The Church is under constant and continuous monitoring (both static and dynamic) however, the investigation, as described in chapter 3, has not been carried out. This limits the results obtained with the analyses.

The work was organized starting from a small model that was considering only the bell tower and the façade. To better simulate the behaviour of the bell tower, the damage was added. Once the calibration was finished on the “small” model, a modal analysis was run with the entire Church. Also a dynamic analysis was performed. This process that start with a small model built for updating the entire model is called model updating.

At the end of this work of thesis, it can be said that the calibration carried out needs more work and it has to be considered that:

- a deeper investigation has to be proposed especially on the Church’s materials in order to gather enough information get a better behaviour of the model.
- a dynamic identification on the entire Church should be planned so that the global behaviour of the structure is known: the calibration of the Church only knowing the behaviour of the bell tower is not feasible.

After the investigation has been carried out, also the modelling process can be improved and updated. The structure has to be studied entirely, both through modal analysis and non-linear dynamic analysis. Also push over analysis is recommended for further validation of the gathered results. Moreover it is suggested to study the Church also with other methods and compare results: in this way a better knowledge of the behaviour of the building is gathered.

In the thesis is also presented a comparison between the frequencies before, during and after a selected seismic event. Also this topic has to be deeply analysed and discuss. The four records considered are not enough to make consideration on the Church’s behaviour.

At the end of this work, it is shown how much experimental investigation, monitoring and modelling can’t be separated. The importance of knowing the global behaviour of the Structure under exam is not enough if no local data on materials are available. To improve the efficiency of the model and get more accurate information, accurate material parameters need to be found. To do this NDT and MDT (described in paragraph 2.4) should be performed.

BIBLIOGRAPHY

- Antonini, O. (1999). *Architettura religiosa aquilana*. L'Aquila: Edizione del Gallo Cedrone.
- ASTM C 1197-91. (1991). *Standard test method for in-situ measurement of masonry deformability properties using the flat jack method*.
- Bezze, F. (2011). *Individuazione strutturale e modellazione della chiesa di San Biagio Amiternum e dell'Oratorio di San Giuseppe dei Mimmi a L'Aquila, edifici storici colpiti dal sisma del 6 Aprile 2009 (in Italian)*. Università degli Studi di Padova (Tesi di Laurea).
- Binda, L., Cantini, L., Saisi, A., & Tiraboschi, C. (2007, June 3-6). Use of flat-jack and sonic tests for the qualification of historic masonry. *X North American Masonry Conference - 10NAMC* , 791-803.
- Binda, L., Mirabella, G., & Abbaneo, S. (1994). The Diagnosis Research Project. *Earthquake Spectra* , 10 (1), 151-170.
- Binda, L., Saisi, A., & Tiraboschi, C. (2000). Investigation procedures for the diagnosis of historic masonries. *Construction and Building Materials* , 14 (4), 199-233.
- Binda, L., Saisi, A., & Zanzi, L. (2003). Sonic tomography and flat jack tests as complementary investigation procedures for the stone pillars of the temple of S.Nicolo' l'Arena (Italy). . *Non-Destructive Testing and Evaluation International - NDT&E International*, Vol. 36, No. 4, pp. 215-227. , 36 (4), 215-227.
- Binda, L., Saisi, A., Zanzi, L., Gianinetto, M., & Roche, G. (2003b, July 1-3). NDT applied to the diagnosis of historic buildings: a case history. *X International Conference Structural Faults and Repair*
- Borri, A., Cangi, G., Caraboni, M., Giancarlo, A., Menghini, F., Procaci, L., et al. (2010). "Sisma del 6 Aprile 2009 in Abruzzo e BCC: il caso della Chiesa di S.Silvestro a L'Aquila" (in Italian). *Bollettino ingegneri* , 4.
- Brencich, L., & Lagomarsino, S. (1998). A macro-element dynamic model for masonry shear walls. *IV International Symposium of Computer methods in structural masonry* , 67-75.
- Caccin, P. (2012). *Sviluppo di procedure automatiche di trattamento e analisi dei dati statici per il monitoraggio strutturale (in Italian)*. Università di Padova: Tesi di Laurea Specialistica.
- Calderone, B., Marone, P., & Pagano, M. (1987). Modelli per la verifica statica degli edifici in muratura in zona sismica (in Italian). *Ingegneria Sismica* , 3, 19-27.
- Casarin, F. (2006). Structural Assessment and vulnerability analysis of a complex historical building (Phd Thesis).
- Casolo, S., & Peña, F. (2007). Rigid element model for in-plane dynamics of masonry walls considering hysteretic behavior and damage. *Earthquake Engineering and Structural Dynamics* , 1029-1048.

D'Ayala, D., & Speranza, E. (2002). An integrated procedure for the assessment of seismic vulnerability of historical buildings. *Proceedings, 12th European Conference on Earthquake Engineering, Barbican Centre, London, Paper reference 561. Elsevier Science, Ltd.*

Diana User's Manual (Vol. Release Note 9.4.4). (2012). Delft: TNO DIANA BV, Edited by J. Manie.

Fattoretto, M. (2012). *Sviluppo di procedure automatiche di stima dei parametri modali per il monitoraggio strutturale (in Italian)*. Univeristà degli Studi di Padova: Tesi di Laurea Specialistica.

Gambarotta, L., & Lagomarsino, S. (1997a). Damage models for the seismic response of brick masonry shear walls. Part I: The mortar joint model and its applications. *Earthquake Engineering and Structural Dynamics* , 26, 423-439.

Gambarotta, L., & Lagomarsino, S. (1997b). Damage models for the seismic response of brick masonry shear walls. Part II: the continuum models and its applications. *Earthquake Engineering and Structural Dynamics* , 26, 441-462.

Gambarotta, L., & Lagomarsino, S. (1996). Sulla risposta dinamica di pareti in muratura (in Italian). *Convegno nazionale: La meccanica delle murature tra teoria e progetto* .

Giuffrè, A. (1993). *Sicurezza e conservazione dei centri storici in area sismica, il caso Ortigia*. Bari: Laterza.

Giuffrè, A., & Carocci, C. (1993). Statica e dinamica delle costruzioni murarie storiche. *Atti del Convegno internazionale CNR "Le pietre da costruzione: il tufo calcareo e la pietra leccese"* (p. 539–598). Bari: Mario Adda Editore.

Lemos, J. V. (2007). Discrete Element Modeling of Masonry Structures. *International Journal of Architectural Heritage* , 190-213.

Linee Guida per la valutazione e riduzione del rischio sismico del patrimonio culturale (in Italian). (2010, Luglio). Ministero per i Beni e le Attività Culturali.

Lourenço, P. B. (1996). *Computational strategies for masonry structures*. Delft University of Technology: PhD thesis.

Magenes, G., Bolognini, D., & Braggio, C. (2000). *Metodi semplificati per l'analisi sismica non-lineare di edifici in muratura (in Italian)*. Roma: CNR-Gruppo Nazionale per la Difesa dai Terremoti.

(2009). *Nuova Circolare della Norme Tecniche per le Costruzioni*. Consiglio Superiore dei Lavori pubblici, published 26.02.2009: Circolare 2.02.2009 n. 617.

(2008). *Nuove Norme Tecniche per le Costruzioni*. DM Infrastrutture 14.01.2008: published on G.U. 4.02.2008.

Silva, B., Costa, A. A., Guedes, J., Arêde, A., & Costa, A. (2008). In-Plane behavior of a stone masonry pier: Experimental test, numerical simulation and retrofitting efficiency evaluation. *International seminar on seismic risk and rehabilitation of stone masonry housing* .

Tomažević, M. (1978). *The computer program POR (in Slovene)*. Report ZRMK,.

9 ANNEXES

9.1 Strains

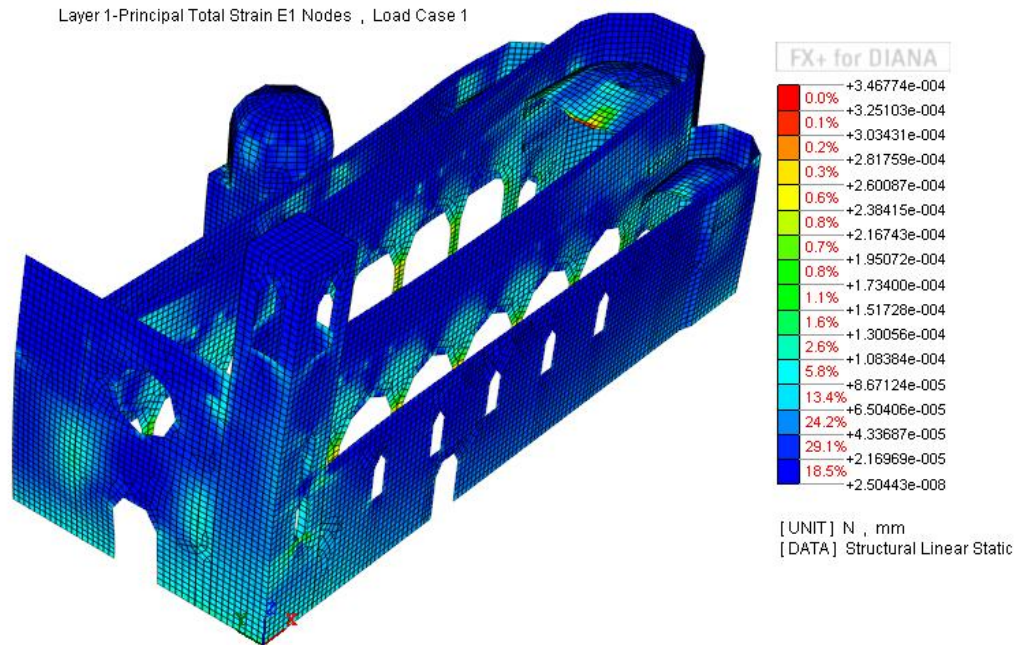


Figure 9-1: Tensile Principal Strain - Layer 1

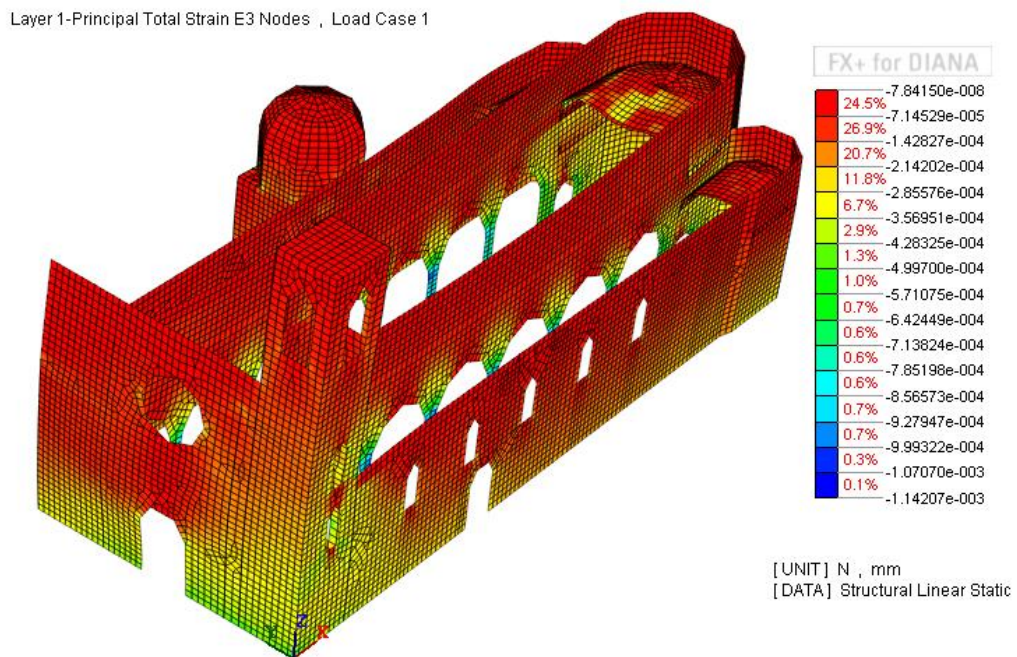


Figure 9-2: Compressive Principal Strain - Layer 1

Layer 3-Principal Total Strain E1 Nodes , Load Case 1

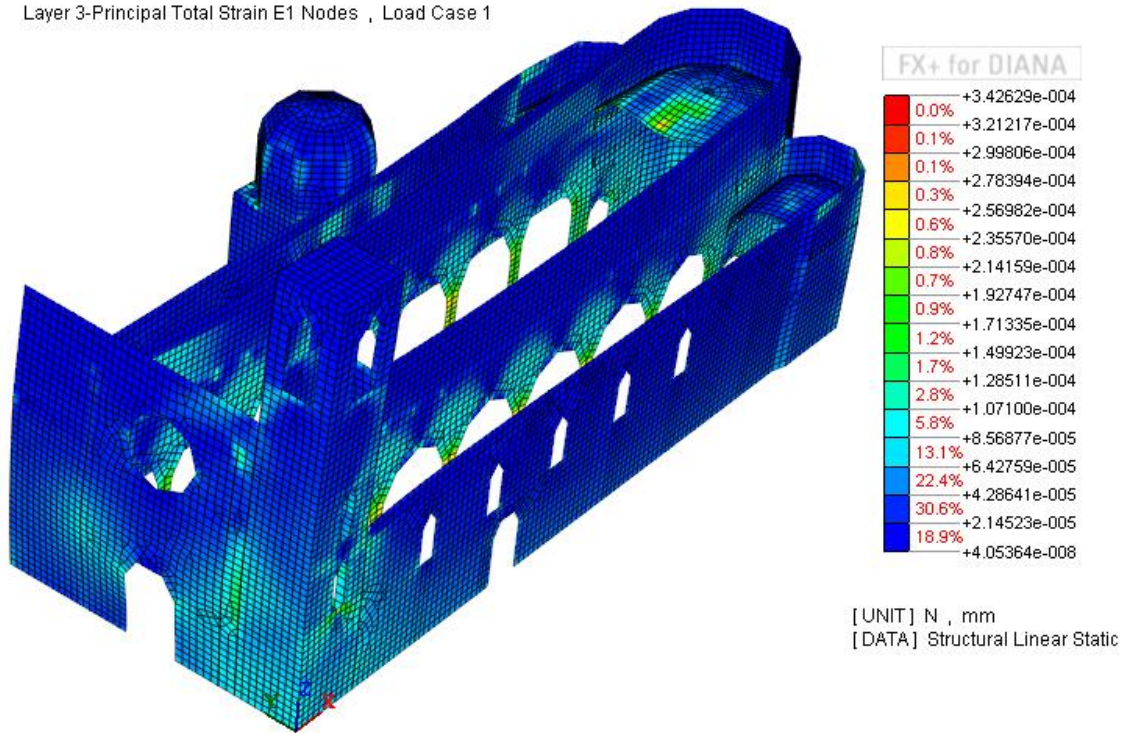


Figure 9-3: Tensile Principal Strain - Layer 3

Layer 3-Principal Total Strain E3 Nodes , Load Case 1

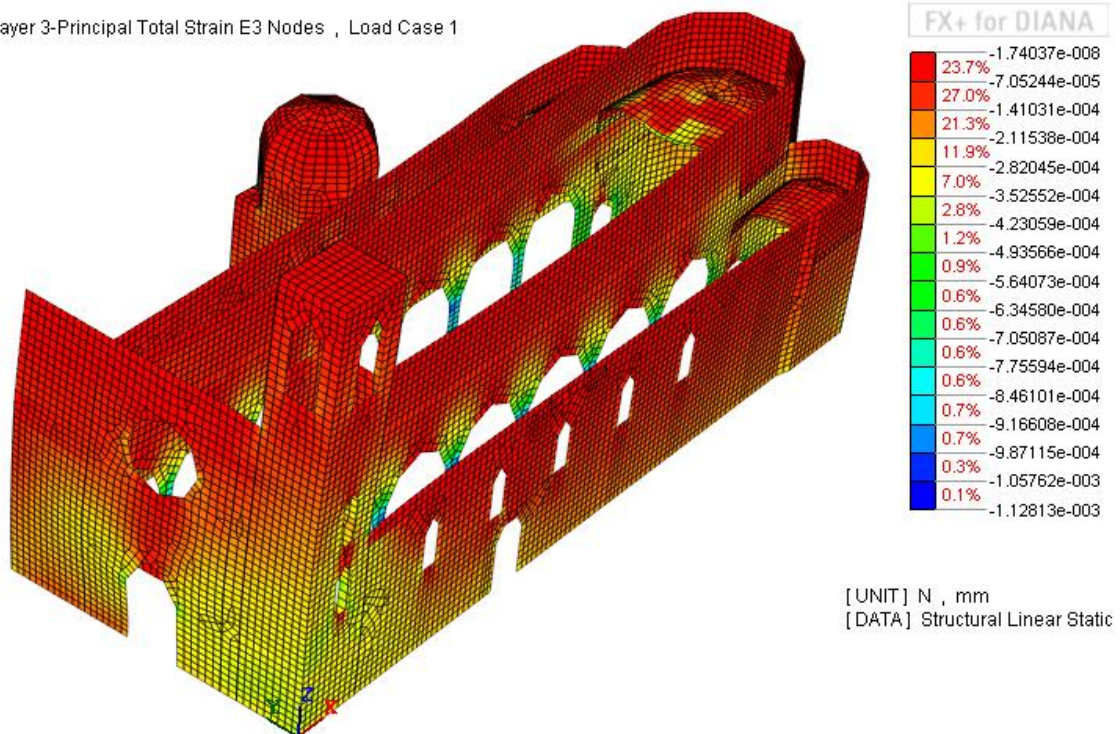


Figure 9-4: Compressive Principal Strain - Layer 3

9.2 Stresses

Layer 1-Principal Stress S1 Nodes(V) , Load Case 1

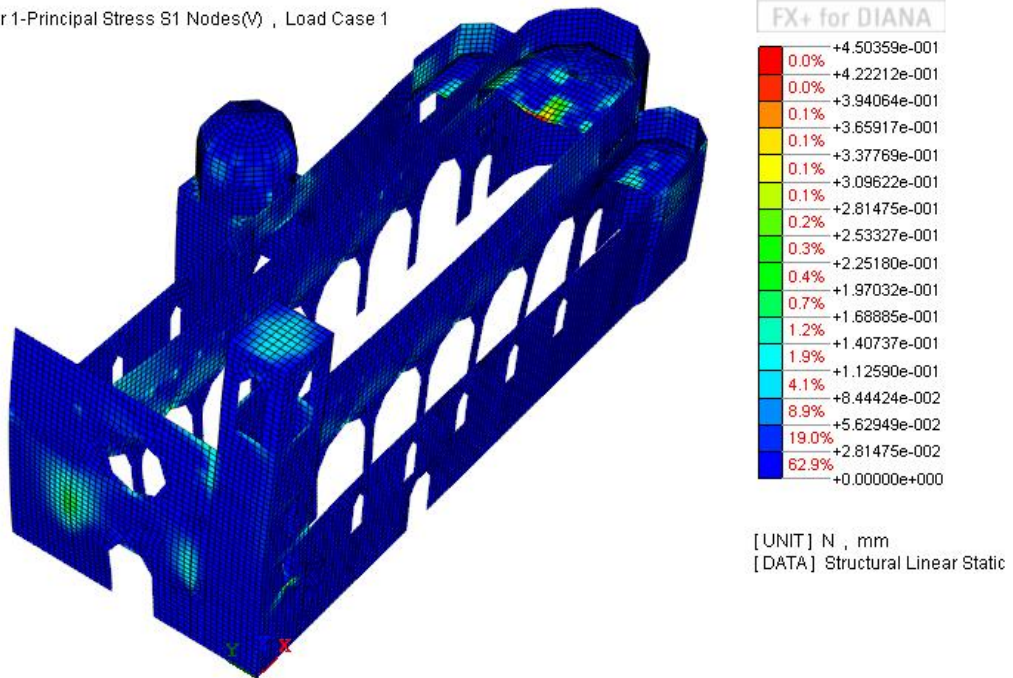


Figure 9-5: Tensile Principal Stress - Layer 1

Layer 1-Principal Stress S3 Nodes(V) , Load Case 1

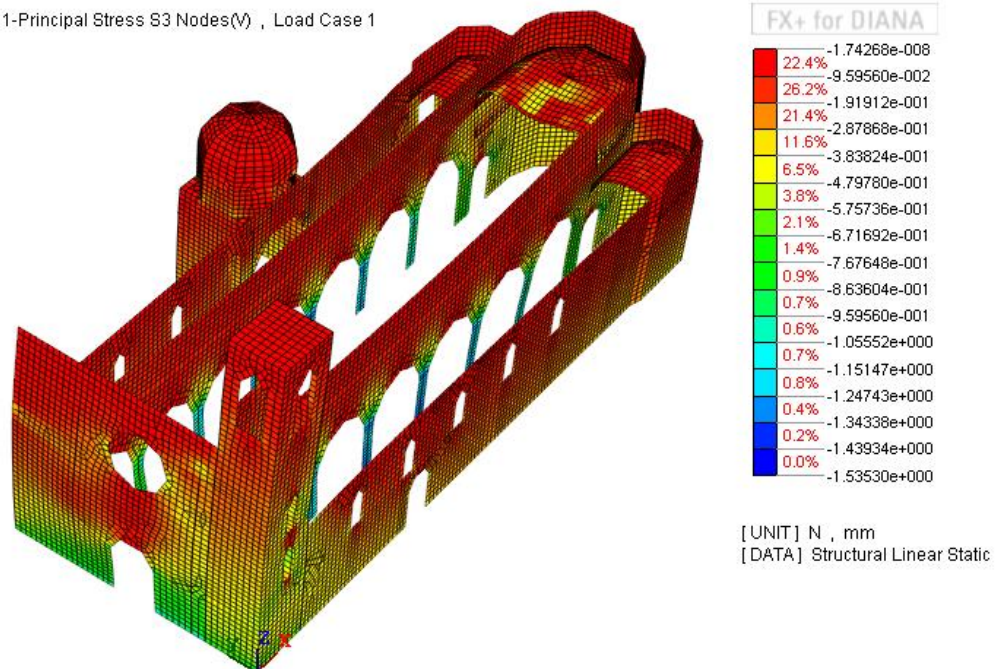


Figure 9-6: Compressive Principal Stress - Layer 1

Layer 3-Principal Stress S1 Nodes(V) , Load Case 1

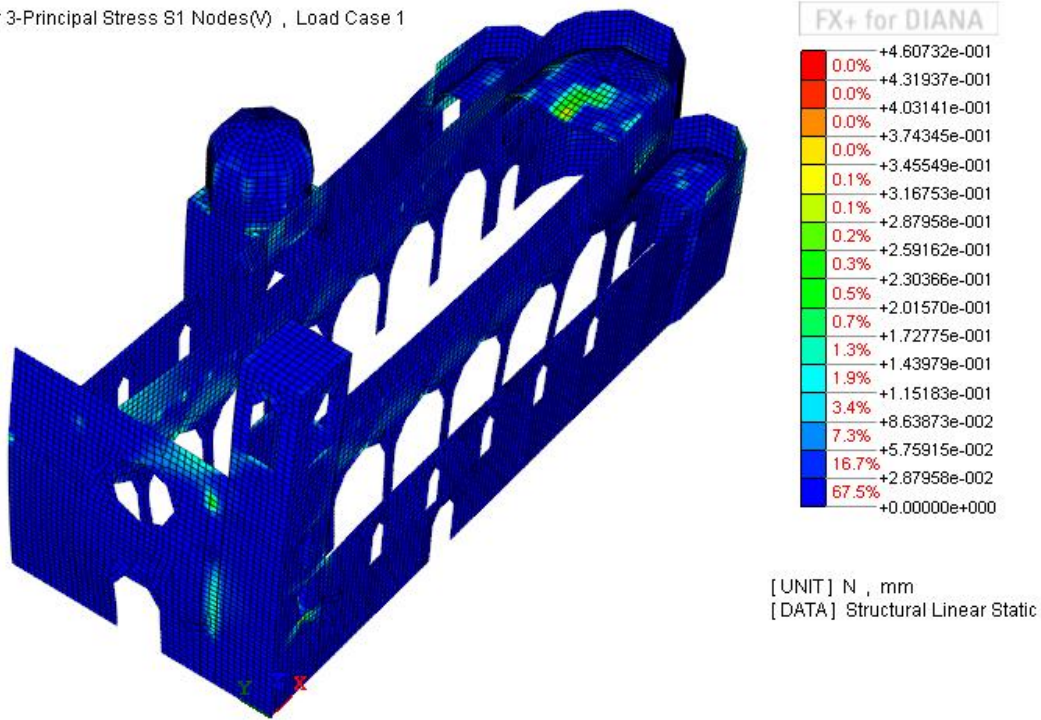


Figure 9-7: Tensile Principal Strain - Layer 3

Layer 3-Principal Stress S3 Nodes(V) , Load Case 1

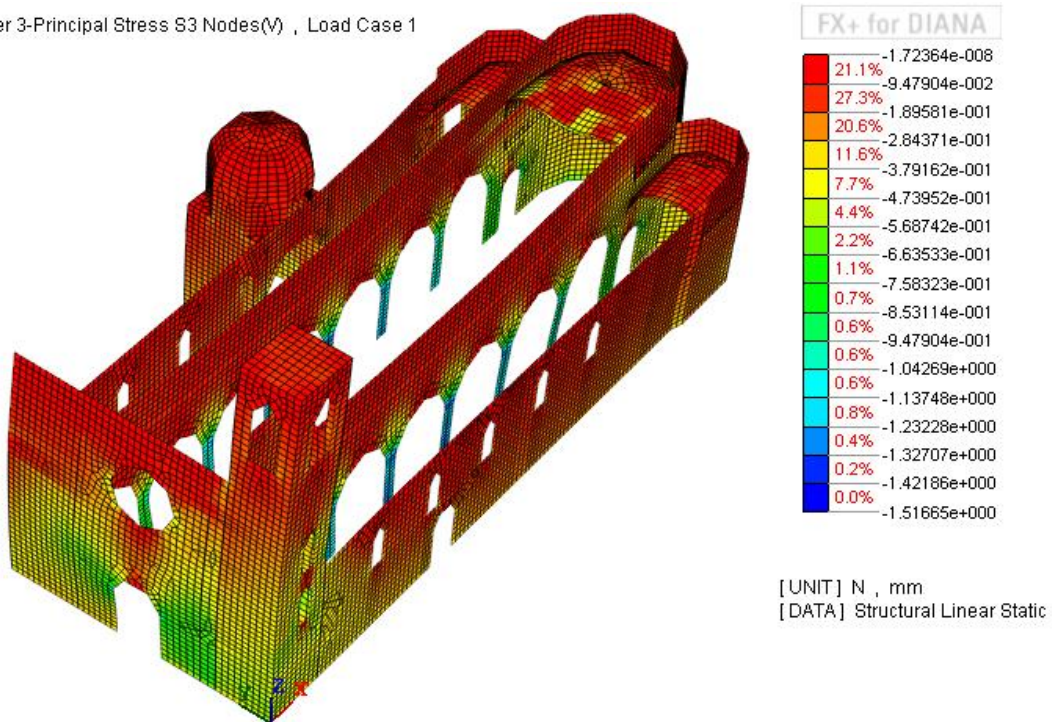


Figure 9-8: Compressive Principal Strain - Layer 3